ALUMINUM COORDINATION COMPOUNDS

By

KIM E. BROWNING

A DISSERTATION PRESENTED TO THE GRADUATE SCHOOL
OF THE UNIVERSITY OF FLORIDA IN PARTIAL FULFILLMENT
OF THE REQUIREMENTS FOR THE DEGREE OF
DOCTOR OF PHILOSOPHY

UNIVERSITY OF FLORIDA

1995

ACKNOWLEDGEMENTS

I would like to thank the following individuals for assisting me with my research and the preparation of my dissertation. Analytical Services of the UF Chemistry Department prepared the FAB Mass Spectra. Dr. Khalil A. Abboud performed the x-ray analysis on the structure discussed in chapter 6. John West produced the Al-27 NMR spectra for solutions and solid samples. I would also like to acknowledge the encouragement, patience and assistance readily available from Gus and Ruth Palenik.

TABLE OF CONTENTS

page

ACKNOWLEDGEMENTS..... ii

LIST OF TABLES..... v

LIST OF FIGURES..... viii

ABSTRACT..... xi

CHAPTERS

1 INTRODUCTION..... 1
Potential Aluminum Health and Environmental Issues..... 1
Coordination Chemistry of Aluminum.. 3
Aluminum Coordination Compounds..... 5
Aluminum Complexes with a Nitrogen Donor Atom..... 6

2 SYNTHESIS AND CHARACTERIZATION OF ALUMINUM COORDINATION COMPOUNDS..... 11
Aluminum as a Lewis Acid..... 11
Synthesis..... 12
Solubility of Aluminum Coordination Compounds..... 20
Methods of Characterization of Aluminum Complexes..... 21

3 CRYSTAL GROWTH TECHNIQUES UTILIZED TO PRODUCE SINGLE CRYSTALS SUITABLE FOR USE IN X-RAY DIFFRACTION STUDIES..... 27
Introduction..... 27
Urea Decomposition..... 27
Vapor Diffusion..... 28
Gel Diffusion..... 30
Base Strength..... 33
Solvent System..... 36
Aluminum Isopropoxide..... 38
Summary of Results..... 39

4 SYNTHESIS, STRUCTURE AND ALUMINUM-27 NMR STUDIES OF COMPLEXES WITH OXINE AND 2-METHYLOXINE..... 41
Introduction..... 41
Experimental..... 44
Discussion..... 48

5 ALUMINUM-27 NMR, INFRARED AND ELEMENTAL ANALYSIS OF ALUMINUM COMPLEXES OF N,O DONOR LIGANDS..... 67
Introduction..... 67
Aluminum-27 NMR..... 67
Elemental Analysis..... 82
Infrared Spectroscopy..... 84
Fast Atom Bombardment Mass Spectrometry..... 86
Conclusion..... 88

6 A PENTAGONAL BIPYRAMIDAL SODIUM COMPOUND: SYNTHESIS AND CRYSTAL STRUCTURE..... 90
Introduction..... 90
Experimental..... 91
Discussion..... 94

7 SYNTHESIS AND STRUCTURE OF A COMPLEX COMPOUND WITH PICOLINIC ACID AND AMMONIUM NITRATE..... 103
Introduction..... 103
Experimental..... 103
Discussion..... 105

8 SYNTHESIS AND ABSOLUTE CONFIGURATION OF SODIUM (+) - TARTRATE MONOHYDRATE..... 115
Introduction..... 115
Experimental..... 115
Discussion..... 117

9 CONCLUSION..... 125
Characterization of Aluminum Coordination Compounds..... 125
Crystal Growth Techniques..... 130
X-ray Diffraction Studies..... 133
Summary..... 137

REFERENCES..... 138

BIOGRAPHICAL SKETCH..... 143

LIST OF TABLES

Table	Title	Page
3-1	Vapor Diffusion Experimental Conditions and Results	30
3-2	Gel Diffusion Experimental Conditions and Results	32
3-3	Base Variation Experimental Conditions and Results	35
3-4	Experimental Conditions for Crystal Growth in Various Solvents and Results	37
4-1	Crystallographic Data for **I** and **II**	49
4-2	Final Atomic Coordinates and Isotropic Thermal Parameters for **I**	51
4-3	Hydrogen Atom Coordinates for **I**	52
4-4	Bond Lengths for **I**	53
4-5	Bond Angles for **I**	53
4-6	Anisotropic Temperature Parameters for Non-Hydrogen Atoms for **I**	55
4-7	Final Atomic Coordinates and Isotropic Thermal Parameters for **II**	58
4-8	Hydrogen Atom Coordinates for **II**	59
4-9	Bond Lengths for **II**	60
4-10	Bond Angles for **II**	60
4-11	Anisotropic Thermal Parameters for **II**	62
5-1	Al-27 NMR Peak Data and Aluminum Coordination	68

5-2 Al-27 NMR Peak Data for Compounds **III** through **VII**..... 72

5-3 Al-27 NMR Data for Solutions Containing 0.30 M Al^{3+} and the Tabulated Concentration of pza at pH 5..... 78

5-4 Elemental Analysis Data for Compounds **III** through **VII** and Pure Tris Complexes of the Ligands..... 83

5-5 FTIR Carbonyl Peak Data..... 84

5-6 FABMS Peak Data..... 87

6-1 Elemental Analysis of **VIII**..... 92

6-2 Crystallographic Data for Compound **VIII**... 95

6-3 Final Atomic Coordinates and Isotropic Thermal Parameters for the Non-Hydrogen Atoms of Compound **VIII**..... 97

6-4 Final Atomic Coordinates and Isotropic Thermal Parameters for the Hydrogen Atoms of Compound **VIII**..... 98

6-5 Bond Lengths of all Atoms of Compound **VIII**..... 98

6-6 Bond Angles for all Atoms of Compound **VIII**..... 99

6-7 Anisotropic Thermal Parameters for the Non-Hydrogen Atoms of Compound **VIII**..... 100

7-1 Crystallographic Data for **IX**..... 106

7-2 Final Atomic Coordinates and Isotropic Thermal Parameters for **IX**..... 109

7-3 Hydrogen Atom Coordinates and Isotropic Thermal Parameters for **IX**..... 110

7-4 Bond Lengths for Non-Hydrogen Atoms in **IX**..... 110

7-5 Bond Lengths involving Hydrogen Atoms in **IX**..... 111

7-6 Bond Angles in **IX**..... 111

7-7 Anisotropic Thermal Parameters for Non-Hydrogen Atoms in **IX**..... 112

8-1 Crystallographic Data for **X**..... 118

8-2 Final Atomic Coordinates and Isotropic Thermal Parameters for **X**..... 120

8-3 Bond Lengths and Angles for **X**..... 120

8-4 Anisotropic Thermal Parameters for Non-Hydrogen Atoms in **X**..... 122

8-5 Least Squares Planes Analysis of Square Antiprismatic and Dodecahedral Geometries for **X**..... 123

LIST OF FIGURES

Figure	Caption	Page
1-1	Representation of Aluminum Complexes with 3-Hydroxy-4-pyridinone and its Derivatives	5
1-2	ORTEP of the Aluminum Citrate Complex and its Al_3O_4 Core	6
1-3	9-Amino-1,2,3,4-tetrahydroacridine	7
1-4	Ligands with O-C-C-N Donor Group. Oxine; 2-Methyloxine; Picolinic acid; 6-Methylpicolinic acid; Pyrazinoic acid; Hypoxanthine; Dipicolinic acid	8
2-1	Representation of a Tris Complex between Aluminum and a Bidentate Ligand	13
2-2	2-Methyloxine	13
2-3	Oxine	14
2-4	Picolinic acid	15
2-5	6-Methylpicolinic acid	16
2-6	Pyrazinoic acid	17
2-7	Hypoxanthine	18
2-8	Dipicolinic acid	19
4-1	Oxine; Methyloxine	41
4-2	ORTEP Drawing of the Tris(oxinato)-aluminum(III) without the Occluded Acetonylacetone	42
4-3	PLUTO Line Drawing of the μ-Oxo-di(bis-(2-methyloxinato)aluminum(III) Complex	43

4-4 ORTEP Drawing of the $Al(meox)_3$ Molecule Showing the Atomic Numbering Scheme and the Thermal Ellipsoids..... 50

4-5 ORTEP of $Al(ox)_3$ Molecule Showing the Numbering Scheme and Thermal Ellipsoids. 57

4-6 Al-27 NMR Spectrum of the Solid **Ia**..... 63

4-7 Al-27 NMR Spectrum of the Solid **IIa**..... 65

4-8 Al-27 NMR Spectrum of $Al(ox)_3$ in C_2H_5OH Solution..... 65

5-1 Ligands in Table 5-1. Iminodiacetic acid; Nitrilotriacetic acid; N-(Hydroxyethyl)-ethylenediaminetriacetic acid; Ethylene-diaminetetraacetic acid; 1,2-Propylene diaminetetraacetic acid; trans-1,2-diaminocyclohexanetetraacetic acid; Diethylenetriaminepentaacetic acid; Pyromeconic acid; Maltol; 3-Hydroxy-2-methyl-4-pyridinone; 3-Hydroxy-1,2-dimethyl-4-pyridinone..... 69

5-2 Al-27 NMR Spectra of **III**, Solid, in d_6-DMSO. 73

5-3 Al-27 NMR Spectra of **IV**, Solid, in d_6-DMSO. 74

5-4 Al-27 NMR Spectra of **V**, Solid, in d_6-DMSO.. 75

5-5 Al-27 NMR Spectra of **VI**, Solid, in d_6-DMSO. 76

5-6 Al-27 NMR Spectra of **VII**, Solid, in d_6-DMSO. 77

5-7 Al-27 NMR Spectrum of an Aqueous Solution Containing 0.30 M Al^{3+} at pH 5.. 79

5-8 Al-27 NMR Spectrum of an Aqueous Solution Containing 0.30 M Al^{3+} and 0.30 M pza at pH 5..... 79

5-9 Al-27 NMR Spectrum of an Aqueous Solution Containing 0.30 M Al^{3+} and 0.60 M pza at pH 5..... 80

5-10 Al-27 NMR Spectrum of an Aqueous Solution Containing 0.30 M Al^{3+} and 0.90 M pza at pH 5..... 80

6-1 Dipicolinic acid..... 90

6-2 ORTEP Representation of **VIII**..... 96

7-1 ORTEP of Compound **IX**..... 107

7-2 Detail Showing Hydrogen Bonding in **IX**..... 108

8-1 ORTEP Drawing of **X** Showing the Atomic Numbering Scheme..... 119

8-2 Sodium Ion Coordination in **X**, Showing the Square Antiprismatic and Dodecahedral Orientations..... 122

Abstract of Dissertation Presented to the Graduate School of the University of Florida in Partial Fulfillment of the Requirements for the Degree of Doctor of Philosophy

ALUMINUM COORDINATION COMPOUNDS

By

Kim E. Browning

May 1995

Chairman: Gus J. Palenik, Ph. D.
Major Department: Chemistry

Long considered a harmless element, studies in recent years have linked aluminum(III) with health and environmental problems ranging from Alzheimer's Disease and Osteoporosis to the deforestation and fish kills associated with acid rain. The coordination chemistry of aluminum(III) must be further understood to explain the mechanism by which aluminum(III) is incorporated into the biosphere and what, if any, role it might play in causing these disorders.

To date, the focus of aluminum(III) coordination chemistry that has been conducted is with ligands containing primarily oxygen donor atoms. Since many naturally occurring compounds also contain nitrogen as a potential donor ligand, the focus of this research has been to study the coordination of aluminum(III) with naturally occurring compounds and similar ligands that contain a potential N,O donor moiety.

The synthesis of aluminum(III) compounds with several N,O donor ligands will be presented. Characterization by X-ray crystallography was possible for some of the coordination compounds despite efforts to grow suitable crystals by various methods. X-ray diffraction techniques were used to examine the similar environments of tris(oxinato)aluminum(III) and tris(2-methyloxinato)aluminum(III). Furthermore, solution as well as solid state Aluminum-27 Nuclear Magnetic Resonance spectra are presented and compared for the synthesized compounds. Aluminum-27 NMR spectroscopy provides information about the coordination number and the type of atoms around the metal center. Beyond X-ray crystallographic techniques, it is probably the most useful for determining the environment around a coordinated aluminum(III) ion. The shift downfield, which is due primarily to the coordination number, varies when different atoms are within the coordination sphere. Therefore, a similar environment around the aluminum(III) ion should produce a similar spectrum.

A discussion of the difficulties associated with aluminum determination is included.

CHAPTER 1

INTRODUCTION

Potential Aluminum Health and Environmental Issues

Traditionally considered to be a harmless element, aluminum is widely used in the preparation of foodstuffs and cosmetics. However, over the past couple of decades, aluminum has been investigated with respect to a wide variety of biological and environmental phenomena.

In the early 1980s, an extraordinarily high concentration of aluminum was found, post mortem, as neurofibrillary tangles and amyloid plaques in the brains of patients who had died of Alzheimer's Disease.[1] At first, aluminum was implicated as the sole causative factor. To test this theory, several studies were performed in various parts of the world to show a causative relationship with respect to available aluminum content in a drinking water and aluminum-containing products such as antacids. The study on aluminum-containing products reported no significant dose-response trend.[2] The drinking water studies showed a slight positive relationship for aluminum content and a negative relationship for fluoride content.[1,3] However, in 1987, it was reported that the precursor protein for the amyloid plaques was coded by a gene

on chromosome 21.[4] It is rather an interesting occurrence that chromosome 21 should be implicated in Alzheimer's Disease. Down's Syndrome patients have an extra copy of chromosome 21. Furthermore, autopsies have shown that virtually all Down's patients that survive into their thirties or forties get Alzheimer's Disease.[4] Upon further research, the metal was also detected in victims of Lou Gehrig's Disease, also known as Amyotrophic Lateral Sclerosis, and other neurological disorders such as epilepsy.[5]

Ordinarily, ingested aluminum is excreted rapidly during normal kidney function.[6] Individuals with kidney failure, however, are subject to aluminum accumulation in several tissues. First, aluminum is incorporated onto the bone surface by the osteoblasts in the place of calcium, thereby weakening the structure.[7] In addition, in healthy bone, the osteoclasts remove the top layers so that the bone can continually be rebuilt. After the aluminum has accumulated on the bone surfaces, the osteoclasts cannot remove it.[7] As a result the damage to the bone cannot be repaired and aluminum adsorption continues to cover the bone surfaces. Once the bone surfaces are saturated, the aluminum then begins to concentrate in the brain.[7] Patients of dialysis dementia, characterized by speech difficulties, seizures and personality changes, have markedly elevated levels of aluminum in their brain tissues in amyloid plaques similar to those in Alzheimer's Disease patients.[8,9]

Aluminum is the most abundant metallic element in the earth's crust, but it is generally not available for uptake into the biosphere. Under atmospheric conditions, elemental aluminum can easily be oxidized to the trivalent aluminum ion, that primarily exists as water insoluble mixed oxides and silicates.[10] When exposed to acidic conditions, such as in acid rain, the oxides dissolve to yield a solution of $Al(H_2O)_6^{3+}$ ions and aluminum ions coordinated to naturally occurring ligands.[11,12] As a mobile element, aluminum is available for uptake by trees and aquatic organisms after it has drained into lakes and rivers. As a result, increased levels of aluminum have been implicated in the deforestation and death of lakes commonly associated with acid rain.[11,13] Because of the similar size and charges, aluminum could compete with calcium, silicon and iron and interfere with normal biological functions.[3,14] In consideration of these facts, an understanding of the reactivity and stability of aluminum and its compounds warrants a thorough investigation.

Coordination Chemistry of Aluminum

In the presence of ligands other than water, the metal ion can undergo exchange and loss of the water molecules.[15] The factors controlling the coordination to a new ligand include the formation of rings due to chelation, the geometry around the metal center and the type of atom bonded to the aluminum(III) ion.

A complex, formed by a ligand substituting for water, would be less stable and less likely to form if there were too much steric strain. Coordination numbers of four, five and six are most commonly reported for Al(III).[10] Too many ligands around the metal center would be less stable due to crowding caused by the relatively small metal ion radius, whereas too few ligands would force Al(III) into a less favorable geometry.

The formation of a five- or six-membered chelate ring will provide stability to the complex due to the formation of an unstrained ring structure. Organic rings of less than five atoms are less stable because ring strain is created. If chelation to a metal ion formed a small ring, the ligand would be forced into a less stable configuration. The strain occurring in the ligand is greater than if a larger ring were formed. As a result, a less stable complex would be formed if chelate rings are less than five-membered.

The donor atom bonded to the metal ion can affect the stability of a complex. From equilibrium studies, a trend of strength of complexation was determined as decreasing for the ligands dicarboxylic acid, hydroxycarboxylic acid, carboxylic acid and amino acid.[16] Al(III), a relatively small ion with a large positive charge, is a hard Lewis acid. Because oxygen has a smaller size and larger negative charge, it has a stronger attraction to the aluminum ion than nitrogen.[10]

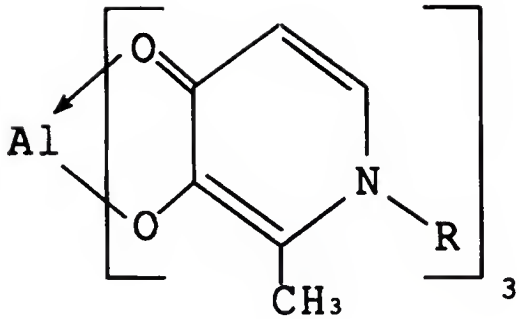

R = H Al(mpp)$_3$

= CH_3 Al(dpp)$_3$

= n-C_6H_{11} Al(mhpp)$_3$

Figure 1-1. Representation of Aluminum Complexes with 3-Hydroxy-4-pyridinone and its Derivatives. Nelson, Karpishin, Rettig and Orvig, *Inorganic Chemistry*, **1988**, *27*, 1045-1051.

Aluminum Coordination Compounds

Complexes of Al(III) have been reported with many O,O donor ligands.[17-23] For the derivatives of 3-hydroxy-4-pyridinone, the complexes with the Al(III) ion, represented in Figure 1-1, were synthesized by the addition of a base or proton scavenger to a solution of ligand and Al(III).[17] By a similar technique, complexes were also formed with maltol and its derivatives, isomaltol, oxalic acid, tropolone and 2,4-pentanedione.[18-22] Each of the compounds was characterized by x-ray diffraction techniques as six coordinate tris chelates with each ligand forming a five- or six-membered ring with the central metal ion. The structure, shown in Figure 1-2, for the complex of Al(III) with citric acid revealed a trinuclear complex ion with each Al(III) in a distorted octahedral environment.[23]

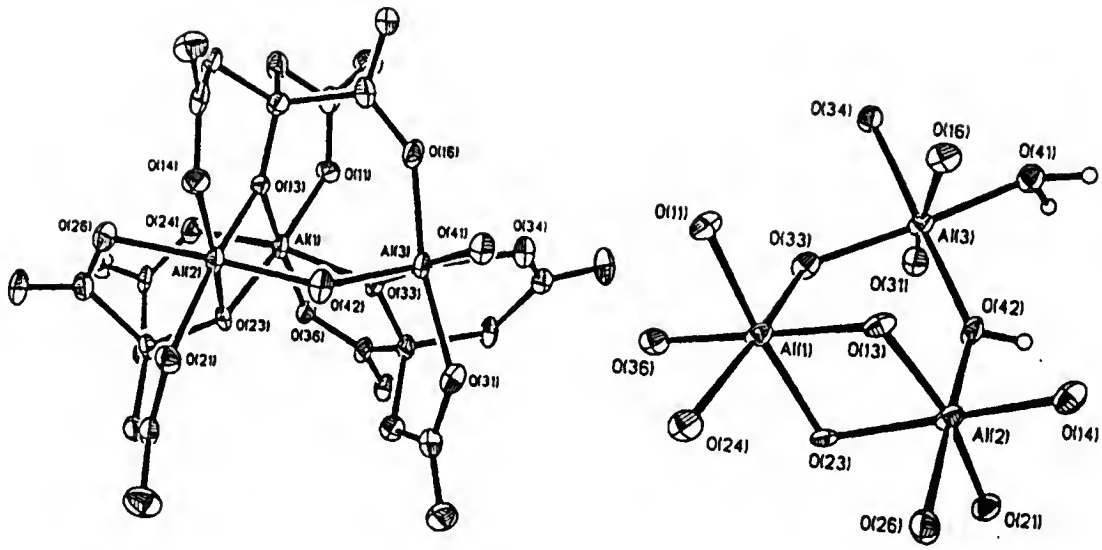

Figure 1-2. ORTEP of the Aluminum Citrate Complex, left, and its Al_3O_4 Core, right. Feng, Gurian, Healy and Barron, *Inorganic Chemistry*, **1990**, *29*, 408-411.

Aluminum Complexes with a Nitrogen Donor Atom

There are many naturally occurring ligands and biological molecules containing nitrogen as a potential donor atom. For example, the pharmaceutical 9-amino-1,2,3,4-tetrahydroacridine (THA), pictured in Figure 1-3, has been used to alleviate symptoms in Alzheimer's Disease patients. It has been proposed that the aromatic ring is hydroxylated to yield a O-C-C-N donor group.[24] Currently, the list of aluminum complexes with a nitrogen as an electron donor is relatively short.[25-43] From these studies, only seven coordination centers with N,O donors have been confirmed by x-ray diffraction techniques.[25-32] In an effort to further understand the behavior of Al(III),

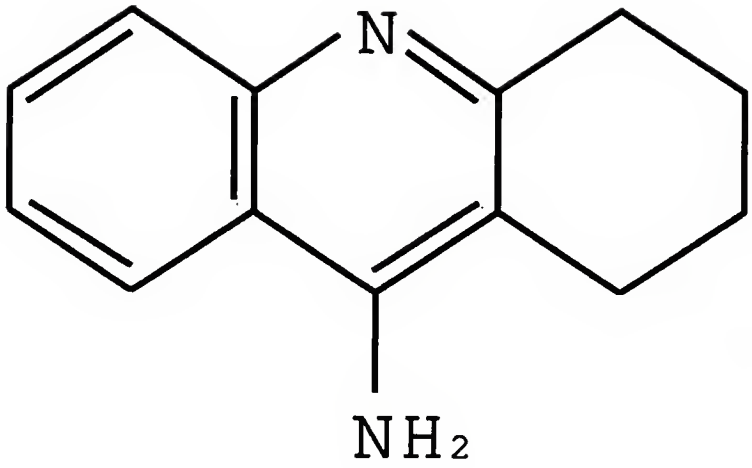

Figure 1-3. 9-Amino-1,2,3,4-tetrahydroacridine (THA).

its complexation to ligands containing a potential donor nitrogen has been investigated. These ligands, shown in Figure 1-4, include oxine, 2-methyl-oxine, picolinic acid, 6-methyl-picolinic acid, pyrazinoic acid, hypoxanthine and 2,6-dipicolinic acid.

Oxine is structurally very similar to the suspected metabolite of THA.[24] The manner in which oxine reacts with the aluminum ion could be important to the reason that THA is effective in alleviating Alzheimer's symptoms. 2-Methyloxine is different from oxine only by the presence of the methyl group adjacent to the ring nitrogen. The steric interaction that could occur due to the presence of the methyl group could change the length and strength of the Al-N bond as well as prevent the formation of the tris complex.

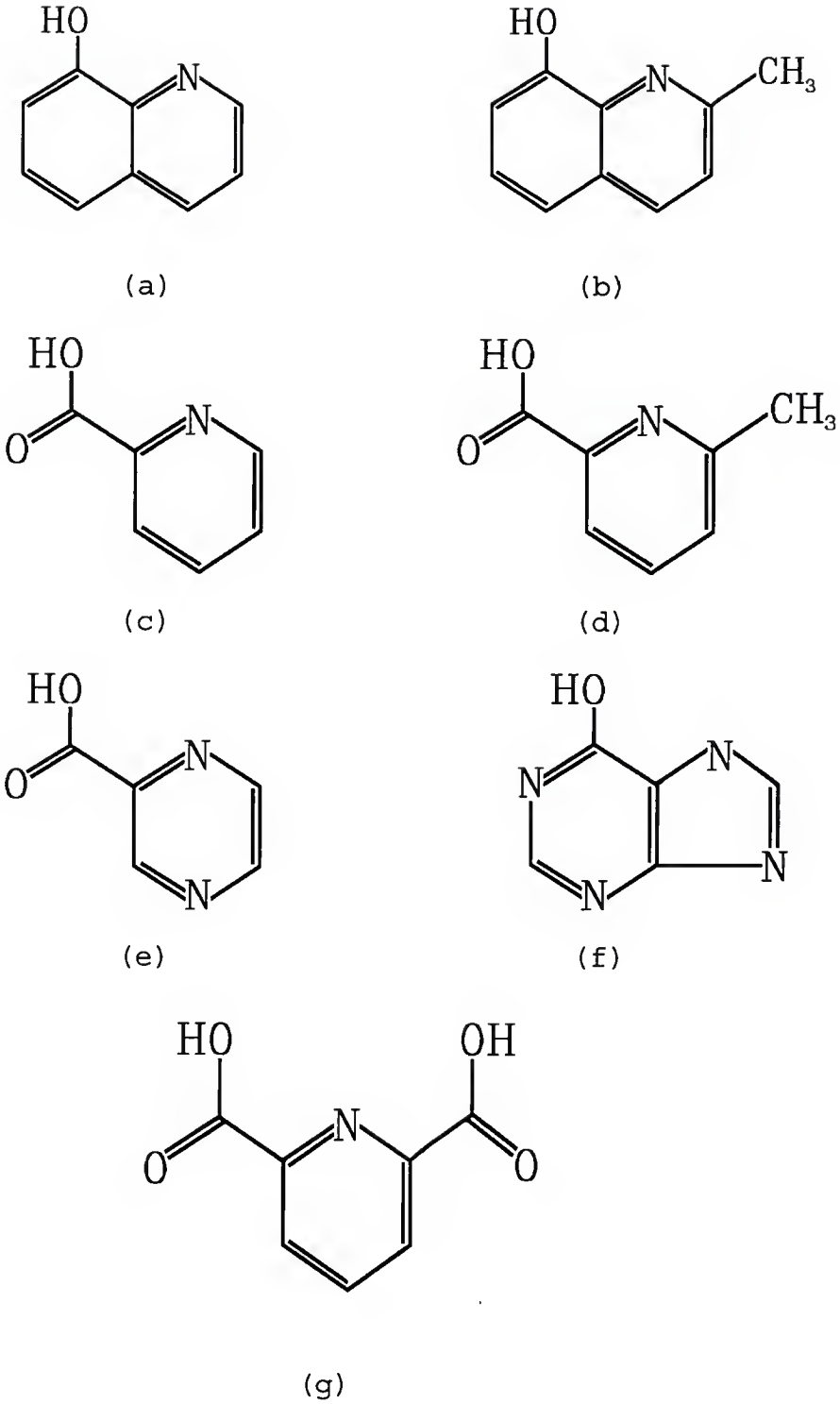

Figure 1-4. Ligands with O-C-C-N Donor Group.
a) Oxine; b) 2-Methyloxine; c) Picolinic acid;
d) 6-Methylpicolinic acid; e) Pyrazinoic acid;
f) Hypoxanthine; g) Dipicolinic acid

Picolinic acid is a naturally occurring compound that has been found bound to aluminum in human breast milk.[44] Picolinic acid is structurally similar to oxine, but without the second ring, the flexibility of the ligand would be greater. If an aluminum and picolinic acid complex could be formed and characterized, a comparison of Al-O and Al-N bond lengths could be made with the oxine compounds. This analysis could possibly determine if the nitrogen is coordinated to the aluminum ion or held close to the ion simply because of its location on the ring. 6-Methylpicolinic acid provides the same potential comparisons for picolinic acid as 2-methyloxine for oxine.

Pyrazinoic acid was chosen for its structural similarity to picolinic acid. However, because of the second nitrogen atom in the aromatic ring, the potential existed to have a greater water solubility for an aluminum complex.

Hypoxanthine is formed in the animal body during the breakdown of adenosine and nucleic acids. The two-ring structure is similar to oxine; however, there are two notable differences. First, there are three nitrogen atoms substituted for ring carbons. Second, and probably more important, is that one of the aromatic rings is a five membered ring instead of six. As a result, the ring strain should pull the nitrogen atom farther from the aluminum ion in a coordination compound.

A naturally occurring ligand, 2,6-pyridinedicarboxylic acid, has the potential to be an electron donor from the nitrogen as well as the two carboxylate oxygens. This molecule, also known by its common name dipicolinic acid, has been reported in a variety of compounds as a tridentate ligand.[45-51] Because dipicolinic acid has the potential to coordinate as a bidentate as well as a tridentate ligand, there is more than one possible mode of coordination. If only one of the carboxylate groups is deprotonated, then dipicolinic acid should act as a bidentate ligand. In a three-to-one ratio, the neutral tris complex could theoretically be formed. Another type of complex could be formed if both of the carboxylic acid groups on dipicolinic acid were deprotonated. Were this to occur, dipicolinate could act as a tridentate ligand by coordinating aluminum with a nitrogen and both oxygen atoms.

The details of the investigation into the aluminum complexes for these ligands are presented in the following chapters. In addition, three compounds without aluminum were inadvertently synthesized during this project. The structure determinations for these compounds is also included.

CHAPTER 2

SYNTHESIS AND CHARACTERIZATION OF ALUMINUM COORDINATION COMPOUNDS

Aluminum as a Lewis Acid

The only non-zero valence state available to aluminum is a positive three. Since it can attain a positive charge, the aluminum ion will readily accept electron pair donors and function as a Lewis acid. The trivalent aluminum ion has a rather small ionic radius of 0.50 Å.[10] As a result, the aluminum ion with a relatively high positive charge coupled with a small ionic radius can be classified as a hard Lewis acid.

In an aqueous solution of an aluminum salt, the metal ion will be surrounded by six water molecules, each of which donates an electron pair to the positive central ion. For a ligand to replace the water molecule and coordinate the metal ion, the complex formed by the exchange should be more stable. One possibility is for the electron donor atom to be a small atom, such as oxygen and nitrogen, and also have a stronger negative charge. An example would be a deprotonated hydroxyl group or carboxylate oxygen. With a negative charge, each of these ions would function as harder Lewis bases and more readily replace the water molecule. The other possibility for

creating a more stable complex is by the formation of one or more five- or six-membered rings by complexation of two or more functional groups belonging to the same donor molecule.

Most nitrogen donor atoms occur as the amine functional group, whether aromatic or aliphatic. In amines, the nitrogen atoms are more likely to become positively charged than negatively. As a result, even though a nitrogen atom can coordinate to an aluminum ion, the electrostatic attraction between the metal ion and an oxygen donor tends to be stronger and, therefore, forms more stable complexes.

Synthesis

The general technique for the synthesis of an aluminum complex involves the combination of a soluble aluminum salt, the ligand and a base. When the ligand is deprotonated, a negatively charged donor atom is created. If the anionic part of the ligand is a harder Lewis base than water, it is then capable of displacing the neutral water molecule. If the ligand can only carry one negative charge and this process is repeated two more times, a neutral aluminum species is formed. Such a non-charged species, especially with a shell of aromatic carbon and hydrogen atoms, will generally have a relatively low water solubility. Therefore, after a certain quantity of the complex is formed, it will begin to precipitate. The solid can then be collected by filtration, rinsed and dried. Depending upon solubility, the complex may

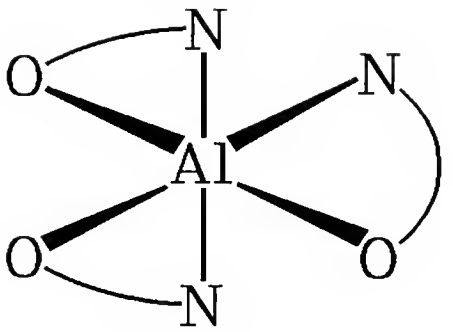

Figure 2-1. Representation of a Tris Complex between Aluminum and a Bidentate Ligand.

be dissolved in an appropriate solvent to be recrystallized. The specific techniques used to synthesize the complexes depend in part on the solubility and the acidity of the particular ligand.

Materials

All materials and solvents used were reagent grade and used as supplied by the manufacturer.

2-Methyloxine (meox)

Ligand reactivity. 8-Hydroxyquinaldine, represented here as meox, is soluble in organic solvents such as ethanol and dimethylsulfoxide (DMSO) but insoluble in water. With a pK_a of 10.1, meox is a rather weak acid that will require a moderately strong base for deprotonation.

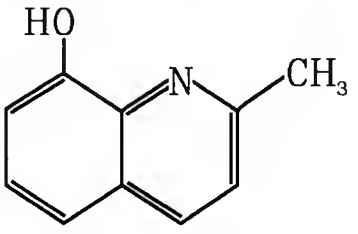

Figure 2-2. 2-Methyloxine, meox.

Preparation of $Al(meox)_3 \cdot CH_3OH \cdot H_2O$ (I). DMSO (39 mL) was placed in a 200 mL round bottom flask which was set in a 90°C oil bath to warm. $Al_2(SO_4)_3 \cdot 18\ H_2O$ (3.31 g, 10 mmole $Al(H_2O)_6^{3+}$) was added and dissolved by stirring. 2-Methyloxine (5.02 g, 32 mmole) was subsequently added to yield a dark amber solution. The solution was neutralized slowly by the addition of 0.5 mL portions of diethylamine (7.5 mL, 72 mmol). The resulting opaque mixture was stirred and heated for an additional 10 minutes and then cooled to room temperature. A dark amber solution (30 mL) was obtained by filtration through a fine glass frit. After two months, large brown crystalline clumps formed which were then redissolved in 15 mL methanol and covered to slowly recrystallize. In two months, small brown needles of diffraction quality were separated from the solution.

Oxine (ox)

Ligand reactivity. 8-Hydroxyquinoline, commonly referred to as oxine, has a similar solubility to meox. However, it is more acidic, with a pK_a of 9.0, and therefore, will be easier to deprotonate the hydroxyl group.

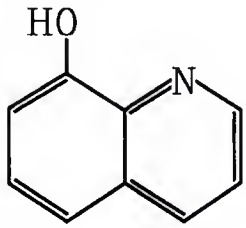

Figure 2-3. Oxine (ox).

Preparation of $Al(ox)_3 \cdot CH_3OH$ (**II**). To avoid the lengthy recrystallization required with **I**, the synthetic scheme was modified to exclude DMSO. $Al(NO_3)_3 \cdot 9H_2O$ (0.181 g, 0.5 mmole) was dissolved in 150 mL of H_2O. Oxine (0.220 g, 1.5 mmole) was added as a solid and slowly dissolved in the acidic aqueous solution to yield a pale yellow solution. The pH of the mixture was slowly raised by dropwise additions of NaOH until a very, thick yellow precipitate formed at pH = 5.2. The solid was collected by filtration and recrystallized from 95% ethanol. Diffraction quality crystals were obtained by recrystallization of the solid from the solution.

Picolinic Acid (pic)

Ligand reactivity. Picolinic acid is very soluble in water and ethanol, but insoluble in organic solvents such as ether. With a pK_a of 5.4, it functions as a moderately weak acid.

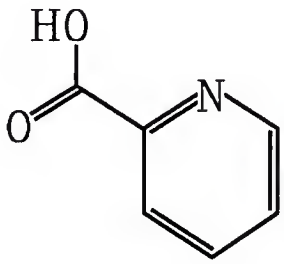

Figure 2-4. Picolinic acid (pic).

Preparation of Al/pic complex (**III**). $Al(NO_3)_3 \cdot 9H_2O$ (1.25 g, 3.33 mmole) was dissolved in 15 mL H_2O. In a separate beaker, pic (1.23 g, 10.0 mmole) was dissolved in 20 mL H_2O.

The solutions were combined to give a clear, colorless solution. $NaHCO_3$ was added slowly as a solid until a thick, white precipitate formed. The pH of the mixture measured 5.0. The result was identical for a concentrated solution of NaOH. The solid was collected by filtration through a glass frit, washed thoroughly with water and dried for further analysis.

6-Methylpicolinic acid (mpic)

Ligand reactivity. 6-Methylpicolinic acid has a solubility similar to picolinic acid. With a pK_a of 5.8, it is only a slightly weaker acid the picolinic acid.

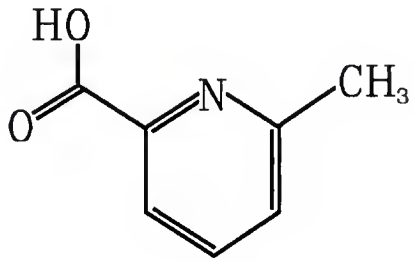

Figure 2-5. 6-Methylpicolinic acid (mpic).

Preparation of Al/mpic complex (**IV**). $Al(NO_3)_3 \cdot 9H_2O$ (1.24 g, 3.3 mmole) was dissolved in 15 mL H_2O. Mpic (1.37 g, 10.0 mmole) was dissolved in 20 mL H_2O to produce a pale beige solution. The solutions were combined to give a clear, almost colorless solution. $NaHCO_3$ was slowly added as a solid until a thick off-white precipitate formed. The pH of the resulting solution was 6.0. The solid was collected by filtration through a glass frit, washed thoroughly with H_2O and dried for further analysis.

Pyrazinoic acid (pza)

Ligand reactivity. Pyrazinoic acid is slightly soluble in hot water and ethanol and insoluble in organic solvents.

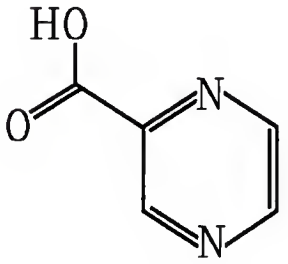

Figure 2-6. Pyrazinoic acid (pza).

Preparation of Al/pza complex (V). Pza (3.00 g, 24.2 mmole) was added to 100 mL H_2O but did not dissolve. In a separate beaker, $Al(NO_3)_3 \cdot 9H_2O$ (3.02 g, 8.05 mmole) was dissolved in 25 mL 95 % ethanol. The solutions were combined and stirred to yield a 125 mL clear and colorless solution with a white suspension. As $NaHCO_3$ (2.03 g, 24.2 mmole) was slowly added as a solid, the suspension disappeared and the mixture became a clear pale pink solution. When all the $NaHCO_3$ had been added, the clear pink solution had a pH of 5.0. Additional $NaHCO_3$ was added until a solid white precipitate formed. The pH of the opaque mixture measured 7.5. The solid was collected by filtration through a medium glass frit and washed thoroughly with water and hot ethanol. The solid was dried in a desiccator for further analysis.

Hypoxanthine (hyp)

Ligand reactivity. Hypoxanthine is not appreciably soluble in any solvent; however, it will react with acid or basic solutions to dissolve in water. It is a very weak acid with a pK_a of 12.

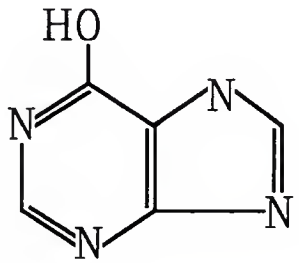

Figure 2-7. Hypoxanthine (hyp).

Preparation of Al/hyp complex (**VI**). Hyp (0.775 g, 5.69 mmole) was added to 80 mL of H_2O with stirring and heated to 80°C. This produced an opaque white solution in which the ligand settled quickly as a fine intensely white powder when not stirring. $Al(NO_3)_3 \cdot 9H_2O$ (0.712 g, 1.90 mmole) was dissolved in a separate 5 mL H_2O. The two solutions were combined to yield a mixture of pH 4.0. The temperature was maintained at 80°C. $NaHCO_3$ (0.482 g, 5.73 mmole) was slowly added as a solid. After addition of the base was complete, the pH of the mixture was 7.5. A large amount of white solid was still visible but only some settled to the bottom when stirring was stopped. A fluffy cream white solid remained suspended above the bottom of the beaker. The temperature was lowered to 60°C and the mixture continued to heat for one hour. Without stirring, only a small amount of white powder settled. The unstirred solution carefully filtered through a

medium frit. The white powder on the bottom of the beaker was discarded. The solid collected by filtration was washed thoroughly with water and dried in a desiccator for further analysis.

Dipicolinic acid (dipic)

Ligand reactivity. Dipicolinic acid is slightly soluble in hot water or ethanol and insoluble in all other solvents. It is a moderately strong acid with a pK_a of 2.2 for its first dissociation.

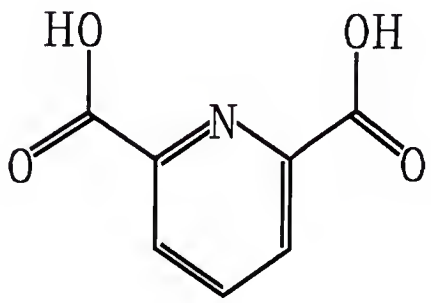

Figure 2-8. Dipicolinic acid (dipic).

Preparation of Al/dipic (**VII**). Dipic (4.00 g, 24.0 mmole) was added with stirring to 100 mL of H_2O at room temperature. $NaHCO_3$ (1.00 g, 11.9 mmole) was added as a solid to partially neutralize the ligand. After the solution was stirred for 20 minutes, the ligand dissolved to yield a clear, colorless solution. $Al(NO_3)_3 \cdot 9H_2O$ (2.99 g, 8.0 mmole) was added as a solid to the solution. After ten minutes, the pH measured 2.0 for the clear and colorless solution. Additional $NaHCO_3$ (3.02 g, 36.0 mmole) was added slowly to the mixture.

After addition of the $NaHCO_3$ was complete, the clear, colorless solution had a pH of 5.0. Within five minutes, the solution started to cloud. Five minutes later, the mixture consisted of an opaque white solid that would remain as a fluffy white suspension when not stirring. The mixture was allowed to stir at room temperature for three days. The solid was collected by vacuum filtration through a course glass frit, rinsed thoroughly with water followed by absolute ethanol and then dried for further analysis.

Solubility of Aluminum Compounds

After a complex has been synthesized, it can be purified by recrystallization. A pure compound would yield accurate and useful information from elemental and spectral analysis. In addition, with the growth of good quality crystals, the structure can be determined by x-ray diffraction techniques. Without the possibility of purifying the synthesized complex, characterization becomes extremely difficult.

Of the seven compounds synthesized, all are insoluble in water. Complexes **I** and **II** were sufficiently soluble in ethanol or methanol to be recrystallized. It was determined that the other compounds must not be the sodium salts of the ligands. When synthesized, the sodium salts were found to be very soluble in water. However, since the pure compounds could not be produced by recrystallization, various crystal growth techniques were employed to obtain pure compounds and

possibly good crystals. The discussion of crystal growth techniques is presented in detail in Chapter 3.

Methods of Characterization of Aluminum Complexes

There are several techniques that can be utilized to characterize an aluminum complex that has been synthesized. These methods include elemental analysis, Infra-red, Al-27 NMR and ICP emission spectroscopies, Fast Atom Bombardment Mass Spectrometry (FABMS) and x-ray diffraction techniques. The first three can be performed upon the insoluble compounds **III** through **VII**. ICP emission spectroscopy, FABMS and x-ray diffraction techniques require that the samples are soluble.

Elemental Analysis

Elemental analysis can be used to determine the percentage of all of the elements in a compound. CHN, which can be performed on solid samples, only determines the percentages of carbon, hydrogen and nitrogen. From these percentages, the ratios of the number of carbon to hydrogen to nitrogen atoms present in the compound can be calculated. Since hydrogen has a very low atomic weight, the percentages and ratios for this element have a large relative error. Therefore, the ratio of carbon atoms to nitrogen atoms provides the most valid numerical data. Since each ligand has a specific number of carbon and nitrogen atoms, the presence of an organic solvent molecule or an ammonium ion in a synthesized compound can easily be confirmed.

By determining the percent of carbon, hydrogen and nitrogen present, the total percent of the other elements, oxygen, aluminum and possibly sodium, can be calculated. Since each ligand has a specific number of oxygen atoms, the corresponding percentage of ligand oxygen can be calculated and then subtracted to yield the percentage accounting for the metal ion and the oxygen present as solvent molecules. The oxygen associated with water can not be accurately determined because of the uncertainty in the amount of hydrogen present. In addition, because the substitution of a sodium and two hydrogen atoms for an aluminum would only produce an error of 2 g/mole, is difficult to prove of disprove the presence of aluminum, as opposed to sodium, based on elemental analysis data.

Infra-red Spectroscopy

IR spectroscopy provides information about the strength, and therefore the length, of a bond. The C=O group in a carboxylic acid has a very strong stretch in the region 1760 to 1700 cm^{-1}.[52] If the acid is deprotonated to form a carboxylate anion, the carbonyl bond loses some of its double bond character due to the delocalization of the electron pair over both of the carboxylate oxygen atoms. As a result, the carbonyl bond strength decreases as the bond length increases. The stretching frequency of a longer bond is slower such that the stretching band shifts to a range of 1650 to 1550 cm^{-1}.[52] If a complex is formed involving the carboxylate group, the

bond length for the carbonyl group would probably be between that for the acid and the anion. Therefore, the carbonyl stretching frequency should lie between those of the unreacted ligand and its sodium salt.[53]

Aluminum-27 NMR Spectroscopy

Al-27 NMR is a technique used to probe into the environment of aluminum in its compounds. A peak will be present for each different aluminum atom. The shift of the peak is indicative of the geometry, symmetry and the type of atoms surrounding the metal center.

Most of the research reported for Al-27 NMR refers to exclusively oxygen atoms bonded to the aluminum and the shifts are referenced relative to $Al(H_2O)_6^{3+}$. Most of the octahedral AlO_6 groups have shifts very near 0 ppm, whereas the tetrahedral AlO_4 groups are shifted to near 80 ppm.[54] However, for an aluminophosphate, the shift of 41 ppm was attributed to the tetrahedral AlO_4 group in the compound.[55] Also, the Al-27 NMR shifts reported for the distorted octahedral environments in tris complexes of O,O bidentate ligands range from 36 to 41 ppm.[17,18] These shifts are in the same range as reported for some tetrahedral aluminum centers. Not all of the studies on coordination compounds have been performed on exclusively oxygen environments. The shift due to the octahedral environment in fluoroaluminates was reported to range from +1.4 to -13.2 ppm.[56] In addition, an Al-27 NMR study including hexacoordinate aluminum complexes formed with

aminopolycarboxylic acids reported that the chemical shifts range from 36.5 to 41.2 ppm.[57] For one of the acids, EDTA, the aluminum ion was determined by x-ray diffraction techniques to be in a distorted octahedral environment in $K[Al(EDTA)]\cdot 2H_2O$ coordinated to two nitrogen atoms and four oxygen atoms.[58] However, there have been a limited number of studies reported Al-27 NMR for the AlN_3O_3 centers produced by the formation of a tris complex with a N,O bidentate ligand. The shifts for the four similar complexes range from 8.1 to 11.4 ppm.[27] These complexes contained an O-C-C-C-N group instead of the O-C-C-N group present in each of the ligands in this study and had coordination spheres fairly close to the ideal octahedron.

ICP Emission Spectroscopy

ICP emission spectroscopy depends upon the emission of light at a specified wavelength after the aluminum ion has been excited in the plasma. The concentration of aluminum can be determined by comparing it to a calibration curve. If the mass of the complex per volume is accurately known for the test solution, then the molecular weight of the complex can be determined. All of the emission lines for aluminum are extremely weak and a rather high detection limit exists. Therefore, not only is a solution required but it must be relatively concentrated. This technique was not feasible to employ due to the very low solubility of the synthesized complexes.

Fast Atom Bombardment Mass Spectrometry

FABMS, a technique developed in the early 1980s, is used to study the composition of a compound. The method has proven useful for compounds of high molecular weight or low volatility and for polar molecules.[59] However, due to beam-induced reduction or inefficient fragmentation, there is a limit to its application.[60] In FABMS, the sample is excited by bombardment with high-energy atoms of either xenon or argon, instead of the more traditional beam of high-energy electrons.[59] The charged molecules and fragments are then separated by the use of a magnetic field. The data that can be extracted include the molecular mass, or masses if the sample is a mixture, and structural hints from the masses of the fragments. Because of the low solubility of the samples, the usefulness of this technique is limited.

X-ray Diffraction Techniques

Also known as x-ray crystallography, this method is used to determine the location and type of each atom present in the complex. The data required are collected by passing an x-ray beam through a single crystal and measuring the intensity and the angle of each diffracted beam relative to the incident beam. The diffractions are caused by the electrons around each atom scattering the x-ray beam. After preliminary calculations, a test structure is proposed. The diffraction pattern that would be produced by the test structure is

compared to the actual pattern and refinements are made to the test structure until the best match is obtained.[61]

Since the x-ray beam is diffracted by each atom's electrons, two atoms with the same number of electrons would diffract the beam in almost the same manner. For example, an aluminum ion and a sodium ion would be difficult, but not impossible, to differentiate. The structure should refine better with the correct atom.

The greatest disadvantage to x-ray diffraction techniques is the requirement of a single crystal approximately 0.1 to 0.3 mm in each dimension. In the absence of a suitable crystal, this technique cannot be employed to determine the structure of a complex.

CHAPTER 3

CRYSTAL GROWTH TECHNIQUES UTILIZED TO PRODUCE SINGLE CRYSTALS SUITABLE FOR USE IN X-RAY DIFFRACTION STUDIES

Introduction

In order to characterize a compound by x-ray crystallography, a single good crystal approximately 0.2 mm in a dimension is required.[61] When a suitable solvent is available, crystals can be grown by slow evaporation of a saturated solution of the compound. If a complex is not soluble, a variety of crystal growth techniques can be employed.[61] The concept used in many methods involves controlling the rate of reaction so that suitable crystals are produced as the compound is formed. In this study, the rate of reaction depends upon the availability of the aluminum ion, the ligand and the base and the strength of the base. The techniques discussed in this chapter include urea decomposition, vapor and aqueous gel diffusion, variation of the solvent system and the base strength.

Urea Decomposition

Theory

Urea decomposes into two molecules of ammonia and one carbon dioxide when it reacts with water. The relatively slow

reaction rate is increased by heat or a large concentration of acid or base. Since urea is very water soluble, it is easily dissolved in a dilute aqueous solution of an aluminum salt and the ligand.

Experimental

Solutions with a three-to-one molar ratio of ligand to aluminum ion were prepared by dissolving the 1.0 and 0.3 mmoles of the ligand and $Al(NO_3)_3 \cdot 9H_2O$, respectively, in 30 mL of water. The ligands tested were pic, mpic, dipic, pza and hyp. Upon gentle heating, 43 to 45°C, ammonia, as well as carbon dioxide bubbles, was gradually produced throughout the solution and the compound was formed.

Results

For each ligand, the crystals that formed were neither large nor of high quality. There was a very large incidence of twinned crystals and inseparable clusters of crystalline product, possibly as a result of the higher temperature.

Vapor Diffusion

Theory

One common technique to control the availability of the reactants is through diffusion.[61,62] By allowing the reactants to only slowly combine, the reaction proceeds at a slower rate than the formal concentrations would normally predict. As a result larger crystals are generally produced. For vapor phase diffusion, a gaseous reactant is slowly incorporated

into the other reactants, usually confined to an aqueous phase.

Experimental

Ammonia is a fairly volatile gas as well as a moderate base. Because of its volatility, it can slowly be absorbed into a solution of the aluminum ion and the ligand. An ammonia chamber was created by sealing a large beaker containing two small beakers or vials. One of the beakers contains an aqueous ammonia solution and the other contains the rest of the reactants. After sealing, the chamber becomes saturated with ammonia vapor which diffuses into the acidic aluminum ion and ligand solution. The solutions for the vapor diffusion experiments were prepared by dissolving the ligand and $Al(NO_3)_3 \cdot 9H_2O$ in water as depicted in Table 3-1.

Results

After several days, a crystalline product began to form in each experiment indicated. However, either the crystals were too small or in inseparable clusters. The ammonia reacted immediately upon contact with the surface of the solution. Instead of single large crystals growing, clusters formed and clung to the surface. The only single crystals discovered were on the bottom of the beaker. Apparently, as these single crystals grew, they became too heavy to be supported by the surface tension of the solution and sank to the bottom of the beaker. The clusters which continued to grow on the surface probably did not sink to the bottom of the

Table 3-1. Vapor Diffusion Experimental Conditions and Results.

Ligand	[ligand], M	[Al^{3+}], M	Result
pic	0.010	0.010	no solid
	0.020	0.010	crystalline
	0.030	0.010	crystalline
	0.045	0.015	crystalline
mpic	0.010	0.010	no solid
	0.020	0.010	no solid
	0.030	0.010	crystalline
	0.045	0.015	crystalline
dipic	0.016	0.008	crystalline
pza	0.010	0.033	crystalline

beaker because of the increased surface tension created by the irregular surface. Once a single crystal sank to the bottom, it did not grow any larger because the crystal growth only occurred at the interface. Because of these limitations, vapor diffusion is not an effective crystal growth technique for the compounds under investigation.

Gel Diffusion

Theory

Vapor diffusion is limited because the reaction is dependent upon the diffusion in only one direction. In addition, the rates of diffusion through air and aqueous solutions are fairly rapid. Diffusion of water soluble compounds through an aqueous gel matrix is much slower.

Because diffusion is slower, a concentration gradient is produced over the distance from the interface.[62] Also, the semisolid gel is strong enough to support the crystals once they form and flexible enough to not restrict growth as the crystals enlarge. Aqueous gel diffusion is particularly suited for these syntheses because the reactants are water soluble and the products are insoluble. In addition, the technique is regarded as a good method for the production of large single crystals.[62]

Experimental

The agar gel used in the experiments was prepared by dissolving the prescribed percentage of agar by weight in water and heating to 98°C. The solution was allowed to boil at this temperature for 5 minutes and then cooled. Reagents added to the agar were first dissolved in the minimum amount of water and then completely mixed into the agar solution before it hardened. The agar was poured into a large vial with a screw top to ensure minimal solvent loss. To provide a consistent reaction interface, any air bubbles were removed using a disposable pipette before the agar set. Experiments performed and results obtained are summarized in Table 3-2.

Results

A crystalline product was produced in most of the experiments. The exceptions were when a white band was produced in every case using hyp and twice with mpic. The white band indicates that either very fine crystals formed or

Table 3-2. Gel Diffusion Experimental Conditions and Results.

Bottom layer	Top layer	Ligand	Results
0.010 M Al^{3+} in 1% agar	0.030 M solution of the sodium salt of the ligand	pic	twins
		mpic	white band
		dipic	small crystals
		pza	fine crystals
		hyp	white band
0.010 M sodium salt of ligand in 0.5% agar	Single $Al(NO_3)_3 \cdot 9H_2O$ crystal	mpic	white band
		pza	flower-like
		hyp	white band
0.1 mM NaOH in 1% agar and a thin layer of pure agar on top	Aqueous solution of 0.03 M Al^{3+} and 0.10 M of the ligand	pic	twinned
		mpic	small crystals
		dipic	small crystals
		pza	flower-like
		hyp	white band
1.0 mM $NaHCO_3$ in 0.5% agar	Aqueous solution of 0.006 M Al^{3+} and 0.020 M of the ligand	pic	small crystals
		mpic	small crystals
		dipic	good crystals*
		pza	flower-like
0.10 M pic and 0.03 M Al^{3+} in 1% agar	0.10 M solution sodium acetate	pic	twinned and double-twinned crystals
0.10 M pic and 0.03 M Al^{3+} in 1% agar	0.10 M solution sodium acetate	pic	twinned and double-twinned crystals

* See Chapter 8 for structure

only $Al(OH)_3$ was produced. Although most of the products were crystalline, only one experiment yielded single crystals of the size and quality required for x-ray diffraction studies. The structure for this compound is presented in Chapter 6.

All of the trials with picolinic acid gave similar results. Large crystals were produced, however, all of these were either twinned or double-twinned. Twinned crystals are formed when two crystals grow together along a common face, frequently producing a mirrored effect. Because the lattice pattern in a twin may not be constant throughout the sample, the x-rays would probably be diffracted differently than they would in a single crystal of the same compound. As a result, twinned crystals are not usually suitable for x-ray diffraction studies.[61] Pyrazinoic acid consistently produced fairly large crystalline structures that were flower-like in appearance. Examination with a microscope revealed that each had the four striated branches arranged in a tetrahedral orientation around a central point. Although they were large enough, the crystalline products were not single crystals. The other crystals formed in the experiments were too small to be useful for x-ray crystallography.

Base Strength

Theory

The syntheses discussed utilized moderately strong bases that are stronger than needed to deprotonate the ligands. In

the presence of either a weak base or a low concentration of a moderate base, the reaction should proceed slowly. In addition, if the conjugate acid formed from the base is volatile, the equilibrium will constantly shift towards the products as the gaseous product evaporates. Furthermore, because the chemical species present can alter crystal growth, the production of twinned crystals and flower-like clusters might not occur.

Experimental

Unless otherwise specified, the aluminum salt used was $Al(NO_3)_3 \cdot 9H_2O$. All reactions were performed in aqueous systems and the ligand to aluminum ion ratio was three-to-one. The specific quantities and compounds used in the reaction are shown in Table 3-3.

Results

No suitable crystals were formed except for the $KAl(SO_4)_2 \cdot 12H_2O$ reactant. However, the reactivity of the ligands can be studied. The sulfate ion, with K_b of 8.3×10^{-13}, is too weakly basic to react to produce an aluminum compound. The acetate ion, with a K_b of 5.6×10^{-10}, was basic enough to produce a crystalline product except for hypoxanthine, which is a very weak acid. Although the reactions did proceed slower than with the concentrated bicarbonate ion as the base, single large crystals were not produced. The brown solution produced in the reaction with hypoxanthine was probably due to the ligand decomposing into a mixture of smaller amines.

Table 3-3. Base Variation Experimental Conditions and Results.

Ligand	Base	Time	Results
0.40 M pic	0.27 M SO_4^{2-} from $KAl(SO_4)_2$	overnight	$KAl(SO_4)_2 \cdot 12H_2O$ crystals formed
0.10 M pic	0.10 M $NaC_2H_3O_2$	10 min	fine crystals
0.10 M pic	0.077 M $NaC_2H_3O_2$	20 min	fine crystals
0.10 M pic	0.070 M $NaC_2H_3O_2$	30 min	small crystals
7.5 mM pic	7.5 mM $NaC_2H_3O_2$	1 week	no solid product
50 mM pic	2 M $NaC_2H_3O_2$ and 9 M $HC_2H_3O_2$		no solid product
14 mM pic	14 mM $NH_4C_2H_3O_2$	overnight	twinned crystals
11 mM pic	0.44 M $NH_4C_2H_3O_2$ and .07 M $HC_2H_3O_2$ in 50 % acetone		no solid product
20 mM pic	20 mM $NaHCO_3$	30 min	twinned crystals
14 mM pic	14 mM $NaHCO_3$	2 hours	twinned crystals
7.5 mM pic	7.5 mM $NaHCO_3$	overnight	powdery solid
0.30 M pic	0.30 M pyridine	2 min	powdery solid
0.15 M pic	0.018 M pyridine	overnight	crystalline
15 mM dipic	7.5 mM SO_4^{2-} from $Al_2(SO_4)_3 \cdot 18H_2O$		no solid product pH rose from 1.5 to 4.5 overnight
8.3 mM dipic	8.3 mM $NaC_2H_3O_2$	3 days	small crystals
15 mM pza	7.5 mM SO_4^{2-} from $Al_2(SO_4)_2 \cdot 18H_2O$		no solid product
6.4 mM pza	7.7 mM $NaC_2H_3O_2$	overnight	flower-like clusters
11 mM hyp	0.44 M $NH_4C_2H_3O_2$ and .07 M $HC_2H_3O_2$ in 50 % acetone	2 weeks	brown solution, no solid product

Solvent System

Theory

When a crystal forms, occasionally solvent molecules are incorporated to fill a space produced by the packing arrangement. When a different solvent is used, the size and shape of the new solvent may cause the molecules to pack in a different manner. A possible result would be for the crystals to grow differently. Crystallization in a series of solvents is a common technique for the production of diffraction quality crystals.[61]

Experimental

All syntheses were performed with a three-to-one ligand to aluminum ion ratio. Unless otherwise noted, the concentration of the ligand is equivalent to the concentration of the base. The source of the aluminum ion was $Al(NO_3)_3 \cdot 9H_2O$. The experimental conditions and results are presented in Table 3-4.

Results

Experiments performed in methyl or ethyl alcohol did not produce a compound other than the sodium salt of the ligand unless a substantial amount of water was present. However, in the presence of water, pic and pza produce characteristic unsuitable crystal forms. In DMSO, pic and pza both produced a white solid that when heated to 100°C to remove water, a clear but brightly colored solution was formed. It is possible that the solution's color was due to a decomposition

Table 3-4. Experimental Conditions for Crystal Growth in Various Solvents and Results.

Solvent	Base	Ligand	Notes
CH_3OH	0.10 M NaOH	pic	65°C, no solid product
CH_3OH	0.10 M $NaHCO_3$	pic	50°C, no solid product
C_2H_5OH	0.15 M NaOH	pic	60°C, no solid product
C_2H_5OH	0.030 M $NaHCO_3$	pic	40°C, no solid product
C_2H_5OH	0.033 M $NaHCO_3$	pic	50°C, sodium picolinate precipitated
75% C_2H_5OH	0.15 M $NaHCO_3$	pic	overnight, twinned crystals at room temp
50% C_2H_5OH	0.15 M $NaHCO_3$	pic	opaque solution within 30 minutes at room temp
25% C_2H_5OH	0.15 M $NaHCO_3$	pic	opaque solution within 5 minutes at room temp
C_2H_5OH	7 mM $NH_4C_2H_3O_2$	pic	room temp, no solid
$HOCH_2CH_2OH$	0.15 M $NaHCO_3$	pic	45°C, no solid product
DMSO	0.53 M $NaHCO_3$	pic	white solid formed; when heated to 100°C, formed a clear peach solution, no solid ppt
C_2H_5OH	0.045 M NaOH	pza	60°C, no solid product
C_2H_5OH	0.034 M NaOH	pza	40°C, no solid product
C_2H_5OH	5 mM $NaHCO_3$	pza	overnight at 50°C, flower-like clusters
DMSO	0.53 M $NaHCO_3$	pza	white solid formed; when heated to 100°C, formed a clear bright yellow solution, no solid remained
C_2H_5OH	0.093 M NaOH	4.7 mM dipic	45°C, sodium salt of dipicolinic acid formed

product because the sodium salts of pic and pza produced the same results when heated to 100°C in DMSO. In addition, no solid remained after the evaporation of the heated DMSO reaction mixture.

Aluminum Isopropoxide

Theory

Used in the Meerwein-Ponndorf-Verley reduction, aluminum isopropoxide, $Al(OC_3H_7)_3$, could provide an alternative aluminum reagent for a synthesis in a non-aqueous environment.[63] In theory, in the presence of a ligand with a hydroxyl group, one of the isopropoxide groups could exchange with the ligand to form free isopropyl alcohol. Removal of the isopropanol by evaporation or distillation should drive the reaction towards completion. This would produce a coordination compound synthesized in the absence of water.

Experimental

In a glove bag flushed with nitrogen gas, aluminum isopropoxide (0.80 g, 3.9 mmole) was transferred to a dried weighing bottle. Pyrazinoic acid (0.52 g, 4.2 mmole) was added as a solid. Isopropyl alcohol was dried over anhydrous $CaSO_4$ and 20 mL was added to the solids. The bottle was capped and transferred to a desiccator. After five days, a white solid, which had formed on the bottom of the bottle, was collected by filtration. Comparable experiments were

performed for pic and mpic, however, no solid was produced in either experiment.

With no effort to exclude atmospheric water, preweighed aluminum isopropoxide (2.6 g, 12 mmole) was stirred in 30 mL of isopropyl alcohol. Approximately 25 mL of a viscous solution was collected after the mixture was centrifuged to remove any solid. Picolinic acid (1.3 g, 11 mmole) was dissolved in 20 mL of isopropyl alcohol. The solutions were combined and within 30 minutes, the mixture began to cloud. After 24 hours, the solution was filtered, the solid washed with isopropanol and tested for solubility. A similar experiment was performed for pza with solid formation being instantaneous.

Results

The solids formed using aluminum isopropoxide were non-crystalline. Furthermore, the products were not soluble in any solvent and therefore could not be recrystallized.

Summary of Results

Although crystalline solids of the various complexes can be readily formed using a variety of techniques, good single crystals are very difficult to produce. Since the compounds with pic and pza formed the same crystal forms under a variety of conditions, it seems that packing of the molecules within the crystal could be the cause. A probable conclusion would

be that x-ray quality crystals may never be grown for these compounds.

CHAPTER 4

SYNTHESIS, STRUCTURE AND AL-27 NMR STUDIES OF COMPLEXES WITH OXINE AND 2-METHYLOXINE

Introduction

Oxine(ox) and 2-methyloxine(meox), shown in Figure 4-1, contain the same N,O donor group. Oxine has been extensively

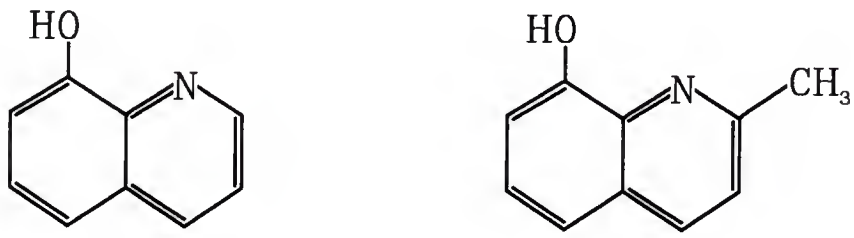

Figure 4-1. Oxine, left; 2-Methyloxine, right.

studied for uses as a complexing agent for the quantitative analysis of metal ions.[64] The crystal structure of the tris(oxinato)aluminum(III) with an occluded acetonylacetone molecule was reported in a 1980 abstract as a distorted octahedron with a meridional conformation.[30] Two more recent investigations confirm the structure of a tris complex between the Al(III) ion and oxine.[25,31] A drawing of the complex is given in Figure 4-2.[31] 2-Methyloxine differs from oxine by the substitution of a methyl group for the hydrogen alpha to the nitrogen atom. The location of the methyl group could produce

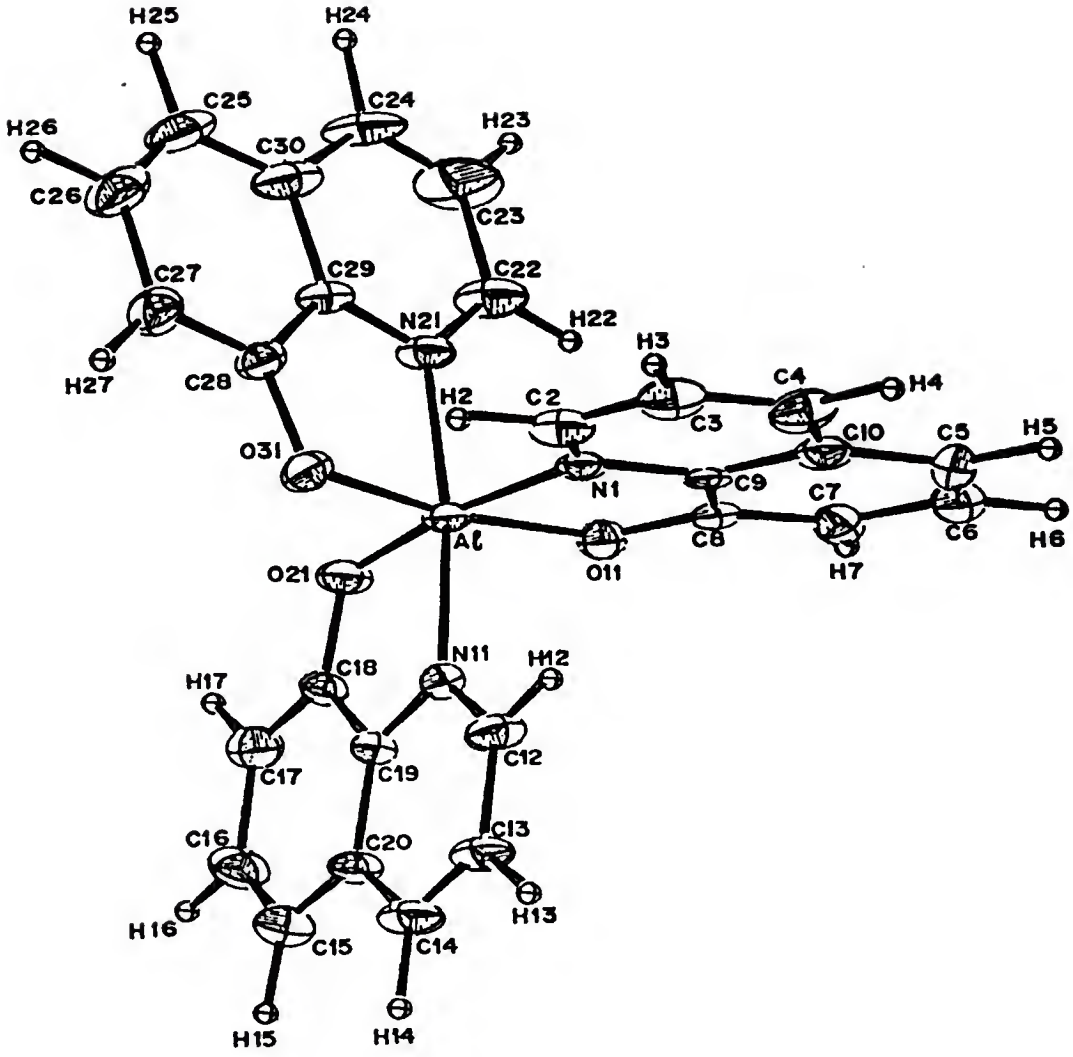

Figure 4-2. ORTEP Drawing of the Tris(oxinato)aluminum(III) without the Occluded Acetonylacetone. Ul-Haque, Horne, and Lyle, *J. Cryst. Spec. Res.*, **1991**, *21*, 411-417.

steric strain and interfere with the nitrogen coordination to a metal ion. The only complex involving aluminum(III) and 2-methyloxine that has been characterized by x-ray crystallography seems to reinforce the steric argument. As

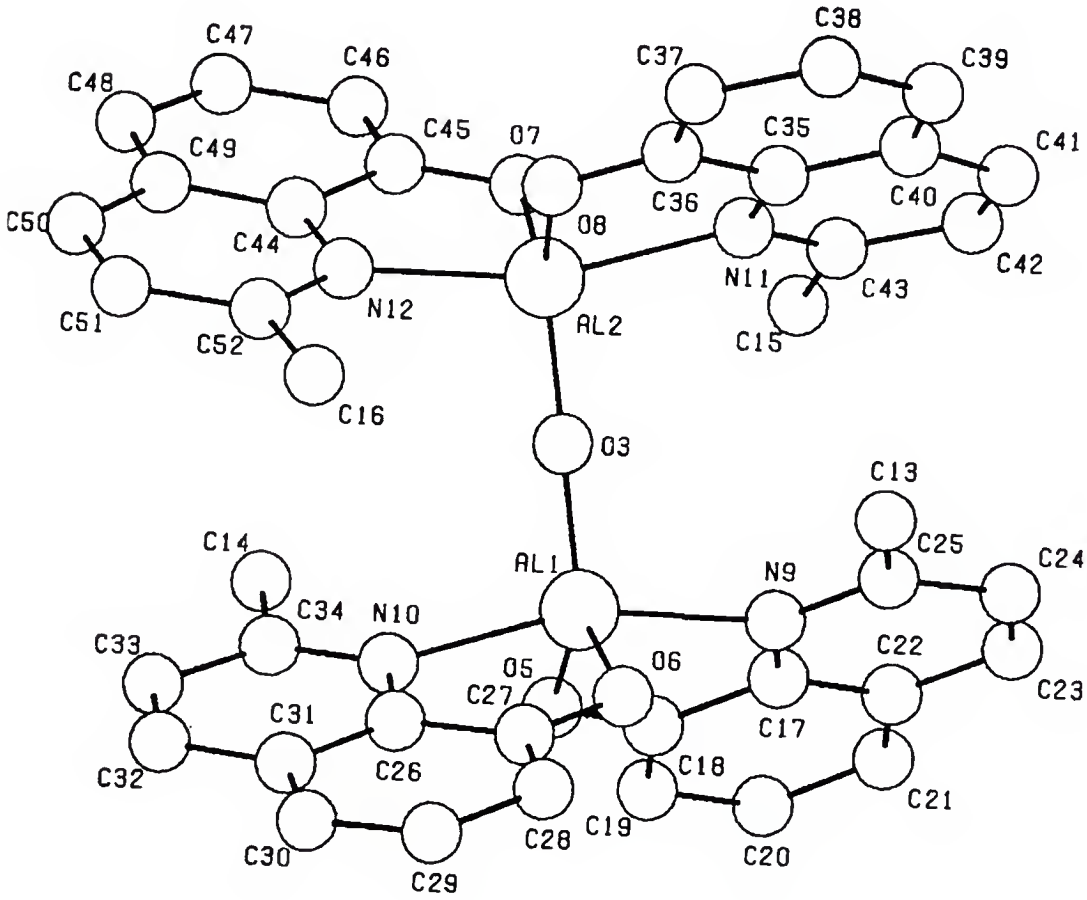

Figure 4-3. PLUTO Line Drawing of the μ-Oxo-di(bis(2-methyloxinato)aluminum(III) Complex. Kushi and Fernando, *Journal of the American Chemical Society*, **1970**, *92*, 91-95.

shown in Figure 4-3, the aluminum ion in μ-oxo-di(bis(2-methyloxinato)-aluminum(III)) is five coordinate with only two 2-methyloxine ligands each.[32]

The synthesis and characterization using x-ray diffraction techniques of the tris complex $Al(meox)_3$, as well as $Al(ox)_3$, are presented in this chapter. An ORTEP drawing of each is included to display the distorted octahedral environment around each aluminum ion. In addition, the results of the Al-27 NMR analysis, including spectra, are discussed for each complex.

Experimental

Synthesis

Materials. All materials and solvents were reagent grade and used as supplied from manufacturer.

Preparation of $Al(meox)_3 \cdot CH_3OH \cdot H_2O$ (I). DMSO (39 mL) was placed in a 200 mL round bottom flask which was set in a 90°C oil bath to warm. $Al_2(SO_4)_3 \cdot 18\ H_2O$ (3.31 g, 10 mmole $Al(H_2O)_6^{3+}$) was added and dissolved by stirring. 2-Methyloxine (5.02 g, 32 mmole) was subsequently added to yield a dark amber solution. The solution was neutralized slowly by the addition of 0.5 mL portions of diethylamine (7.5 mL, 72 mmol). The resulting opaque mixture was stirred and heated for an additional 10 minutes and then cooled to room temperature. A dark amber solution (30 mL) was obtained by filtration through a fine glass frit. After two months, large brown crystalline

clumps formed which were then redissolved in 15 mL methanol and covered to slowly recrystallize. In two months, small brown needles of diffraction quality were separated from the solution.

Preparation of $Al(ox)_3 \cdot CH_3OH$ (**II**). To avoid the lengthy recrystallization required with **I**, the synthetic scheme was modified to exclude DMSO. $Al(NO_3)_3 \cdot 9H_2O$ (0.181 g, 0.5 mmole) was dissolved in 150 mL of H_2O. Oxine (0.220 g, 1.5 mmole) was added as a solid and slowly dissolved in the acidic aqueous solution to yield a pale yellow solution. The pH of the mixture was slowly raised by dropwise additions of NaOH until a very, thick yellow precipitate formed at pH = 5.2. The solid was collected by filtration and recrystallized from 95% ethanol. Diffraction quality crystals were obtained by recrystallization of the solid from the solution.

Aluminum-27 NMR Spectroscopy

Preparation of $Al(meox)_3$ (**Ia**). 2-Methyloxine (4.81 g, 30.2 mmole) was added to 200 mL H_2O. NaOH (1.21 g, 30.2 mmole) was added to dissolve the ligand. $Al(NO_3)_3 \cdot 9H_2O$ (3.79 g, 10.1 mmole) was dissolved in 50 mL H_2O and added dropwise to the clear brown solution to form a thick yellow precipitate. After complete addition, the mixture was stirred for 10 minutes. The solid was collected by filtration through a glass frit, washed thoroughly with H_2O and absolute C_2H_5OH and dried. Elemental analysis: 69.79 % C, 4.70 % H, 8.12 % N

for Ia. 69.36 % C, 5.04 % H, 8.09 % N for $Al(meox)_3 \cdot H_2O$. Submitted for Al-27 NMR analysis.

Preparation of $Al(ox)_3$ (**IIa**). Oxine (4.51 g, 31.1 mmole) dissolved in 50 mL 100% C_2H_5OH to give dark amber solution. $Al(NO_3)_3 \cdot 9H_2O$ (3.81 g, 10.2 mmole) was added to mixture with stirring and a thick yellow precipitate formed. NaOH solution was added until reaction cleared and then reformed a precipitate. The bright yellow solid was collected by filtration, washed thoroughly with H_2O and C_2H_5OH, and dried. Elemental analysis: 68.02 % C, 4.62 % H, 8.06 % N for IIa. 68.91 % C, 4.79 % H, 8.31 % N for $Al(ox)_3 \cdot C_2H_5OH$. Submitted for Al-27 NMR analysis.

Preparation of saturated $Al(ox)_3 \cdot C_2H_5OH$ solution (**IIb**). **IIa** (0.5 g, 1 mmole) was added to 350 mL 100% C_2H_5OH and stirred at room temperature for 1 hour. A bright yellow solution was collected by filtration through a glass frit and evaporated slowly to yield 50 mL of a dark orange solution. Recrystallization of a small fraction yielded exclusively one crystal form of fluorescent yellow crystals, confirmed by X-ray crystallography to be $Al(ox)_3 \cdot C_2H_5OH$. The solution was submitted for Al-27 NMR analysis.

Al-27 NMR spectral analysis. Al-27 NMR spectra were collected on a NT-300 NMR spectrometer with spectrometer frequency 78.176839 MHz. The samples were spun at the magic angle at rates of 1.4 and 2.05 kHz for **Ia** and **IIa**, respectively.

X-ray Crystallographic Analysis

X-ray diffraction study of **I**. A needle shaped crystal having the dimensions 0.22 × 0.16 × 0.14 mm was mounted on a glass fiber for diffraction studies. All subsequent data were collected on a Nicolet P3 Diffractometer, using filter-monochromated Cu Kα radiation for **I**. The unit cell dimensions were determined for 25 automatically centered reflections; space group tetragonal P4/n by intensity statistics and satisfactory structure solution and refinement; 2020 unique reflections, 1945 with $I>3\sigma(I)$; $0\leq h\leq 10$, $0\leq k\leq 10$, $0\leq l\leq 10$. Two intensity standards, which were measured every 98 reflections, showed no change during data collection. The program used for F_{obs} refinement was SHELXTL Revision 5.1 (Sheldrick, 1985) All non-hydrogen atoms were located from an E-map. Twenty of the thirty hydrogen atoms were located using a difference Fourier map. Final refinement values for 361 parameters were R = 8.67, wR = 10.67 and w = 9.07. Calculations and figures were performed on an Eclipse Model 30 desktop computer. Atomic scattering factors used in the SHELXTL program are the analytical form given in *International Tables for X-ray Crystallography* (1974).

X-ray diffraction study of **II**. Method and instrumentation used to solve the X-ray structure of **II** were the same as above with the following exceptions. A tabular crystal having the dimensions 0.32 × 0.32 × 0.10 mm was mounted. The data were collected using graphite-monochromated

Mo Kα radiation. The unit cell dimensions were determined for 17 automatically center reflections, $1.0° \leq 2\theta \leq 30.0°$; space group monoclinic $P2_1/n$; 1421 unique reflections, 1062 with $I > 3\sigma(I)$, $0 \leq h \leq 8$, $0 \leq k \leq 10$, $-13 \leq l \leq 13$. Eighteen of the twenty-two hydrogen atoms were located using a difference Fourier map. Final refinement values for 325 parameters were R = 9.18, wR = 7.15 and w = 7.13.

Discussion

X-ray diffraction analysis

Crystallographic data for each complex is summarized in Table 4-1.

$Al(meox)_3 \cdot CH_3OH \cdot H_2O$ (I). An ORTEP drawing of the $Al(meox)_3$ molecule is given in Figure 4-4. Final atomic coordinates for all non-hydrogen atoms and all hydrogen atoms found, bond lengths and bond angles appear in Tables 4-2 through 4-5, respectively. The anisotropic thermal parameters are listed in Table 4-6.

Despite the presence of the sterically hindering methyl group adjacent to the nitrogen atom, the aluminum ion is definitely coordinated to the nitrogen and oxygen atoms of three 2-methyloxine ligands. The Al-N bond distances in **I**, ranging from 2.122 to 2.179 Å, correspond well with the relatively long Al-N bond distance of 2.18 Å reported for $H_3Al \cdot 2N(CH_3)_3$.[65] However, the Al-N bonds in **I** are significantly longer than the Al-N bonds in μ-oxo-di(bis(2-methyloxinato)

Table 4-1. Crystallographic Data for **I** and **II**.

	I	**II**
Complex	$Al(meox)_3 \cdot CH_3OH \cdot H_2O$	$Al(ox)_3 \cdot CH_3OH$
Formula	$AlC_{31}H_{30}N_3O_5$	$AlC_{28}H_{22}N_3O_4$
MW	551.55	491.48
Crystal system	Tetragonal	Monoclinic
Space Group	P4/n	$P2_1/n$
a, Å	22.1970	10.8620
b, Å	22.1970	13.2381
c, Å	11.1804	16.8528
β, °	90.000	97.511
V_c, Å^3	5508.6	2402.5
Z	8	4
D_{calc}, g/cm^3	1.33	1.36
Radiation	Cu Kα	Mo Kα
λ, Å	1.54178	0.71069
μ cm^{-1}	8.95	4.49
F(000)	2095.61	951.81
Crystal dimensions	0.22 × 0.16 × 0.14	0.32 × 0.32 × 0.10
2θ	0.0, 100.0	1.0, 30.0
Observed reflections	2020	1421
Collected reflections	1945	1062
Number of parameters	361	325
Final *R*	0.0867	0.0918
R_w	0.1067	0.0715

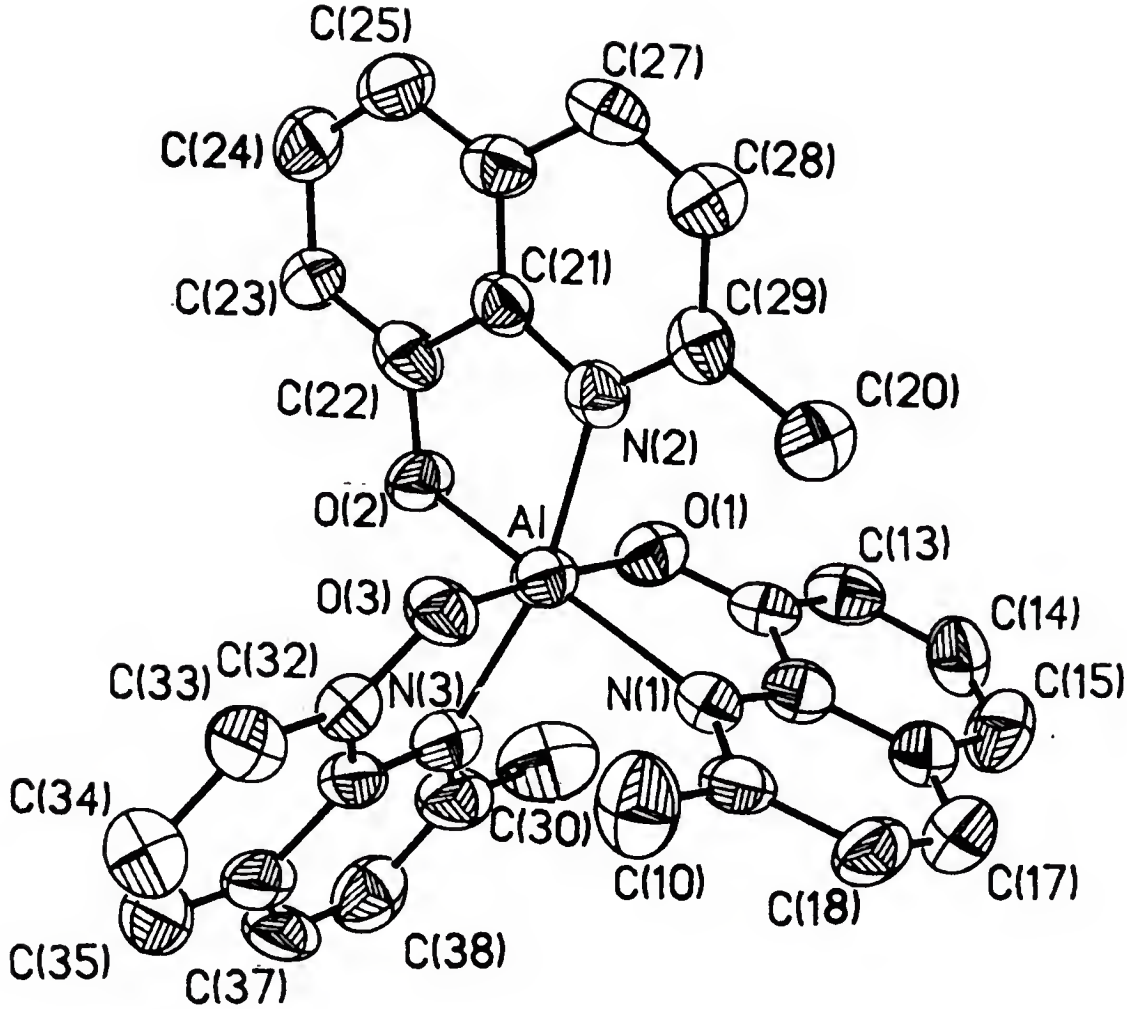

Figure 4-4. ORTEP Drawing of the Al(meox)$_3$ Molecule Showing the Atomic Numbering Scheme and the Thermal Ellipsoids.

Table 4-2. Final Atomic Coordinates ($\times 10^4$) and Isotopic Thermal Parameters ($Å^2 \times 10^3$) for **I**. Estimated Standard Deviations are given in Parentheses.

	x	y	z	U
Al	0.8192 (1)	0.4832 (1)	0.1185 (2)	46 (1)
O(1)	0.8291 (2)	0.5569 (2)	0.0533 (5)	57 (2)
N(1)	0.7596 (3)	0.4725 (3)	-0.0348 (5)	48 (2)
C(11)	0.7611 (4)	0.5262 (4)	-0.0956 (7)	50 (3)
C(12)	0.7996 (3)	0.5700 (4)	-0.0488 (8)	52 (3)
C(13)	0.8048 (4)	0.6254 (4)	-0.1064 (8)	60 (4)
C(14)	0.7716 (4)	0.6351 (5)	-0.2123 (8)	75 (4)
C(15)	0.7360 (4)	0.5926 (4)	-0.2612 (8)	72 (4)
C(16)	0.7295 (4)	0.5362 (4)	-0.2054 (7)	56 (3)
C(17)	0.6956 (4)	0.4883 (5)	-0.2484 (8)	68 (4)
C(18)	0.6939 (4)	0.4347 (4)	-0.1891 (8)	58 (3)
C(19)	0.7251 (3)	0.4276 (4)	-0.0781 (7)	50 (3)
C(10)	0.7220 (4)	0.3667 (4)	-0.0192 (8)	78 (4)
O(2)	0.8687 (2)	0.5023 (2)	0.2471 (4)	51 (2)
N(2)	0.9011 (3)	0.4510 (3)	0.0434 (5)	44 (2)
C(21)	0.9443 (3)	0.4564 (3)	0.1302 (6)	44 (3)
C(22)	0.9263 (4)	0.4830 (4)	0.2399 (7)	54 (3)
C(23)	0.9659 (3)	0.4875 (4)	0.3339 (7)	55 (3)
C(24)	1.0262 (4)	0.4667 (4)	0.3176 (7)	63 (4)
C(25)	1.0447 (4)	0.4420 (4)	0.2131 (8)	60 (3)
C(26)	1.0040 (4)	0.4367 (4)	0.1162 (7)	50 (3)
C(27)	1.0201 (4)	0.4124 (4)	0.0016 (7)	53 (3)
C(28)	0.9774 (3)	0.4079 (3)	-0.0848 (7)	50 (3)
C(29)	0.9172 (4)	0.4273 (3)	-0.1629 (7)	57 (3)
C(20)	0.8725 (4)	0.4221 (4)	-0.1629 (7)	57 (3)
O(3)	0.8059 (2)	0.4060 (2)	0.1692 (4)	51 (3)
N(3)	0.7455 (3)	0.5022 (3)	0.2332 (5)	49 (2)
C(31)	0.7314 (3)	0.4496 (4)	0.2893 (7)	51 (3)
C(32)	0.7656 (4)	0.3987 (4)	0.2537 (7)	53 (3)
C(33)	0.7542 (4)	0.3423 (4)	0.3063 (8)	71 (4)
C(34)	0.7092 (5)	0.3378 (5)	0.3980 (9)	83 (4)
C(35)	0.6764 (4)	0.3870 (6)	0.4337 (8)	85 (5)
C(36)	0.6866 (4)	0.4447 (5)	0.3822 (7)	64 (4)
C(37)	0.6561 (4)	0.5004 (5)	0.4062 (7)	73 (4)
C(38)	0.6687 (4)	0.5510 (5)	0.3514 (9)	71 (4)
C(39)	0.7148 (4)	0.5521 (4)	0.2593 (7)	66 (3)
C(30)	0.7277 (4)	0.6110 (4)	0.1977 (10)	90 (4)
O(4)	0.8433 (3)	0.5559 (3)	0.4583 (6)	94 (3)
C(4)	0.8249 (5)	0.5063 (6)	0.5319 (10)	112 (6)
O(5)	0.6755 (3)	0.7031 (3)	0.4787 (7)	117 (4)

Equivalent isotropic U defined as one third of the trace of the orthogonalized U_{ij} tensor

Table 4-3. Hydrogen Atom Coordinates ($\times 10^4$) for **I**.

	x	y	x
H(13)	0.8434	0.6558	-0.0747
H(14)	0.7812	0.6715	-0.2853
H(15)	0.7028	0.6083	-0.3354
H(17)	0.6493	0.4771	-0.3092
H(18)	0.6544	0.4089	-0.2414
H(101)	0.7131	0.3604	0.0660
H(24)	1.0569	0.4653	0.4023
H(25)	1.0875	0.4191	0.1925
H(27)	1.0614	0.3915	-0.0093
H(28)	0.9869	0.3763	-0.1527
H(201)	0.8500	0.4616	-0.1594
H(202)	0.8388	0.3809	-0.1610
H(33)	0.7949	0.3076	0.3074
H(34)	0.7034	0.2863	0.4238
H(35)	0.6609	0.3839	0.5353
H(37)	0.6266	0.4813	0.4740
H(38)	0.6482	0.6029	0.3477
H(301)	0.7000	0.6511	0.2198
H(302)	0.7772	0.6173	0.2270
H(5)	0.6325	0.7075	0.4869

aluminum(III)) which range from 2.054 to 2.110 Å.[32] In addition, they are even longer when compared to the Al-N bond lengths of 2.028 to 2.073 Å in tris(oxinato)aluminum(III).[31] The steric interaction of the methyl groups with the aromatic rings is probably responsible for the lengthening of the Al-N bonds in the tris(2-methyloxinato)aluminum(III) complex. The longest Al-N bond length and shortest Al-O bond length are to ring 1. A potential cause may be that the molecule is twisting outward to allow more space between the methyl group on ring 2 and ring 1.

Table 4-4. Bond Lengths (Å) for **I**. Estimated Standard Deviations are given in Parentheses.

Al-O(1)	1.805(6)	Al-N(1)	2.179(6)
Al-O(2)	1.858(5)	Al-N(2)	2.127(6)
Al-O(3)	1.829(5)	Al-N(3)	2.122(6)
O(1)-C(12)	1.347(10)	N(1)-C(11)	1.372(10)
N(1)-C(19)	1.347(10)	C(11)-C(12)	1.398(12)
C(11)-C(16)	1.430(11)	C(12)-C(13)	1.393(12)
C(13)-C(14)	1.412(13)	C(13)-H(13)	1.146(8)
C(14)-C(15)	1.347(14)	C(14)-H(14)	1.168(10)
C(15)-C(16)	1.407(13)	C(15)-H(15)	1.163(9)
C(16)-C(17)	1.389(13)	C(17)-C(18)	1.361(14)
C(17)-H(17)	1.257(9)	C(18)-C(19)	1.431(11)
C(18)-H(18)	1.200(8)	C(19)-C(10)	1.504(12)
C(10)-H(11)	0.983(9)	O(2)-C(22)	1.351(10)
N(2)-C(21)	1.369(9)	N(2)-C(29)	1.362(9)
C(21)-C(22)	1.418(11)	C(21)-C(26)	1.406(11)
C(22)-C(23)	1.374(11)	C(23)-C(24)	1.429(12)
C(24)-C(25)	1.354(12)	C(24)-H(24)	1.167(8)
C(25)-C(26)	1.415(12)	C(25)-H(25)	1.102(8)
C(26)-C(27)	1.435(11)	C(27)-C(28)	1.356(11)
C(27)-H(27)	1.035(8)	C(28)-C(29)	1.422(11)
C(28)-H(28)	1.055(7)	C(29)-C(20)	1.488(11)
C(20)-H(21)	1.010(8)	C(20)-H(22)	1.181(8)
O(3)-C(32)	1.311(9)	N(3)-C(31)	1.361(11)
N(3)-C(39)	1.332(11)	C(31)-C(32)	1.419(12)
C(31)-C(36)	1.441(11)	C(32)-C(33)	1.407(13)
C(33)-C(34)	1.435(14)	C(33)-H(33)	1.186(9)
C(34)-C(35)	1.371(16)	C(34)-H(34)	1.186(11)
C(35)-C(36)	1.423(16)	C(35)-H(35)	1.190((9)
C(36)-C(37)	1.436(15)	C(37)-C(38)	1.310(15)
C(37)-H(37)	1.087(9)	C(38)-C(39)	1.452(13)
C(38)-H(38)	1.239(10)	C(39)-C(30)	1.505(13)
C(30)-H(31)	1.111(10)	C(30)-H(32)	1.154(10)
O(4)-C(4)	1.432(15)	O(5)-H(5)	0.964(7)

Table 4-5. Bond Angles (°) for **I**. Estimated Standard Deviations are given in Parentheses.

O(1)-Al-N(1)	81.7(3)	C(22)-C(23)-C(24)	118.6(7)
O(1)-Al-O(2)	92.0(3)	C(23)-C(24)-C(25)	121.7(8)
N(1)-Al-O(2)	173.1(3)	C(23)-C(24)-H(24)	116.9(7)
O(1)-Al-N(2)	92.4(2)	C(25)-C(24)-H(24)	120.9(8)
N(1)-Al-N(2)	99.9(2)	C(24)-C(25)-C(26)	120.1(8)
O(2)-Al-N(2)	83.0(2)	C(24)-C(25)-H(25)	128.9(8)
O(1)-Al-O(3)	173.9(3)	C(26)-C(25)-H(25)	110.6(7)
N(1)-Al-O(3)	92.5(2)	C(21)-C(26)-C(25)	119.4(7)

Table 4-5 -- Continued.

O(2)-Al-O(3)	94.0(2)	C(21)-C(26)-C(27)	116.8(7)
N(2)-Al-O(3)	86.8(2)	C(25)-C(26)-C(27)	123.8(7)
O(1)-Al-N(3)	99.1(3)	C(26)-C(27)-C(28)	119.4(7)
N(1)-Al-N(3)	91.6(2)	C(26)-C(27)-H(27)	119.6(7)
O(2)-Al-N(3)	86.7(2)	C(28)-C(27)-H(27)	120.1(7)
N(2)-Al-N(3)	164.8(3)	C(27)-C(28)-C(29)	121.3(7)
O(3)-Al-N(3)	82.8(2)	C(27)-C(28)-H(28)	114.9(7)
Al-O(1)-C(12)	118.6(5)	C(29)-C(28)-H(28)	120.3(7)
Al-N(1)-C(11)	106.3(5)	N(2)-C(29)-C(28)	120.4(7)
Al-N(1)-C(19)	135.1(5)	N(2)-C(29)-C(20)	120.7(7)
C(11)-N(1)-C(19)	118.5(6)	C(28)-C(29)-C(20)	118.9(7)
N(1)-C(11)-C(12)	115.7(7)	C(29)-C(20)-H(201)	103.5(7)
N(1)-C(11)-C(16)	123.3(7)	C(29)-C(20)-H(202)	118.0(6)
C(12)-C(11)-C(16)	120.9(8)	H(201)-C(20)-H(202)	111.0(7)
O(1)-C(12)-C(11)	117.7(7)	Al-O(3)-C(32)	116.6(5)
O(1)-C(12)-C(13)	122.8(7)	Al-N(3)-C(31)	106.6(5)
C(11)-C(12)-C(13)	119.5(8)	Al-N(3)-C(39)	133.8(6)
C(12)-C(13)-C(14)	118.6(8)	C(31)-N(3)-C(39)	119.6(7)
C(12)-C(13)-H(13)	116.0(8)	N(3)-C(31)-C(32)	115.5(7)
C(14)-C(13)-H(13)	124.1(8)	N(3)-C(31)-C(36)	123.8(8)
C(13)-C(14)-C(15)	122.7(9)	C(32)-C(31)-C(36)	120.7(8)
C(13)-C(14)-H(14)	126.6(9)	O(3)-C(32)-C(31)	118.0(7)
C(15)-C(14)-H(14)	107.9(8)	O(3)-C(32)-C(33)	122.2(8)
C(14)-C(15)-C(16)	120.2(9)	C(31)-C(32)-C(33)	119.7(7)
C(14)-C(15)-H(15)	116.8(9)	C(32)-C(33)-C(34)	119.0(9)
C(16)-C(15)-H(15)	121.3(8)	C(32)-C(33)-H(33)	116.5(7)
C(11)-C(16)-C(15)	118.0(8)	C(34)-C(33)-H(33)	118.5(8)
C(11)-C(16)-C(17)	116.3(8)	C(33)-C(34)-C(35)	121.4(10)
C(15)-C(16)-C(17)	125.7(8)	C(33)-C(34)-H(34)	108.5(9)
C(16)-C(17)-C(18)	121.0(8)	C(35)-C(34)-H(34)	129.7(9)
C(16)-C(17)-H(17)	141.4(9)	C(34)-C(35)-C(36)	121.0(9)
C(18)-C(17)-H(17)	93.9(7)	C(34)-C(35)-H(35)	112.7(10)
C(17)-C(18)-C(19)	120.4(8)	C(36)-C(35)-H(35)	119.0(10)
C(17)-C(18)-H(18)	101.5(7)	C(31)-C(36)-C(35)	118.0(9)
C(19)-C(18)-H(18)	136.4(8)	C(31)-C(36)-C(37)	113.3(8)
N(1)-C(19)-C(18)	120.3(7)	C(35)-C(36)-C(37)	128.7(8)
N(1)-C(19)-C(10)	122.3(7)	C(36)-C(37)-C(38)	123.4(8)
C(18)-C(19)-C(10)	117.2(7)	C(36)-C(37)-H(37)	94.5(9)
C(19)-C(10)-H(101)	124.2(8)	C(38)-C(37)-H(37)	142.1(11)
Al-O(2)-C(22)	116.1(5)	C(37)-C(38)-C(39)	119.8(9)
Al-N(2)-C(21)	106.8(4)	C(37)-C(38)-H(38)	137.2(9)
Al-N(2)-C(29)	134.7(5)	C(39)-C(38)-H(38)	102.7(8)
C(21)-N(2)-C(29)	118.5(6)	N(3)-C(39)-C(38)	120.1(8)
N(2)-C(21)-C(22)	116.9(7)	N(3)-C(39)-C(30)	121.6(8)
N(2)-C(21)-C(26)	123.6(7)	C(38)-C(39)-C(30)	118.2(8)
C(22)-C(21)-C(26)	119.5(7)	C(39)-C(30)-H(301)	119.3(9)
O(2)-C(22)-C(21)	116.8(7)	C(39)-C(30)-H(302)	99.0(8)
O(2)-C(22)-C(23)	122.4(7)	H(301)-C(30)-H(302)	111.5(8)
C(21)-C(22)-C(23)	120.8(8)		

Table 4-6. Anisotropic Temperature Parameters ($Å^2 \times 10^3$) for Non-Hydrogen Atoms for **I**. Estimated Standard Deviations are given in Parentheses.

Atom	U_{11}	U_{22}	U_{33}	U_{23}	U_{13}	U_{12}
Al	41(1)	52(2)	47(1)	-5(1)	-2(1)	1(1)
O(1)	49(4)	61(4)	61(3)	-5(3)	-8(3)	-1(3)
N(1)	39(4)	56(4)	47(4)	-1(4)	7(3)	2(3)
C(11)	45(5)	51(5)	55(5)	-4(5)	6(4)	4(4)
C(12)	35(5)	57(6)	63(3)	-0(5)	9(5)	1(4)
C(13)	50(6)	51(6)	80(7)	2(5)	9(5)	-5(4)
C(14)	80(8)	91(8)	54(6)	22(6)	8(6)	5(7)
C(15)	77(7)	74(7)	64(6)	15(6)	-17(6)	14(6)
C(16)	45(5)	73(6)	51(5)	7(5)	5(4)	9(5)
C(17)	61(7)	86(8)	57(6)	-2(6)	-14(5)	-1(6)
C(18)	45(6)	75(7)	54(5)	-18(5)	-10(4)	-1(5)
C(19)	34(5)	64(6)	53(5)	-7(4)	7(4)	-6(4)
C(10)	107(8)	59(6)	70(6)	10(5)	-9(6)	-16(6)
O(2)	41(3)	72(4)	41(3)	-15(3)	-6(3)	4(3)
N(2)	47(4)	41(4)	44(4)	3(3)	3(3)	-8(3)
C(21)	42(5)	48(5)	41(4)	4(4)	4(4)	-8(4)
C(22)	57(6)	55(6)	51(5)	-5(5)	18(5)	5(5)
C(23)	39(5)	78(6)	47(5)	4(5)	-8(4)	-9(4)
C(24)	56(6)	84(7)	49(5)	-1(5)	-15(5)	-12(5)
C(25)	47(5)	72(6)	61(6)	-6(5)	-5(5)	7(5)
C(26)	41(5)	49(5)	61(5)	4(5)	7(5)	-2(4)
C(27)	45(5)	50(5)	65(5)	-1(5)	21(5)	2(4)
C(28)	54(5)	42(5)	55(5)	-15(4)	-3(4)	6(4)
C(29)	58(6)	36(5)	45(4)	4(4)	6(4)	1(4)
C(20)	61(6)	58(6)	51(5)	-28(4)	-4(5)	9(5)
O(3)	49(3)	55(3)	51(3)	-3(3)	12(3)	6(3)
N(3)	42(4)	55(5)	51(4)	-15(4)	-3(3)	5(3)
C(31)	34(5)	72(6)	46(5)	-6(5)	-2(4)	-6(4)
C(32)	44(5)	69(7)	47(5)	9(5)	-6(5)	-2(5)
C(33)	53(6)	86(7)	74(6)	22(6)	6(5)	4(5)
C(34)	79(8)	100(9)	71(7)	19(7)	5(6)	-8(6)
C(35)	65(7)	148(11)	40(5)	6(6)	-8(5)	-30(7)
C(36)	39(5)	118(9)	37(5)	-20(6)	-2(4)	-6(5)
C(37)	41(6)	133(10)	46(6)	-18(6)	13(5)	-15(6)
C(38)	71(7)	82(7)	61(6)	-17(6)	-12(6)	12(6)
C(39)	48(5)	92(7)	59(6)	-21(5)	3(4)	4(5)
C(30)	80(7)	63(7)	126(9)	-28(7)	-0(7)	27(6)
O(4)	113(6)	94(5)	75(4)	-30(4)	11(4)	10(4)
C(4)	94(9)	163(12)	79(8)	-5(8)	19(7)	-30(8)
O(5)	84(5)	129(7)	136(7)	-8(5)	21(5)	6(5)

The form of the thermal ellipsoid is $\exp[-2\pi^2(h^2a^{*2}U_{11} + k^2b^{*2}U_{22} + l^2c^{*2}U_{33} + 2klb^*c^*U_{23} + 2hla^*c^*U_{13} + 2hka^*b^*U_{12})]$

<u>$Al(ox)_3 \cdot CH_3OH$ (II).</u> The ORTEP drawing of **II** is given in Figure 4-5. Atomic coordinates for all non-hydrogen atoms and hydrogen atoms found, bond lengths and bond angles are given in Tables 4-7 through 4-10, respectively. The anisotropic thermal parameters appear in Table 4-11.

As expected, the aluminum ion is in a distorted octahedral environment created by three oxine ligands. The three nitrogen and three oxygen atoms are arranged in the meridional as opposed to the facial conformation. The complex is isostructural with the $Al(ox)_3$ molecule in a compound previously reported.[31]

Although **II** is quite similar to **I**, there are notable differences between the bond lengths and angles between the aluminum, nitrogen and oxygen atoms for the two complexes. In $Al(meox)_3$, the Al-O bond lengths are 1.805, 1.829 and 1.858 Å. On the average, these are slightly shorter than the Al-O bond distances in $Al(ox)_3$ of 1.842, 1.845 and 1.884 Å. In addition, the Al-N bond lengths for Al-N bonds are longer for $Al(meox)_3$. The Al-N bond distances in **I** range from 2.122 to 2.179 Å. In **II**, the Al-N bonds, which range from 2.026 to 2.077 Å, are an average difference of 0.100 Å shorter than for the $Al(meox)_3$ complex. As the bond to the oxygen gets shorter, the ligand molecule pivots to also provide a longer Al-N bond distance. As a result, the $Al(meox)_3$ is distorted farther from the ideal octahedron than $Al(ox)_3$.

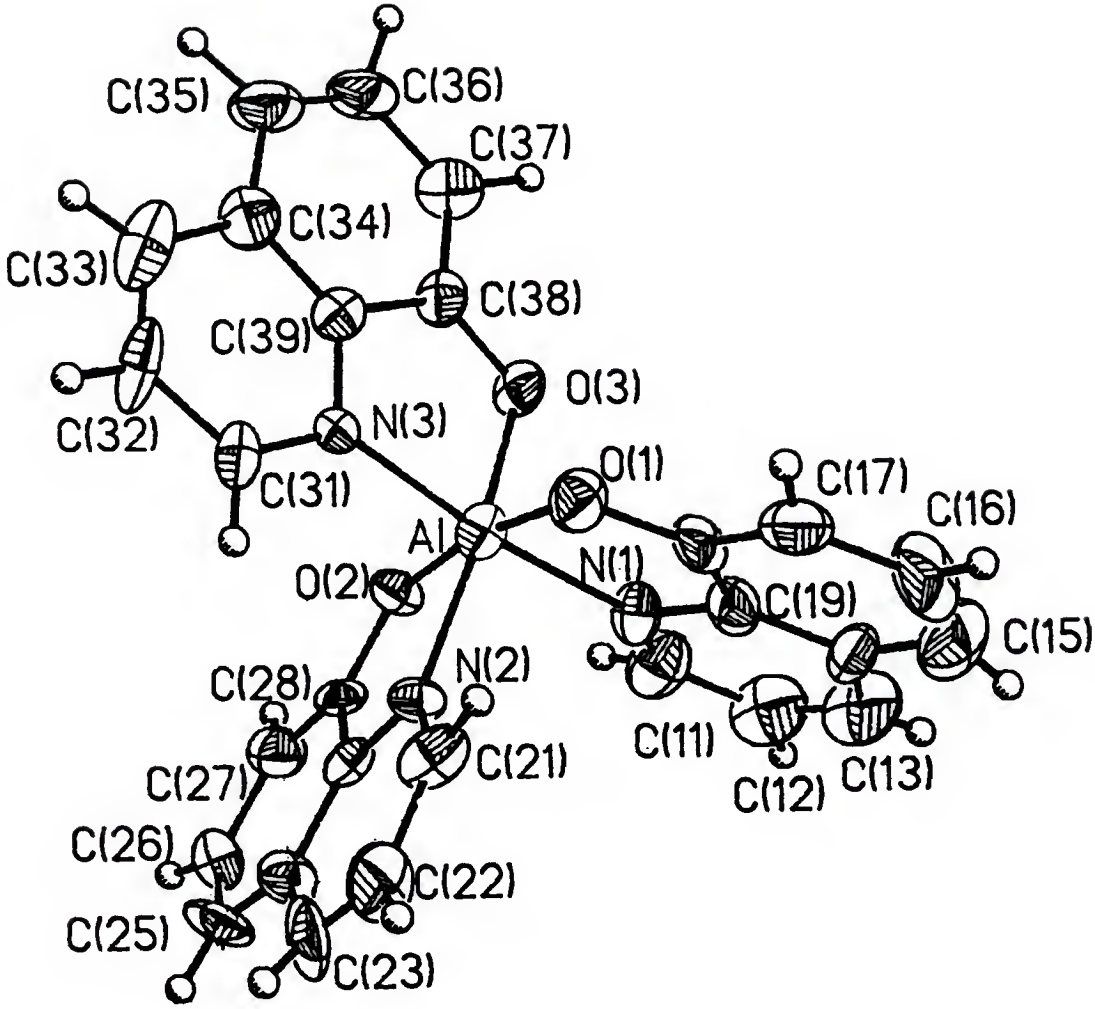

Figure 4-5. ORTEP of $Al(ox)_3$ Molecule Showing the Atomic Numbering Scheme and Thermal Ellipsoids.

Table 4-7. Final Atomic Coordinates ($\times 10^4$) and Isotropic Thermal Parameters ($Å^2 \times 10^3$) for **II**. Estimated Standard Deviations are given in Parentheses.

Atom	x	y	z	U
Al	0.4265(3)	0.0274(2)	0.7389(2)	38(1)*
O(1)	0.2599(5)	0.0105(4)	0.7561(3)	42(2)*
N(1)	0.4464(7)	0.0749(5)	0.8542(4)	38(3)*
C(11)	0.5443(10)	0.1074(8)	0.9009(7)	54(5)*
C(12)	0.5401(13)	0.1397(9)	0.9793(8)	66(6)*
C(13)	0.4303(16)	0.1354(9)	1.0089(7)	77(6)*
C(14)	0.3236(12)	0.1046(7)	0.9626(6)	51(5)*
C(15)	0.2008(12)	0.0982(9)	0.9863(7)	76(5)*
C(16)	0.1072(11)	0.0649(9)	0.9317(9)	71(6)*
C(17)	0.1220(9)	0.0336(8)	0.8527(6)	50(4)*
C(18)	0.2367(8)	0.0374(7)	0.8287(6)	39(4)*
C(19)	0.3355(8)	0.0739(6)	0.8841(5)	40(4)*
O(2)	0.5956(5)	0.0229(5)	0.7371(3)	33(2)*
N(2)	0.4551(6)	-0.1228(5)	0.7720(4)	30(3)*
C(21)	0.3771(9)	-0.1959(9)	0.7901(5)	43(4)*
C(22)	0.4186(11)	-0.2922(9)	0.8134(6)	55(5)*
C(23)	0.5385(12)	-0.3132(8)	0.8134(6)	57(5)*
C(24)	0.6254(9)	-0.2414(7)	0.7930(5)	37(4)*
C(25)	0.7559(11)	-0.2558(7)	0.7925(6)	52(5)*
C(26)	0.8301(10)	-0.1776(9)	0.7751(6)	47(4)*
C(27)	0.7783(9)	-0.0833(8)	0.7574(6)	44(4)*
C(28)	0.6537(8)	-0.0632(7)	0.7555(5)	31(4)*
C(29)	0.5780(7)	-0.1459(6)	0.7751(4)	26(3)*
O(3)	0.4114(5)	0.1581(4)	0.7009(3)	36(2)*
N(3)	0.3811(6)	-0.0107(5)	0.6223(4)	31(3)*
C(31)	0.3649(9)	-0.0989(7)	0.5836(6)	44(4)*
C(32)	0.3391(10)	-0.1056(9)	0.5010(7)	59(5)*
C(33)	0.3278(9)	-0.0196(11)	0.4552(6)	56(5)*
C(34)	0.3404(8)	0.0749(9)	0.4916(6)	44(4)*
C(35)	0.3336(10)	0.1669(9)	0.4531(6)	59(5)*
C(36)	0.3520(9)	0.2581(8)	0.4940(7)	49(5)*
C(37)	0.3796(8)	0.2577(7)	0.5800(6)	45(4)*
C(38)	0.3880(8)	0.1655(7)	0.6218(6)	36(4)*
C(39)	0.3694(7)	0.0745(7)	0.5755(5)	30(3)*
O(4)	0.9547(8)	0.0461(7)	0.3444(7)	137(5)*
C(4)	0.9648(14)	0.1254(13)	0.3919(11)	178(10)*

* Equivalent isotropic U defined as one third of the trace of the orthogonalized U_{ij} tensor

Table 4-8. Hydrogen Atom Coordinates ($\times 10^4$) for **II**.

Atom	x	y	z
H(11)	0.6093	0.1143	0.8760
H(12)	0.6192	0.1599	1.0192
H(13)	0.4324	0.1558	1.0513
H(15)	0.2114	0.1052	1.0335
H(16)	0.0293	0.0557	0.9408
H(17)	0.0521	0.0261	0.8154
H(21)	0.2834	-0.1815	0.7796
H(22)	0.3567	-0.3365	0.8245
H(23)	0.5486	-0.3627	0.8086
H(25)	0.7843	-0.3126	0.8011
H(26)	0.9172	-0.1800	0.7650
H(27)	0.8209	-0.0347	0.7443
H(31)	0.3750	-0.1579	0.6148
H(32)	0.3176	-0.1677	0.4742
H(33)	0.3096	-0.0363	0.4026
H(35)	0.3219	0.1658	0.3898
H(36)	0.3406	0.3349	0.4728
H(37)	0.3823	0.3264	0.6163

The average intraligand O-Al-N bond angle for **I** is 82.5° which is slightly more acute than the average of 82.9° for **II**. The interligand bond angles around aluminum range from 86.7° to 99.9° with an average of 92.8° for $Al(meox)_3$. For $Al(ox)_3$, these bond angles, varying from 87.6° to 96.9, average to 92.5°. The average of the bond angles for $Al(ox)_3$ correspond more closely to the 90° angles present in an ideal octahedron.

The comparison of the bond angles for the oxygen and nitrogen atoms trans to each other corroborates that the $Al(ox)_3$ is closer to the ideal octahedral environment than $Al(meox)_3$. In **I**, the trans bond angles range from 164.8° to 173.9° for an average deviation 9.4° from an ideal 180° angle.

Table 4-9. Bond Lengths (Å) for **II**. Estimated Standard Deviations are given in Parentheses.

Al-O(1)	1.884(6)	Al-N(1)	2.026(8)
Al-O(2)	1.842(6)	Al-N(2)	2.077(8)
Al-O(3)	1.845(6)	Al-N(3)	2.026(7)
N(1)-C(11)	1.310(13)	O(1)-C(18)	1.329(12)
C(11)-C(12)	1.395(18)	N(1)-C(19)	1.365(12)
C(12)-C(13)	1.352(22)	C(11)-H(11)	0.872(12)
C(13)-C(14)	1.372(19)	C(12)-H(12)	1.054(13)
C(14)-C(15)	1.445(19)	C(13)-H(13)	0.761(12)
C(15)-C(16)	1.353(17)	C(14)-C(19)	1.407(14)
C(16)-C(17)	1.423(19)	C(15)-H(15)	0.793(11)
C(17)-C(18)	1.360(14)	C(16)-H(16)	0.888(12)
C(18)-C(19)	1.413(12)	C(17)-H(17)	0.926(10)
N(2)-C(21)	1.347(13)	O(2)-C(28)	1.320(11)
C(21)-C(22)	1.393(16)	N(2)-C(29)	1.363(10)
C(22)-C(23)	1.332(17)	C(21)-H(21)	1.028(10)
C(23)-C(24)	1.413(16)	C(22)-H(22)	0.930(12)
C(24)-C(25)	1.431(16)	C(23)-H(23)	0.670(10)
C(25)-C(26)	1.367(16)	C(24)-C(29)	1.383(12)
C(26)-C(27)	1.387(15)	C(25)-H(25)	0.818(10)
C(27)-C(28)	1.375(14)	C(26)-H(26)	0.983(10)
C(28)-C(29)	1.434(13)	C(27)-H(27)	0.839(11)
N(3)-C(31)	1.339(12)	O(3)-C(38)	1.328(11)
N(3)-C(31)	1.339(12)	N(3)-C(39)	1.372(11)
C(31)-C(32)	1.385(15)	C(31)-H(31)	0.940(10)
C(32)-C(33)	1.372(18)	C(32)-H(32)	0.953(12)
C(33)-C(34)	1.392(19)	C(33)-H(33)	0.910(11)
C(34)-C(35)	1.413(17)	C(34)-C(39)	1.409(12)
C(35)-C(36)	1.357(16)	C(35)-H(35)	1.059(10)
C(36)-C(37)	1.441(15)	C(36)-H(36)	1.080(11)
C(37)-C(38)	1.406(14)	C(37)-H(37)	1.094(10)
C(38)-C(39)	1.435(13)	O(4)-C(4)	1.316(21)

Table 4-10. Bond Angles (°) for **II**. Estimated Standard Deviations are given in Parentheses.

O(1)-Al-N(1)	82.8(3)	C(21)-C(22)-H(22)	114.7(11)
O(1)-Al-O(2)	168.3(3)	C(23)-C(22)-H(22)	127.0(12)
N(1)-Al-O(2)	92.5(3)	C(22)-C(23)-C(24)	122.9(10)
O(1)-Al-N(2)	87.6(3)	C(22)-C(23)-H(23)	112.3(15)
N(1)-Al-N(2)	92.7(3)	C(24)-C(23)-H(23)	120.2(15)
O(2)-Al-N(2)	81.9(3)	C(23)-C(24)-C(25)	127.2(9)

Table 4-10 -- continued.

O(1)-Al-O(3)	96.9(3)	C(23)-C(24)-C(29)	115.2(9)
N(1)-Al-O(3)	92.0(3)	C(25)-C(24)-C(29)	117.5(9)
O(2)-Al-O(3)	93.9(3)	C(24)-C(25)-C(26)	120.9(9)
N(2)-Al-O(3)	173.9(3)	C(24)-C(25)-H(25)	118.2(11)
O(1)-Al-N(3)	90.1(3)	C(26)-C(25)-H(25)	120.9(13)
N(1)-Al-N(3)	171.5(3)	C(25)-C(26)-C(27)	119.6(10)
O(2)-Al-N(3)	95.3(3)	C(25)-C(26)-H(26)	128.4(11)
N(2)-Al-N(3)	91.8(3)	C(27)-C(26)-H(26)	111.3(10)
O(3)-Al-N(3)	84.1(3)	C(26)-C(27)-C(28)	123.4(10)
Al-O(1)-C(18)	114.3(5)	C(26)-C(27)-H(27)	121.7(11)
Al-N(1)-C(11)	130.9(8)	C(28)-C(27)-H(27)	114.9(10)
Al-N(1)-C(19)	111.2(5)	O(2)-C(28)-C(27)	127.7(9)
C(11)-N(1)-C(19)	117.9(8)	O(2)-C(28)-C(29)	116.3(8)
N(1)-C(11)-C(12)	123.0(11)	C(27)-C(28)-C(29)	116.1(9)
N(1)-C(11)-H(11)	112.9(11)	N(2)-C(29)-C(24)	123.3(8)
C(12)-C(11)-H(11)	123.6(11)	N(2)-C(29)-C(28)	114.1(7)
C(11)-C(12)-C(13)	118.5(11)	C(24)-C(29)-C(28)	122.7(8)
C(11)-C(12)-H(12)	123.9(13)	Al-O(3)-C(38)	122.7(8)
C(13)-C(12)-H(12)	117.3(12)	Al-N(3)-C(31)	133.6(6)
C(12)-C(13)-C(14)	121.5(11)	Al-N(3)-C(39)	110.2(5)
C(12)-C(13)-H(13)	114.4(17)	C(31)-N(3)-C(39)	116.1(7)
C(14)-C(13)-H(13)	123.9(19)	N(3)-C(31)-C(32)	122.8(9)
C(13)-C(14)-C(15)	127.0(11)	N(3)-C(31)-H(31)	116.9(9)
C(13)-C(14)-C(19)	116.5(12)	C(32)-C(31)-H(31)	120.2(10)
C(15)-C(14)-C(19)	116.5(9)	C(31)-C(32)-C(33)	102.2(11)
C(14)-C(15)-C(16)	118.0(11)	C(31)-C(32)-H(32)	122.5(11)
C(14)-C(15)-H(15)	104.6(12)	C(33)-C(32)-H(32)	116.8(11)
C(16)-C(15)-H(15)	135.8(15)	C(32)-C(33)-C(34)	120.1(10)
C(15)-C(16)-C(17)	124.4(12)	C(32)-C(33)-H(33)	109.8(14)
C(15)-C(16)-H(16)	125.2(16)	C(34)-C(33)-H(33)	130.0(14)
C(17)-C(16)-H(16)	110.3(12)	C(33)-C(34)-C(35)	127.1(10)
C(16)-C(17)-C(18)	119.2(9)	C(33)-C(34)-C(39)	115.8(10)
C(16)-C(17)-H(17)	118.9(11)	C(35)-C(34)-C(39)	117.1(10)
C(18)-C(17)-H(17)	120.2(11)	C(34)-C(35)-C(36)	122.6(10)
O(1)-C(18)-C(17)	123.8(8)	C(34)-C(35)-H(35)	114.0(10)
O(1)-C(18)-C(19)	118.7(8)	C(36)-C(35)-C(35)	123.1(11)
C(17)-C(18)-C(19)	117.5(9)	C(35)-C(36)-C(37)	120.3(10)
N(1)-C(19)-C(14)	122.6(8)	C(35)-C(36)-H(36)	129.7(10)
N(1)-C(19)-C(18)	113.0(8)	C(37)-C(36)-H(36)	109.7(9)
C(14)-C(19)-C(18)	124.4(9)	C(36)-C(37)-C(38)	119.9(9)
Al-O(2)-C(28)	118.1(6)	C(36)-C(37)-H(37)	123.1(9)
Al-N(2)-C(21)	132.2(6)	C(38)-C(37)-H(37)	116.5(9)
Al-N(2)-C(29)	109.7(5)	O(3)-C(38)-C(37)	123.9(9)
C(21)-N(2)-C(29)	118.2(7)	O(3)-C(38)-C(39)	118.6(8)
N(2)-C(21)-C(22)	122.1(9)	C(37)-C(38)-C(39)	117.5(8)
N(2)-C(21)-H(21)	117.9(10)	N(3)-C(39)-C(34)	124.9(8)
C(22)-C(21)-H(21)	119.6(10)	N(3)-C(39)-C(38)	112.4(7)
C(21)-C(22)-C(23)	118.2(11)	C(34)-C(39)-C(38)	122.7(9)

Table 4-11. Anisotropic Thermal Parameters ($Å^2 \times 10^3$) for **II**. Estimated Standard Deviations are given in Parentheses.

Atom	U_{11}	U_{22}	U_{33}	U_{23}	U_{13}	U_{12}
Al	41(2)	41(2)	31(2)	-3(2)	5(1)	-1(2)
O(1)	30(4)	59(5)	37(4)	0(3)	7(3)	2(4)
N(1)	43(5)	35(5)	34(5)	-14(4)	4(4)	-7(5)
C(11)	62(9)	55(8)	48(8)	11(6)	15(7)	-13(7)
C(12)	77(10)	59(9)	58(10)	-8(7)	-7(8)	-16(8)
C(13)	127(13)	56(9)	41(8)	-24(7)	-16(9)	-6(9)
C(14)	99(10)	27(7)	31(7)	2(5)	27(7)	7(7)
C(15)	101(10)	70(9)	65(8)	18(7)	45(8)	-2(8)
C(16)	46(8)	77(10)	100(12)	13(9)	48(8)	13(7)
C(17)	51(8)	49(7)	49(8)	16(6)	4(6)	10(6)
C(18)	30(7)	41(7)	51(8)	11(6)	22(5)	11(6)
C(19)	52(7)	27(6)	43(6)	-1(5)	15(5)	3(5)
O(2)	27(4)	29(4)	42(4)	8(3)	8(3)	5(4)
N(2)	22(5)	33(5)	33(5)	6(4)	-3(4)	2(4)
C(21)	51(8)	41(8)	36(7)	4(6)	2(6)	-22(7)
C(22)	46(8)	64(9)	63(8)	6(7)	33(7)	-2(7)
C(23)	87(10)	30(7)	62(8)	-23(6)	35(7)	0(8)
C(24)	27(7)	41(7)	43(7)	4(6)	2(5)	6(6)
C(25)	71(9)	18(7)	61(8)	4(6)	-11(7)	12(7)
C(26)	47(7)	46(8)	48(7)	-4(7)	13(6)	12(7)
C(27)	42(8)	48(8)	41(7)	7(6)	2(6)	7(6)
C(28)	25(6)	44(7)	22(6)	10(5)	-2(4)	10(6)
C(29)	27(5)	32(6)	17(5)	1(4)	1(4)	-11(5)
O(3)	50(4)	29(4)	28(4)	-8(3)	1(3)	-8(4)
N(3)	41(5)	28(5)	27(5)	3(4)	8(4)	10(4)
C(31)	54(8)	45(8)	33(7)	-10(6)	13(6)	5(6)
C(32)	77(10)	70(10)	35(8)	-32(7)	22(7)	-22(8)
C(33)	34(7)	98(11)	39(7)	-24(8)	11(5)	-22(8)
C(34)	32(7)	53(8)	44(7)	-11(7)	-7(5)	-2(6)
C(35)	81(10)	44(8)	49(8)	16(7)	-4(7)	10(8)
C(36)	55(8)	38(8)	54(8)	24(6)	9(6)	5(7)
C(37)	44(7)	35(7)	55(8)	5(6)	2(6)	-14(6)
C(38)	26(6)	50(8)	31(7)	-10(6)	-4(5)	-1(6)
C(39)	21(5)	39(6)	31(6)	1(5)	2(4)	-5(5)
O(4)	84(7)	93(8)	229(12)	-59(8)	8(7)	-6(6)
C(4)	120(14)	61(16)	270(21)	-171(16)	85(14)	-71(13)

The form or the thermal ellipsoid is $\exp[-2\pi^2(h^2a^{*2}U_{11} + k^2b^{*2}U_{22} + l^2c^{*2}U_{33} + 2klb^*c^*U_{23} + 2hla^*c^*U_{13} + 2hka^*b^*U_{12})]$

angle. For $Al(ox)_3$, the trans bond angles range from 168.3° to 173.9° for an average deviation from ideality of 8.8°.

Aluminum-27 NMR Spectroscopy

The Al-27 NMR spectrum for **Ia** is shown in Figure 4-6. Two different aluminum environments are present as exhibited by the two wide peaks on the Al-27 NMR. The first peak is centered around 54 ppm with a height of 580. The second, smaller peak is centered around 221 ppm with a height of 160. An Al-27 NMR study including hexacoordinate aluminum complexes with aminopolycarboxylic acids reported that chemical shifts range from 36.5 to 41.2 ppm.[57] The complex with one of the acids investigated by Iyer et al., has been characterized by

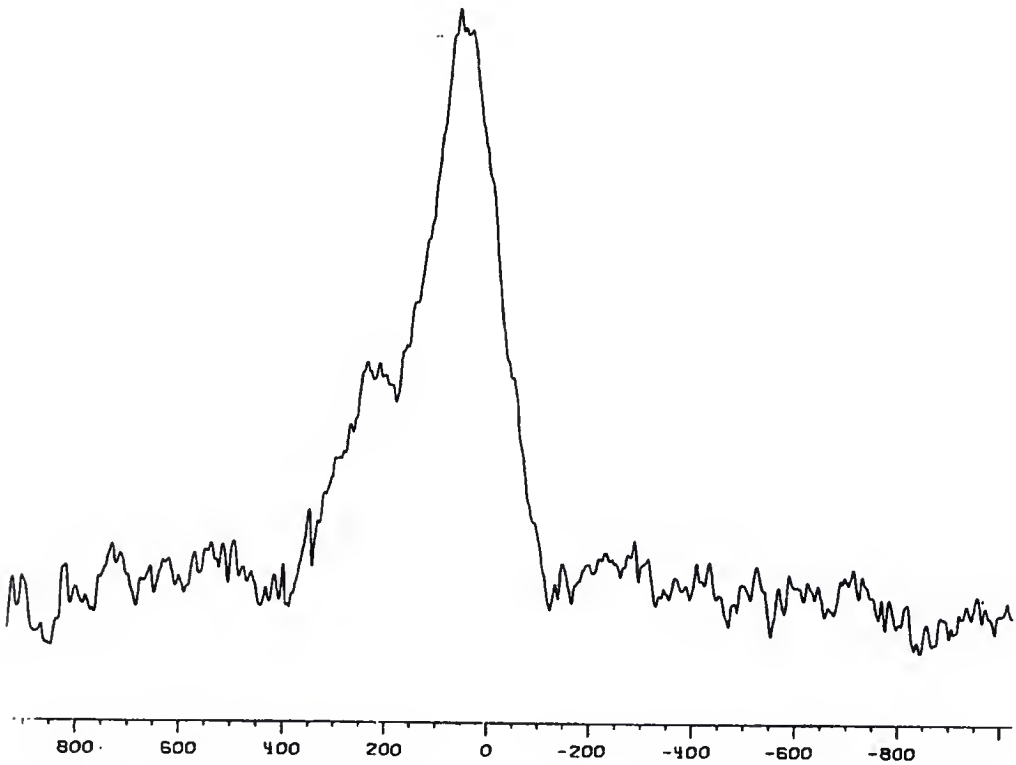

Figure 4-6. Al-27 NMR Spectrum of the Solid **Ia**.

x-ray crystallography. The aluminum ion in $K[Al(EDTA)]\cdot 2H_2O$ has been shown to be in a distorted octahedral environment coordinated to two nitrogen and four oxygen atoms.[58] The Al-27 NMR shifts reported for tris complexes of O,O bidentate ligands range from 36 to 41 ppm.[17,18] The peak at 54 ppm is probably due to the aluminum ion surrounded by three nitrogen and three oxygen atoms in a rather distorted octahedral environment. Two structures, with the AlN_3O_3 confirmed by x-ray studies, had chemical shifts of 8.1 and 8.2 ppm.[27] The chemical shifts for **I** and **II** should be larger than these two reported studies because environments around the aluminum in **I** and **II** are much more distorted from the ideal octahedral coordination[27]. The distorted octahedral environment could be viewed as approaching a pentacoordinate geometry, which is generally indicated with chemical shifts near 60 ppm. To date, there has not been an aluminum complex reported with a chemical shift near 220 ppm.

The Al-27 NMR spectrum of the solid **IIa** is shown in Figure 4-7. There are three different aluminum environments in the solid sample, as evidenced by the three peaks in the Al-27 NMR spectrum. Two peaks of almost equal height, 587 and 601, are centered around 5 ppm and 73 ppm, respectively. A third smaller peak appears centered at -120 ppm.

Solution **IIb** was prepared to separate the mixture. The Al-27 NMR spectrum of the solution, shown in Figure 4-8, has only one rather broad peak ($W_{½}$ = 5400 Hz) centered at 54 ppm.

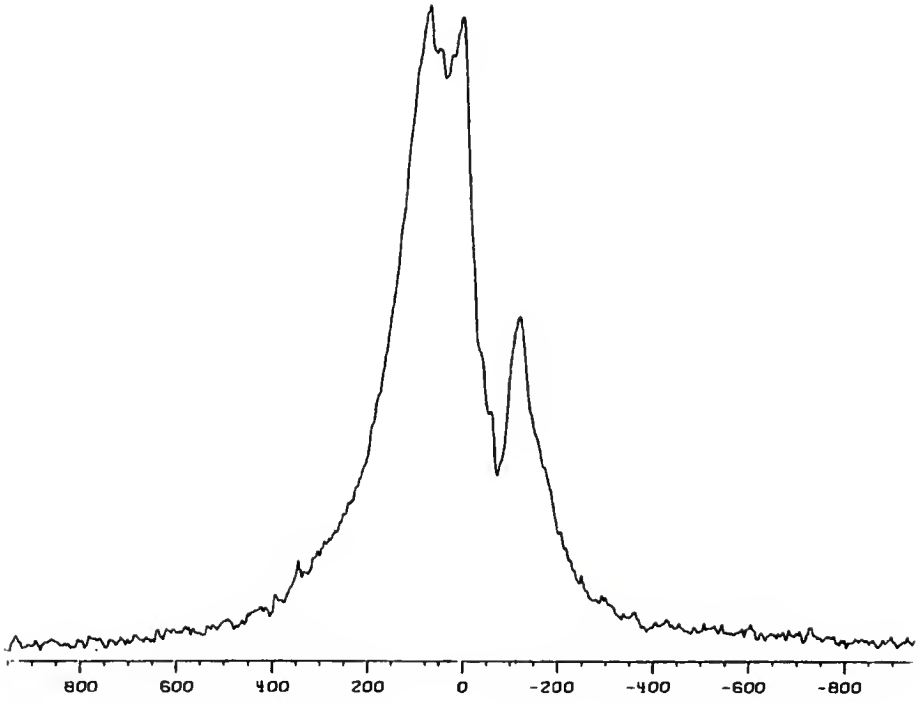

Figure 4-7. Al-27 NMR Spectrum of the Solid **IIa**.

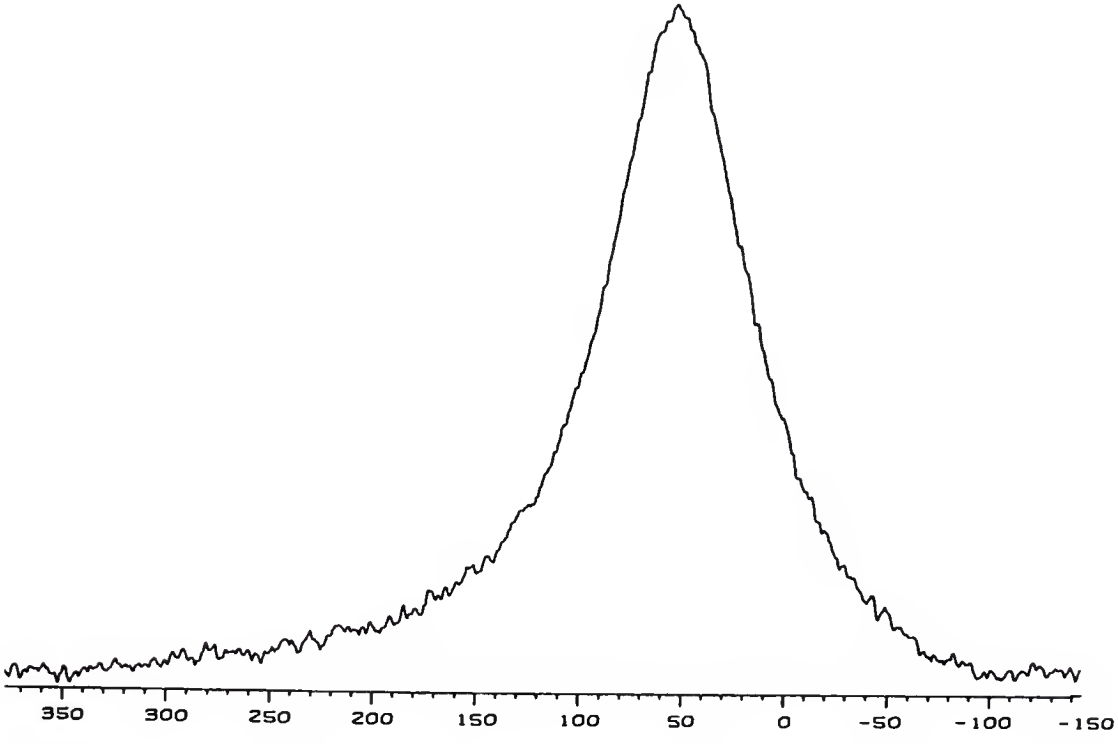

Figure 4-8. Al-27 NMR Spectrum of $Al(ox)_3$ in C_2H_5OH Solution.

Because the structure was confirmed by a second x-ray analysis, the environment of the aluminum complex in solution is known to be $Al(ox)_3$ -- a distorted octahedral environment with three nitrogen and three oxygen atoms. Possible explanations for the intermediate peak at 73 ppm in the solid not directly corresponding to the 54 ppm peak in the solution include the presence of the solvent molecules and other complex molecules in the crystal lattice, steric strains due to packing or solvent effects. Since the location of each nitrogen and oxygen atom around the aluminum atom has been verified using x-ray diffraction techniques, the relatively large value of 54 ppm should be added to the range of chemical shifts reported for a distorted octahedral environment around an aluminum ion.

Relatively few compounds with an AlN_3O_3 center have been studied with both x-ray crystallography and Al-27 NMR spectroscopy. $Al(meox)_3$ and $Al(ox)_3$ seem to be the least ideal octahedral aluminum complexes with three nitrogen and three oxygen atoms to be studied thus far.

CHAPTER 5

ALUMINUM-27 NMR, INFRARED, MASS SPECTROMETRIC AND ELEMENTAL ANALYSIS OF ALUMINUM COMPLEXES OF N,O DONOR LIGANDS

Introduction

The techniques for the characterization of aluminum complexes were discussed in Chapter 2. Because suitable crystals were not produced for compounds **III** through **VII**, x-ray crystallography could not be employed. Therefore, the remaining methods discussed in Chapter 2 were used to characterize the synthesized compounds.

Aluminum-27 NMR

Theory

A limited number of aluminum coordination compounds with nitrogen as a donor atom have been analyzed by Al-27 NMR. The Al-27 chemical shift is determined by the number and types of atoms and the symmetry around the aluminum atom.[54] The chemical shifts as well as the donor atoms for some octahedral environments in aluminum complexes are presented in Table 5-1. All of the chemical shifts shown are relative to $Al(H_2O)_6^{3+}$.

Although shifts near 0 ppm and 80 ppm are generally produced by octahedral and tetrahedral environments, respectively, the peaks due to the hexavalent coordination

Table 5-1. Al-27 NMR Data and Aluminum Coordination.

Compound	δ, ppm	N atoms	O atoms	H_2O	Ref
$Al(H_2O)_3(IDA)^a$	18.2	1	2	3	57
$Al(IDA)_2{}^a$	36.5	2	4	0	57
$Al(H_2O)_2(NTA)^b$	25.4	1	3	2	57
$Al(H_2O)(HEDTA)^c$	32.8	2	3	1	57
$Al(EDTA)^d$	41.2	2	4	0	57
$Al(PDTA)^e$	40.7	2	4	0	57
$Al(DCTA)^f$	40.5	2	4	0	57
$Al(oz)_3{}^g$	8.2	3	3	0	27
$Al(BrOz)_3{}^h$	11.4	3	3	0	27
$Al(moz)_3{}^i$	8.1	3	3	0	27
$Al(aloz)_3{}^j$	9.0	3	3	0	27
$Al(DTPA)^{2-k}$	37.5	1	5	0	57
$Al(pa)_3{}^l$	39	0	6	0	18
$Al(ma)_3{}^m$	40	0	6	0	18
$Al(mpp)_3{}^n$	37	0	6	0	17
$Al(dpp)_3{}^o$	36	0	6	0	17

Notes: Ligands are shown in Figure 5-1 a) Iminodiacetic acid, b) Nitrilotriacetic acid, c) N-(Hydroxyethyl)ethylenediaminetriacetic acid, d) Ethylenediaminetetraacetic acid, e) 1,2-Propylenediaminetetraacetic acid, f) *trans*-1,2-Diaminocyclohexanetetraacetic acid, g) 2-(2'-Hydroxyphenyl)-2-oxazoline, h) 2-(5'-Bromo-2'-hydroxyphenyl)-2-oxazoline, i) 2-(2'-Hydroxy-3'-methylphenyl)-2-oxazoline, j) 2-(2'-Hydroxy-3'-allylphenyl)-2-oxazoline, k) Diethylenetriaminepentaacetic acid, l) Pyromeconic acid, m) Maltol, n) 3-Hydroxy-2-methyl-4-pyridinone, o) 3-Hydroxy-1,2-dimethyl-4-pyridinone

compounds shown here lie about midway between the two. Also, the compounds with one or more nitrogen atoms coordinated to the aluminum are shifted farther than the similar complexes that contain only oxygen donor atoms. In addition, the more

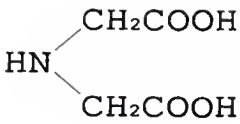

(a)

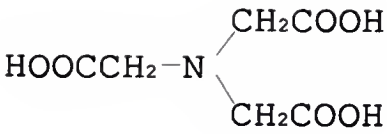

(b)

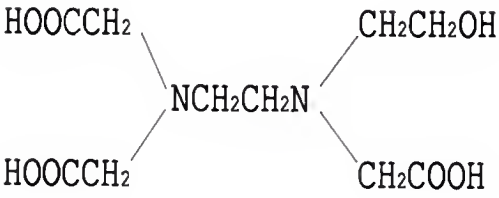

(c)

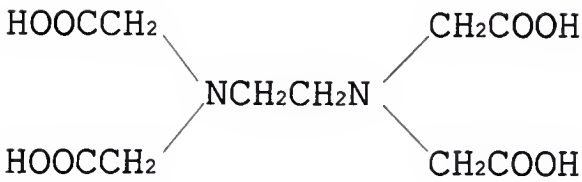

(d)

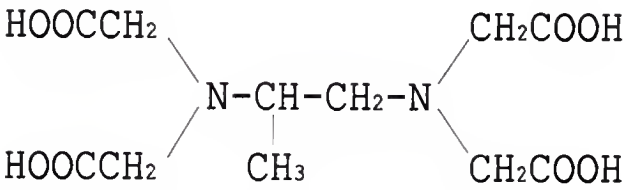

(e)

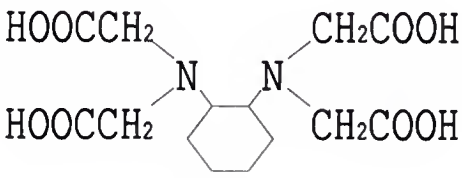

(f)

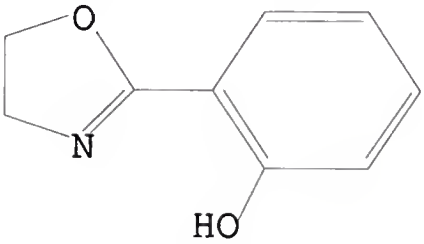

(g)

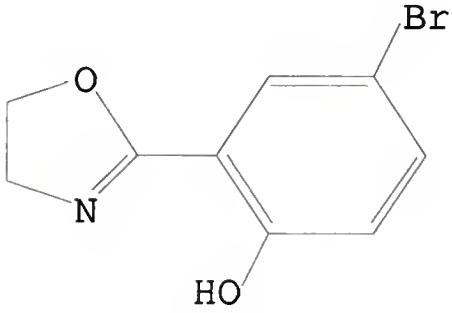

(h)

Figure 5-1. Structures of Ligands in Table 5-1.

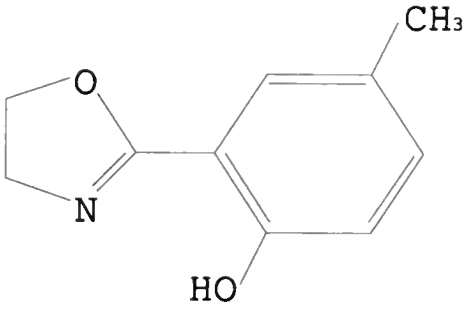

(i)

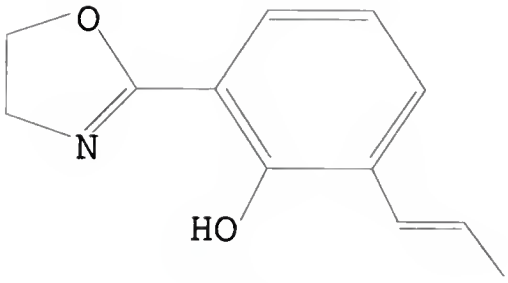

(j)

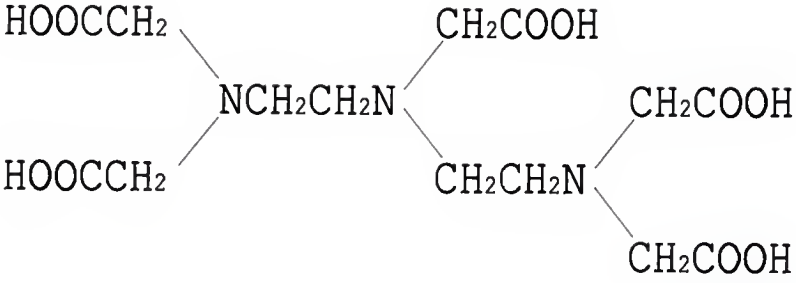

(k)

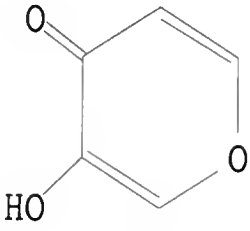

(l)

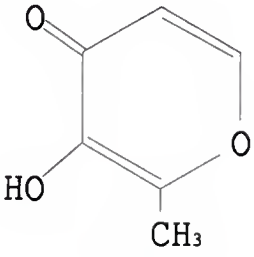

(m)

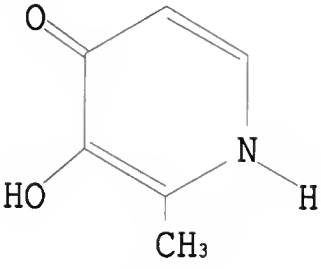

(n)

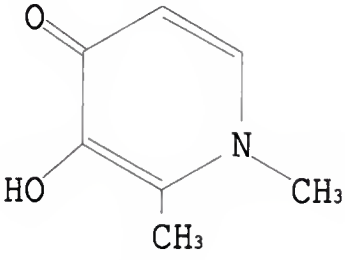

(o)

Figure 5-1 -- Continued.

water molecules are present in the place of chelating ligands, the smaller the chemical shift. Because some of the data reported were for aqueous species without x-ray data, the precise symmetry of several of the compounds can not be known. However, it has been reported that the chemical shift for a distorted octahedral compound will be larger than for one with an ideal geometry.[39] This could explain the smaller chemical shift when more water molecules are present.

Although not included in this table, the results of the Al-27 NMR spectra for $Al(meox)_3$ (**Ia**) and $Al(ox)_3$ (**IIa**) are summarized below. In the solid **Ia**, the main peak appeared at 54 ppm, but there was also a smaller peak at 221 ppm. For the solid **IIa**, there were three peaks present. The two larger peaks, of almost equal height, occurred at 5 and 73 ppm. A much smaller peak was present at -120 ppm. After **IIa** was dissolved in ethanol and left to concentrate by evaporation (**IIb**), only one large peak was present at 54 ppm. It should be noted that the crystals formed from this solution were characterized by x-ray crystallography and the $Al(ox)_3$ structure confirmed.

Experimental

Compounds **III** through **VII** were analyzed in the solid and solution state using a NT-300 Al-27 NMR spectrophotometer with spectrometer frequency 78.176839 MHz. The magic-angle spinning frequency was between 1.1 and 2.4 kHz.

Table 5-2. Al-27 NMR Peak Data for Compounds **III** through **VII**.

Ligand	Compound	δ, ppm for solid	δ, ppm for solution
pic	**III**	94	65
		-198	15
mpic	**IV**	167	68
		-202	
		-317	
pza	**V**	0	70
hyp	**VI**	7	68
		74	80
dipic	**VII**	85	68
		162	
		-236	

The solutions were prepared by heating the solid in d_6-DMSO at 40°C to produce clear colorless solutions. The peak data are summarized in Table 5-2. The spectra are shown in Figures 5-2 through 5-6.

During the synthesis of compound **V**, the solution containing pza and the aluminum ion began to turn a pale pink color as the pH was raised, however, the solid formed is white. Solutions containing varying aluminum ion to ligand ratios were prepared by dissolving the appropriate amounts of pza and $Al(NO_3)_3 \cdot 9H_2O$, followed by the slow addition of solid $NaHCO_3$ to raise the pH to 5. The solutions were submitted for Al-27 NMR spectral analysis under the same experimental

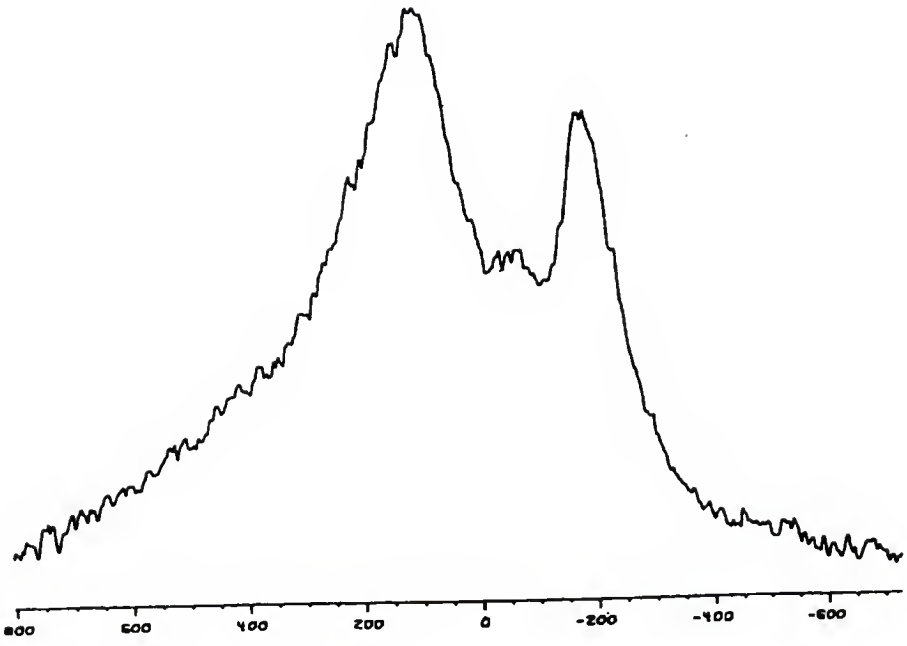

(a)

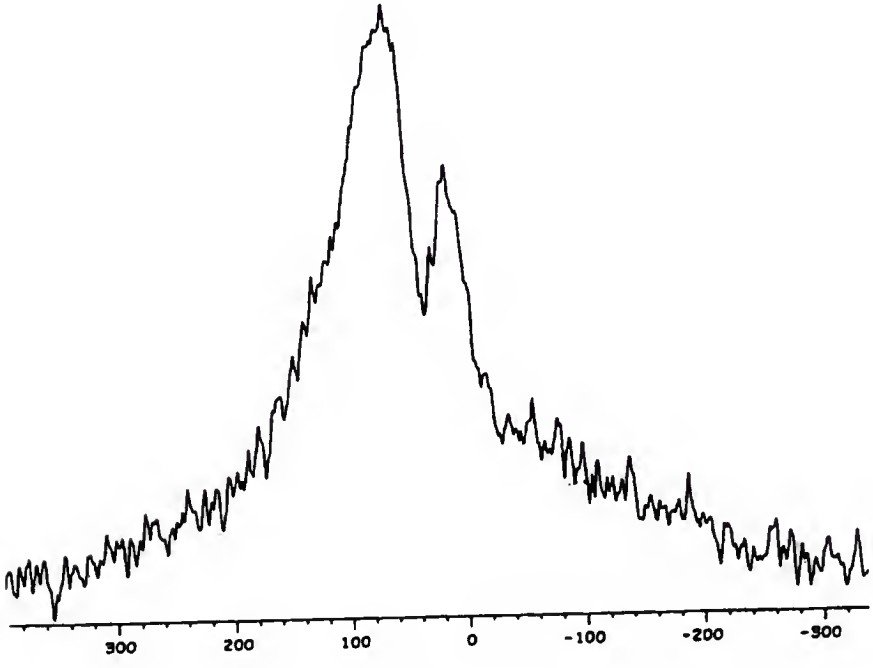

(b)

Figure 5-2. Al-27 NMR Spectra of **III**, a) Solid, b) in d_6-DMSO.

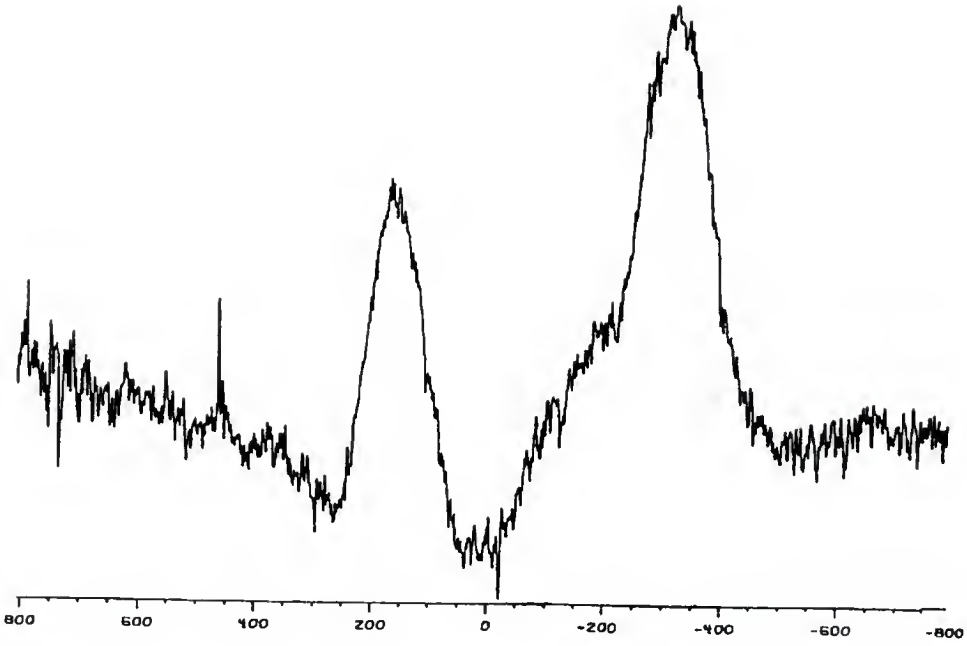

(a)

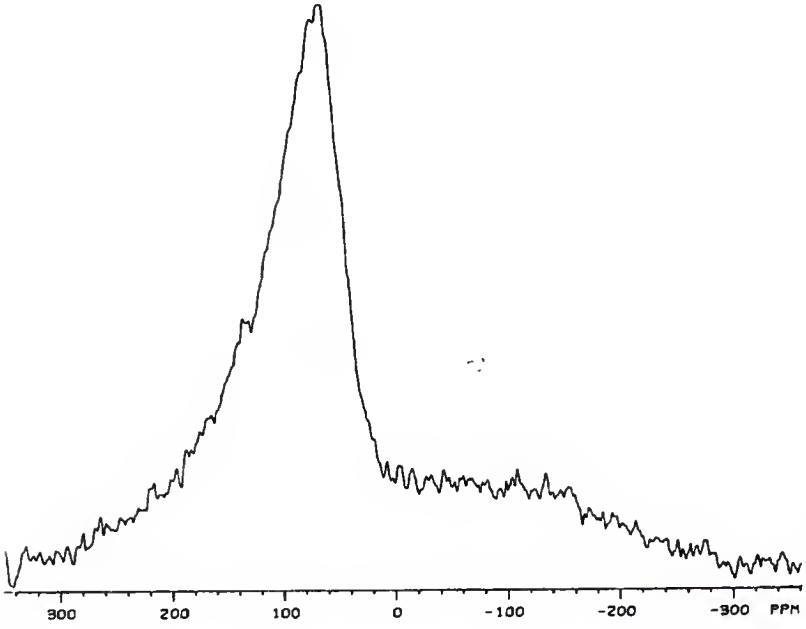

(b)

Figure 5-3. Al-27 NMR Spectra of **IV**, a) Solid, b) in d_6-DMSO.

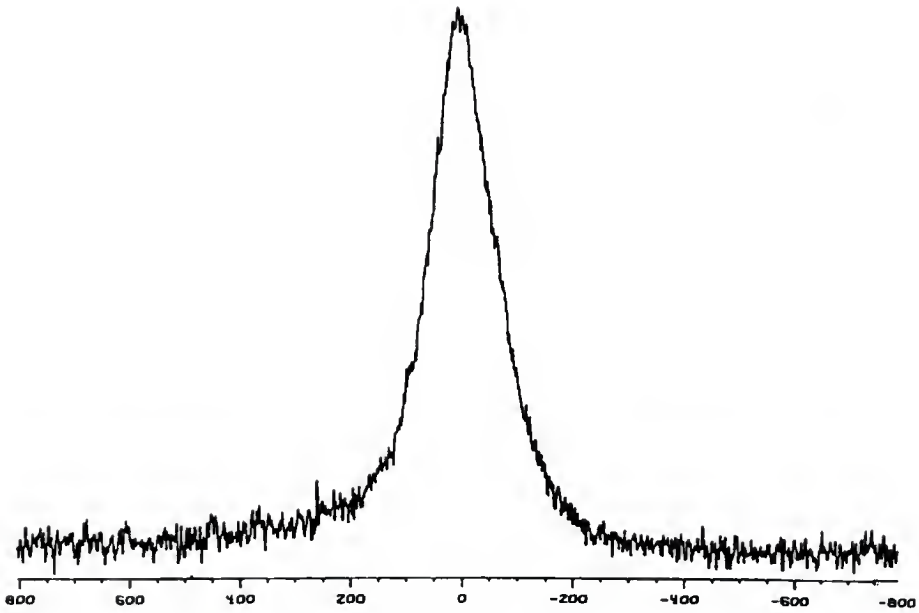

(a)

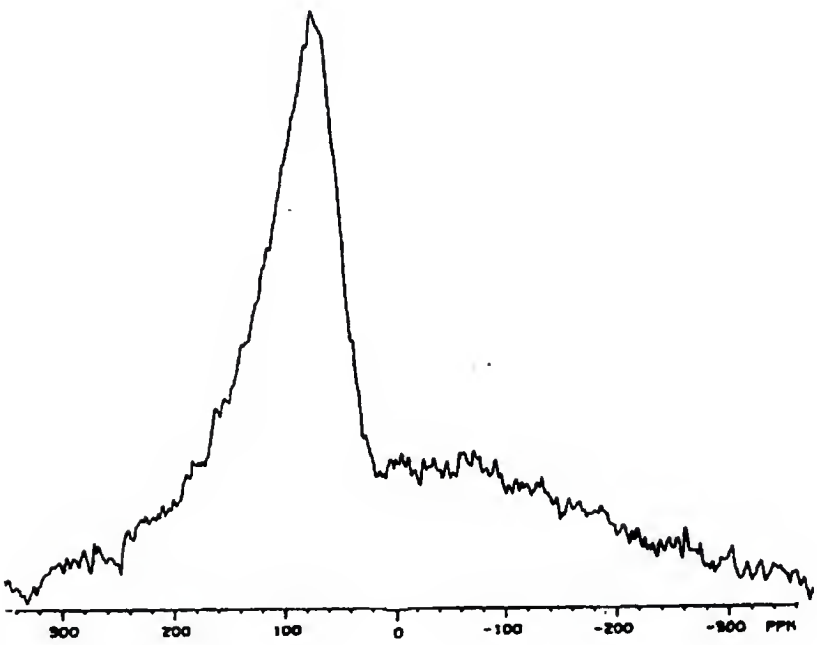

(b)

Figure 5-4. Al-27 NMR Spectra of **V**, a) Solid, b) in d_6-DMSO.

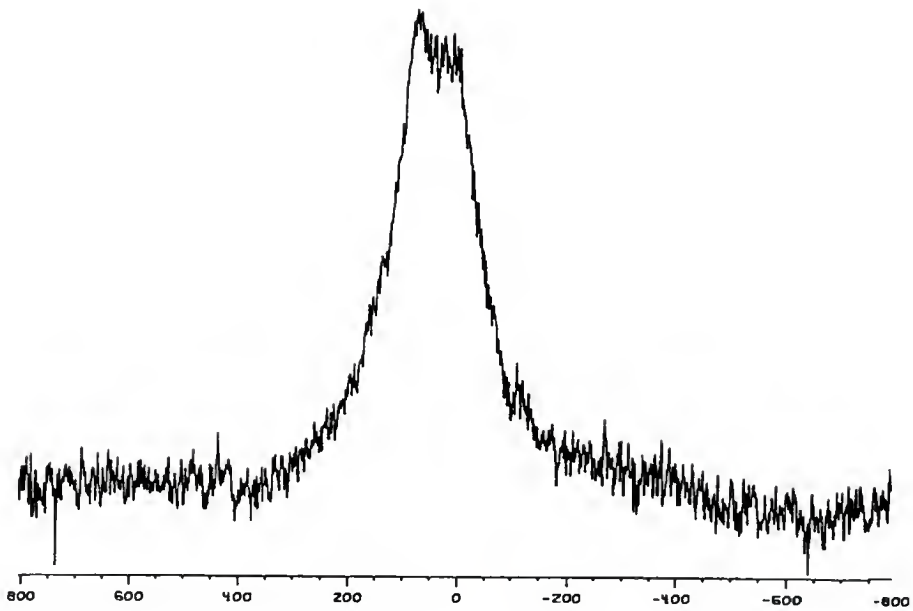

(a)

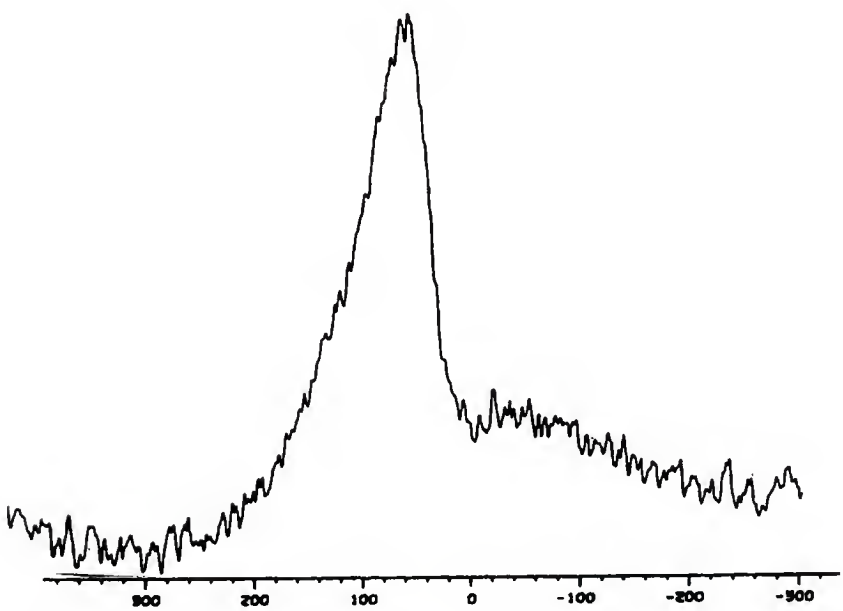

(b)

Figure 5-5. Al-27 NMR Spectra of **VI**, a) Solid, b) in d_6-DMSO.

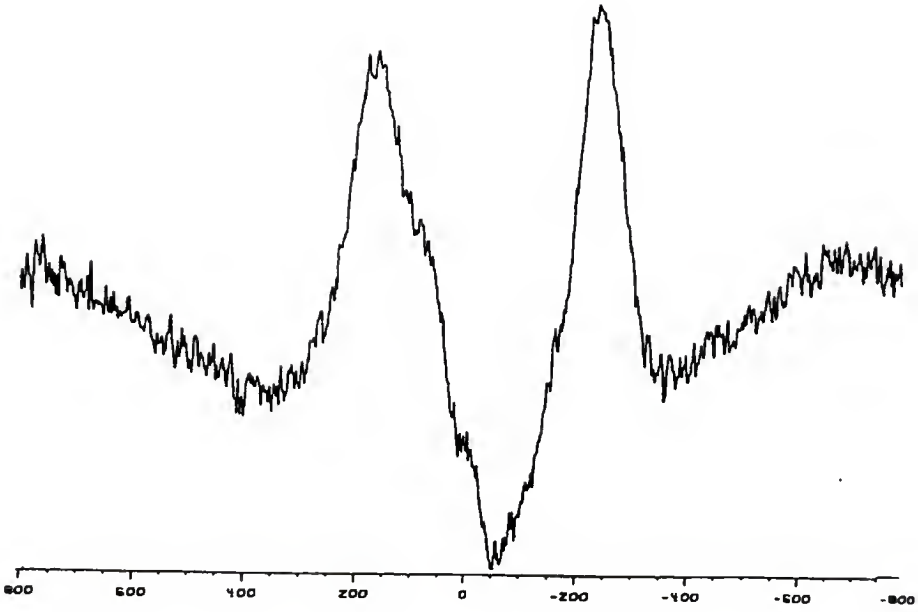

(a)

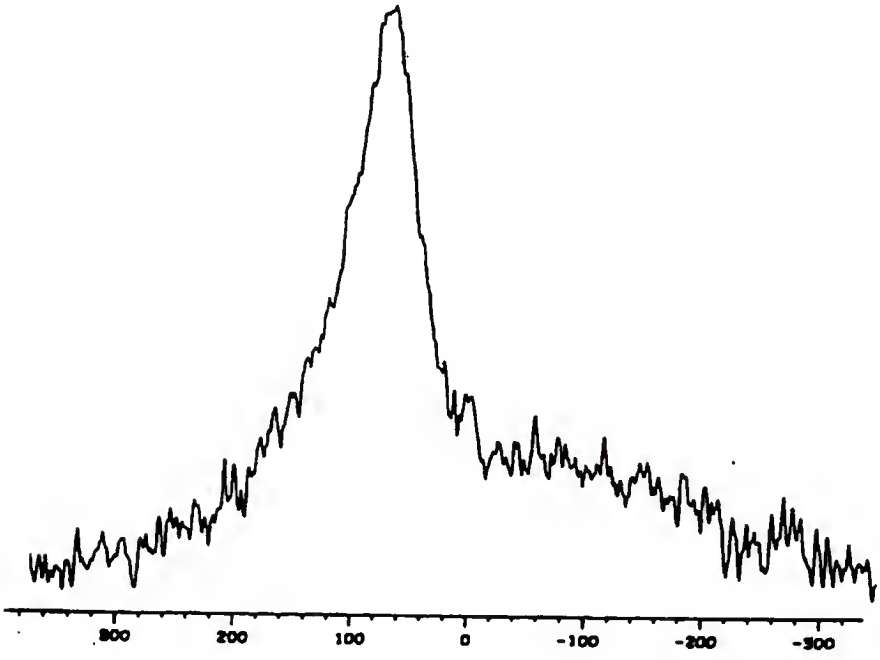

(b)

Figure 5-6. Al-27 NMR Spectra of **VII**, a) Solid, b) in d_6-DMSO.

Table 5-3. Al-27 NMR Data for Solutions Containing 0.30 M Al^{3+} and the Tabulated Concentration of pza at pH 5.

[pza], M	shift, ppm	rel. ht.
0 M	0	21.8
	2	0.3
	63	1.0
0.30 M	0	21.7
	18	0.3
	28	0.1
	60	0.1
0.60 M	0	21.8
	8	1.3
	17	0.5
	60	0.1
0.90 M	0	21.8
	7	5.6
	16	3.6
	60	0.1

conditions as all other samples. The data are summarized in Table 5-3. The spectra are shown in Figures 5-7 through 5-10.

Results

Most of the solid and solution samples produced more than one peak using Al-27 NMR. It is clear that each of these contains a mixture of aluminum environments. However, in each solution, there is a peak near 68 ppm which is rather close to one of the large peaks, at 73 ppm, in the spectrum of the solid **IIa**. This could confirm the presence of a tris aluminum

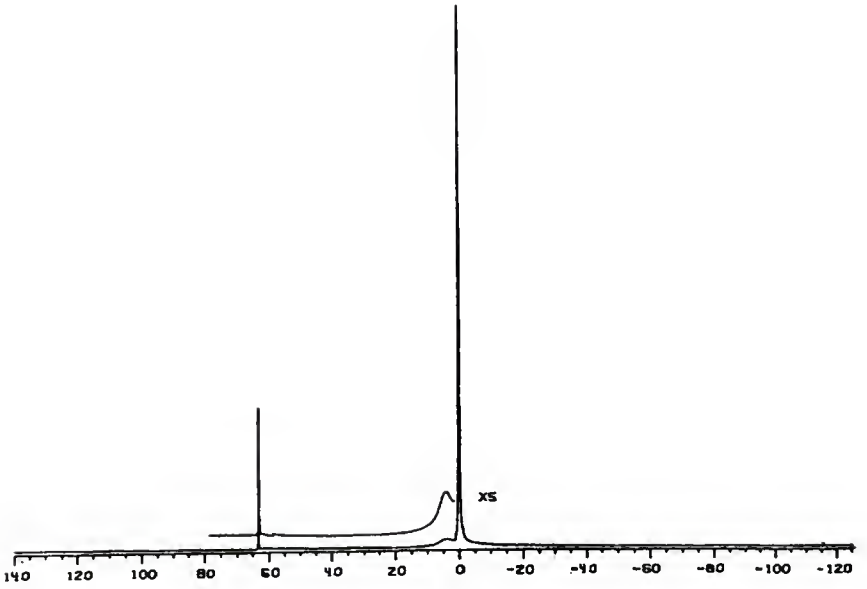

Figure 5-7. Al-27 NMR Spectrum of an Aqueous Solution Containing 0.30 M Al^{3+} at pH 5.

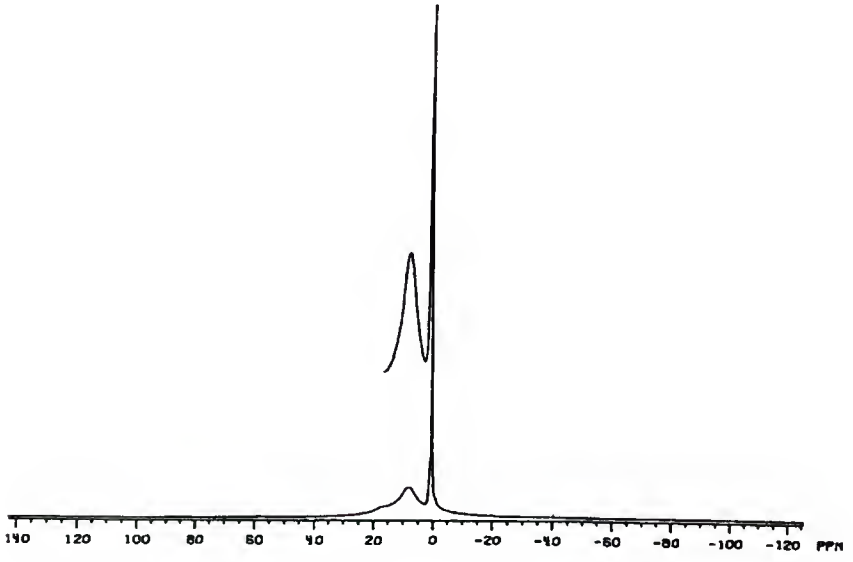

Figure 5-8. Al-27 NMR Spectrum of an Aqueous Solution Containing 0.30 M Al^{3+} and 0.30 M pza at pH 5.

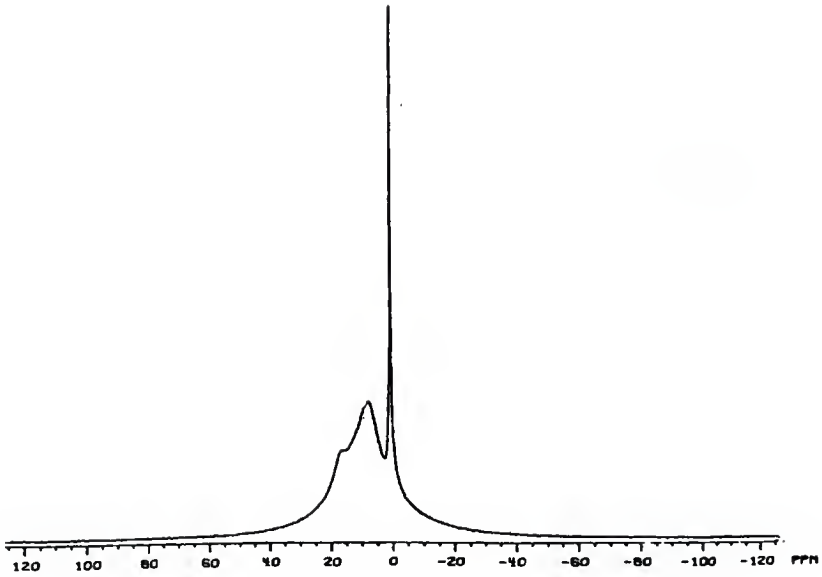

Figure 5-9. Al-27 NMR Spectrum of an Aqueous Solution Containing 0.30 M Al^{3+} and 0.60 M pza at pH 5.

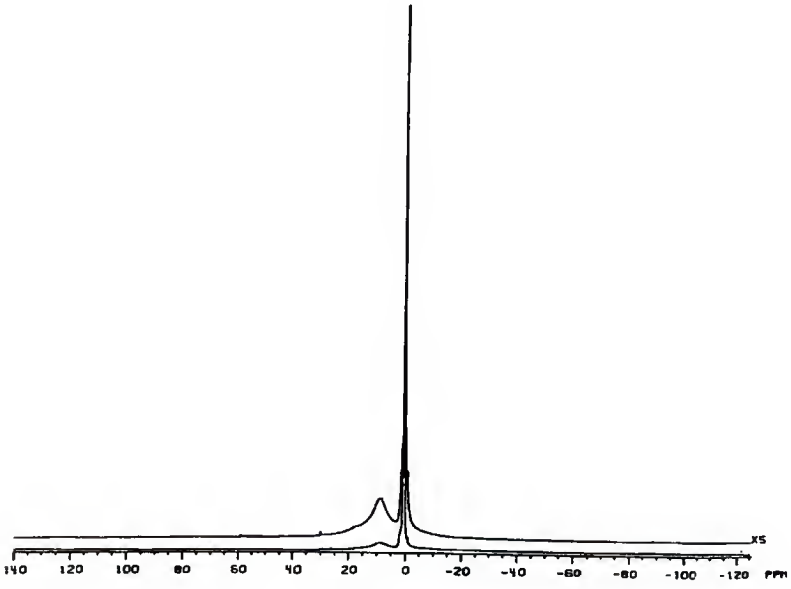

Figure 5-10. Al-27 NMR Spectrum of an Aqueous Solution Containing 0.30 M Al^{3+} and 0.90 M pza at pH 5.

complex experiencing the same effects as $Al(ox)_3$ between solid and solution phases. It should be noted that when **IIa** was dissolved to form **IIb**, the only peak present in the Al-27 NMR spectrum was at 54 ppm. Also, there are no peaks near 70 for any of the solid samples except for **VI** with hypoxanthine. It does not seem likely for the ion $[Al(DMSO)_6]^{3+}$ to be responsible for these peaks since its chemical shift has been reported as near 3 ppm.[40] The peak at 7 ppm for the solid sample **VI** could be a DMSO complex of aluminum.

The Al-27 NMR data confirms the presence of aluminum in each sample but also suggests the existence of more than one product for all of the samples except **V**. Furthermore, since no coordination compounds have been assigned to the myriad of chemical shifts present in the spectra, little information can be gained about the environment of the aluminum ions in the compounds that have been analyzed.

Compound **V**, with pyrazinoic acid, has only one peak in both the solid and solution phases, but these occur at distinctly different chemical shifts. The solution peak is at 70 ppm similar to the other solutions. The solid, however, has one peak at 0 ppm, characteristic of $Al(H_2O)_6^{3+}$ or a perfect octahedral environment. The series of solutions containing aluminum ion and varying amounts of pza show that in the absence of the ligand, there are no peaks between approximately 2 and 60 ppm. The main peak in each spectra is at 0 ppm, which is most probably due to a large amount of

unreacted $Al(H_2O)_6^{3+}$. However, in the spectra for solutions with the ligand present, peaks near 7, 17 and 28 ppm are present. These are possibly due to species formed from the hydrated aluminum ion being involved in a series of pH dependent equilibria. These equations seem to represent a

$$Al^{3+} + Hpza \rightleftharpoons Al(pza)^{2+} + H^+ \quad (1)$$

$$Al(pza)^{2+} + Hpza \rightleftharpoons Al(pza)_2^+ + H^+ \quad (2)$$

$$Al(pza)_2^+ + H_2O \rightleftharpoons Al(pza)_2(OH) + H^+ \quad (3)$$

$$Al(pza)_2^+ + Hpza \rightleftharpoons Al(pza)_3(s) + H^+ \quad (4)$$

reasonable set of chemical reactions possible in an aqueous solution with a ligand such as pza. Once the tris complex is formed, it precipitates and, as a result, only three peaks other than the hexaaquaaluminum(III) ion should be present. The series is similar to that proposed for aluminum and picolinic acid, a ligand of similar reactivity.[34] Further tests or x-ray studies to confirm the structure of the complexes.

Elemental Analysis

Each of the solid samples were submitted for elemental analysis. The results are summarized in Table 5-4 as percentages of carbon, hydrogen and nitrogen present. Also included are mole ratios, scaled to the number of nitrogen atoms per ligand molecule, and, at the bottom of the table,

Table 5-4. Elemental Analysis Data for Compounds **III** through **VII** and Pure Tris Complexes of the Ligands.

Compound	Data type	Carbon	Hydrogen	Nitrogen
III	% comp.	48.06	3.08	9.34
	ratio	6.00	4.58	1.00
IV	% comp.	38.38	3.85	6.90
	ratio	6.49	7.75	1.00
V	% comp.	26.12	4.30	11.85
	ratio	5.15	10.18	2.00
VI	% comp.	32.74	3.03	30.90
	ratio	4.94	5.49	4.00
VII	% comp.	33.84	3.57	5.40
	ratio	7.31	9.25	1.00
$Al(pic)_3$	% comp.	54.96	3.08	10.73
$Al(mpic)_3$	% comp.	57.93	4.17	9.65
$Al(pza)_3$	% comp.	45.46	2.29	21.21
$Al(hyp)_3$	% comp.	41.67	2.08	38.89
$Al(dipic)_3$	% comp.	48.01	2.30	8.00

the percentages that would be present if the samples were unsolvated tris complexes of the ligand.

The data confirms the presence of the ligand in each of the compounds because the molar ratios of carbon to nitrogen are, for the most part, very close to those of the ligands. However, because the amount of hydrogen is high, most likely due to the presence of water molecules, the molar ratios involving hydrogen do not correspond to those of the deprotonated ligands. The percentages for the tris complexes were included to illustrate the amount of error that would

exist due to impurities if the synthesized compounds were the tris complexes. Furthermore, the Al-27 NMR confirmed the presence of more than one aluminum environment in all of the samples except for **V**. As a result, the elemental percentages would not match those of any particular compound.

Infrared Spectroscopy

The IR spectra for pic, mpic, pza and dipic and the sodium salts were prepared on a Perkin-Elmer Fourier Transform Infrared Spectrophotometer. IR spectra were also taken for compounds **III**, **IV**, **V** and **VII**. The data for the carbonyl stretching frequency in each compound is summarized in Table 5-5. Hypoxanthine was not included because it has no carboxylic acid group.

Table 5-5. FTIR Carbonyl Peak Data, cm^{-1}.

Ligand	Unreacted ligand	Sodium salt	Disodium salt	Aluminum compound	Compound
pic	1715	1584	-	1672	**III**
mpic	1677	1587	-	1683	**IV**
pza	1713	1612	-	1678	**V**
dipic	1693	1634 1731	1618	1610 1666	**VII**

Each aluminum compound has a carbonyl stretching frequency between 1660 and 1690 cm^{-1}, between characteristic carboxylic acid and carboxylate ion regions.[52] For **III** and **V**, the single peak occurs between the peaks for the sodium salt

and the ligand. This would indicate that in the aluminum compound, the coordination of the ligand to the metal ion produces a change in the double bond character that is distinct from the perturbation caused by the presence of the sodium near the carboxylate ion. For mpic, the ligand stretching frequency is lower, probably due to the formation of an acid dimer.[52] However, the peak for **IV** is near those for **III** and **V**, and, as such, has the ligand coordinated to the aluminum ion. For **VII**, there are two peaks present. The peak at 1666 cm^{-1} is in the region of the other aluminum compounds and is, therefore, probably due to a coordinated carboxylate group. The other peak is close to the one peak for the disodium dipicolinate salt. The presence of two peaks could indicate two differently reacting carboxylate groups in one compound or two compounds with different carboxylate groups. For the other aluminum compounds, it should be noted that, despite the presence of more than one aluminum environment, there is only one visible carbonyl stretching band. Either, the ligand is coordinated by the same strength bond in every compound in the mixture or the coordination is so similar that there is not a distinguishable difference in the carbonyl stretching frequency.

Fast Atom Bombardment Mass Spectrometry

FABMS were prepared for **III**, **IV**, **V** and **VI**. Data from these are given in Table 5-6. Most peaks smaller than ten percent relative abundance have been omitted.

For **III**, the sample containing pic, the peak at m/z=204 is possibly due to $AlL(H_2O)_3^+$. There was no peak corresponding to one ligand molecule, but a peak m/z=79 is probably due to the ligand fragment left after the loss of carbon dioxide. In addition, small peaks due to combinations of aluminum, the ligand and hydroxide were present. The peaks for $AlL(OH)_2$-2 (m/z=181), $AlL_2(OH)$+3 (m/z=291), and AlL_3-3(OH) (m/z=342) appear with m/z=291 being the weakest. Furthermore, a small peak is present for AlL_3+1. It seems likely that the free ligand would more easily decarboxylate than a coordinated ligand. Instead the coordinated ligand seems to lose a hydroxyl group, leaving the coordination sphere intact. Although the spectrum does support the presence of a tris complex, the actual proportions of the complexes originally present would be difficult to determine due to the extensive fragmentation of the complexes and ligand molecules.

For sample **IV**, the largest peak corresponds to L+1, with a decent size fragment due to the decarboxylation of the ligand. Other prevalent peaks, m/z=166, m/z=299 and m/z=436 are most likely due to complexes such as AlL+3, AlL_2, and AlL_3+1, respectively. Although there are many fragments produced, with the ligand being the greatest in abundance,

Table 5-6. FABMS Peak Data.

Sample **III**		Sample **IV**		Sample **V**		Sample **VII**	
m/z	RA*	m/z	RA*	m/z	RA*	m/z	RA*
50	11.14	94	22.08	69	10.06	137	100.0
51	39.43	120	28.28	81	2.44	138	16.75
52	12.82	138	100.0	107	21.99	165	25.96
63	11.26	139	40.00	125	100.0	177	19.65
77	26.99	166	51.92	138	33.78	273	32.53
78	14.36	167	15.72	153	11.64	301	1.95
79	24.66	178	46.24	165	13.03	313	1.41
130	11.53	213	52.48	187	13.34	391	0.04
131	16.82	214	11.52	397	1.06		
159	36.97	257	43.12				
181	57.88	299	10.64				
203	29.60	436	15.16				
204	100.0						
291	0.15						
326	61.85						
327	46.16						
342	59.59						
343	17.48						
362	70.88						
363	16.01						
394	0.11						

* RA stands for the percent relative abundance.

the original sample contained a fair percentage of the tris complex.

With only a few peaks at large masses, the spectrum for compound **V**, containing pza, does not provide much detail about the ratios of complexes present in the original sample. Although the ligand was the most prevalent ion, it is apparent by the peaks at m/z=107 and m/z=81 that the ligand decomposed by losing small fragments such as H_2O and CO_2. The small peak at m/z=397 is most probably due to AlL_3+1. One other small peak at m/z=187, which could be due to $AlL(OH)_2$+3 or AlL_2-2CO_2, seems to be the only other indication of an aluminum complex.

The spectrum of **VI**, with the largest peak (m/z=137) corresponding to L+1, does not provide much information on the relative amounts of complexes present in the sample. The remaining large peaks, m/z=165, m/z=177, and m/z=273, are probably due to AlL+3, AlL(OH)-2 and 2HL+1, respectively. Two of the smaller peaks, m/z=301 and m/z=313, are probably due to AlL_2+4 and AlL_2(OH)-1. There is no peak present near m/z=432, where AlL_3 would be. The nearest peak, m/z=391, is smaller by 41 units. It seems reasonable that one ring is a complex could have fragmented. The small peak at M-43 could be due to the loss of part of one of the rings. By a similar fragmentation, any AlL_3 that could have been present may have been responsible for this peak.

Conclusion

The structure of the compounds **III** through **VII** can not be determined from the data provided by the three techniques discussed in this chapter. Without more thorough calibration of the Al-27 NMR scale, the available data merely confirms the presence of the aluminum ion in more than one possible environment in a single sample. In addition, without a pure sample, elemental analysis provides little information beyond the confirmation of the ligand's presence. Finally, the carbonyl stretching frequency data confirms the coordination of the aluminum ion to the ligand yet does not provide any further information. Without the use of x-ray

crystallography, the structures of the aluminum coordination compounds synthesized for this work are virtually impossible to elucidate.

CHAPTER 6

A PENTAGONAL BIPYRAMIDAL SODIUM COMPOUND: SYNTHESIS AND CRYSTAL STRUCTURE

Introduction

A naturally occurring ligand, 2,6-pyridinedicarboxylic acid, shown in Figure 6-1, can act as an electron donor from the nitrogen as well as the two carboxylate oxygens. Known by the trivial name dipicolinic acid, this molecule has been reported in a variety of compounds as a tridentate ligand.[45-51] There are several modes of coordination of the carboxylate and carboxylic acid groups. Dipic has been shown to coordinate metal ions via the carbonyl oxygen in the carboxylic acid and by the hydroxy group in the carboxylate ion. In addition, the carboxylate oxygen atoms sometimes act as donor atoms to a second metal ion, thereby linking together chains of asymmetric units.[47,48]

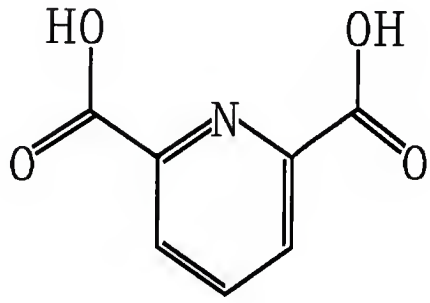

Figure 6-1. Dipicolinic acid.

The structure discussed in this chapter was initially classified as an aluminum compound because of the experimental conditions and the Al-27 NMR spectrum proving the existence of an uncharacterized aluminum dipic complex. However, further investigation, including structure refinement, supported the presence of sodium as the central metal ion instead of aluminum.

Experimental

Synthesis

Materials. All chemicals were used as supplied by the manufacturer.

Preparation of $Na(C_7H_4NO_4)(C_7H_5NO_4)\cdot 3H_2O$ (**VIII**). With stirring, 0.50 g agar was added to 100 mL H_2O. The temperature of the mixture was slowly raised to and maintained at 98°C for 5 minutes. The 0.5 % agar solution was removed from heat and allowed to cool. After the agar reached 50°C, 1.68 g $NaHCO_3$ (20.0 mmole) was dissolved in the agar. Without touching the sides, 15 mL of the basic agar medium was poured into a vial (approximately 2 cm diameter) and allowed to cool overnight. In 15 mL H_2O, both 0.1251 g $Al(NO_3)_3\cdot 9H_2O$ (0.33 mmole) and 0.1673 g dipicolinic acid (1.0 mmole) were dissolved to provide a solution 0.022 M in Al^{3+} and 0.67 M in ligand. The solution was transferred to the vial above the solidified 0.20 M $NaHCO_3$ agar and tightly sealed to prevent loss of solvent. After 24 days, clear colorless crystals had

grown to the size suitable for x-ray diffraction studies. Large crystals and the remaining solid was pasteured from the agar, washed with water and dried for further analysis.

Elemental Analysis

The percentages of carbon, hydrogen and nitrogen in compound **VIII** are listed in Table 6-1 with the calculated values for the compounds $Al(C_7H_3NO_4)(C_7H_4NO_4)\cdot 3H_2O$ and $Na(C_7H_4NO_4)(C_7H_5NO_4)\cdot 3H_2O$. Although the agreement is reasonable

Table 6-1. Elemental Analysis of **VIII**.

	Na compound	**VIII**	Al compound
% C	40.99	40.92	40.79
% H	3.69	3.58	3.18
% N	6.83	6.69	6.79

for either set of data, the error for carbon and hydrogen is one-half and one-fourth, respectively, for the sodium compound. However, the percentage of nitrogen present is slightly closer for the aluminum compound. Some of the error in the percentages can be traced to the agar medium in which **VIII** was grown. Although the crystals were pasteured out of the agar and then washed, trace amounts of the cellulose gel could affect the elemental analysis results.

X-ray Crystallographic Analysis

A clear colorless crystal measuring 0.34 × 0.26 × 0.13 mm was mounted on a glass fiber for diffraction studies. All subsequent data were collected at room temperature on a Siemans R3m/V diffractometer equipped with a graphite

monochromator utilizing Mo Kα radiation (λ = 0.71073 Å). The cell parameters were refined for 50 reflections with 20.0° ≤ 2θ ≤ 22.0°. 3305 reflections were collected using the ω-scan method. Four reflections were measured every 96 reflections to monitor instrument and crystal stability (maximum correction was 1 %). Absorption corrections were applied based on measured crystal faces using *SHELXTL plus* (Sheldrick, 1990); absorption coefficient, μ = 0.16 mm^{-1} (min. and max. transmission factors are 0.955 and 0.981, respectively).

The structure was solved by direct methods in *SHELXTL plus* (Sheldrick, 1990) from which the locations of all of the non-hydrogen atoms were obtained. During the initial elemental assignment, an aluminum ion was entered as the central metal atom. Fifteen hydrogen atoms were located from a Difference Fourier map. The assignment of aluminum as the central metal ion was changed to a sodium to obtain electroneutrality. The structure was refined in *SHELXTL plus* using full-matrix least squares. The non-hydrogen atoms were treated anisotropically, whereas the hydrogen atoms were refined with isotropic thermal parameters. H7 is disordered between O7 and O7′. The disorder could not be resolved but H7′ was refined in a position approximately midway between O7 and O7′. 313 parameters were refined and Σ w $(|F_o| - |F_c|)^2$ was minimized; $w=1/(\sigma|F_o|)^2$, $\sigma(F_o) = 0.5kI^{-1/2}\{[\sigma(I)]^2 + (0.02I)^2\}^{1/2}$, I(intensity) = $(I_{peak} - I_{background})$(scan rate), and $\sigma(I) = (I_{peak} + I_{background})^{1/2}$(scan rate), k is the correction due to

decay and Lp effects, 0.02 is a factor used to down weight intense reflections and to account for instrument instability. The linear absorption coefficient was calculated from values from the *International Tables for X-ray Crystallography* (1974). Scattering factors for non-hydrogen atoms were taken from Cromer & Mann (1968) with anomalous-dispersion corrections from Cromer & Liberman (1970), while those of the hydrogen atoms were from Stewart, Davidson & Simpson (1965).

Discussion

X-ray Diffraction Analysis.

Crystallographic data for the compound are summarized in Table 6-2. Compound **VIII** is shown as an ORTEP drawing in Figure 6-2. Final atomic parameters for the non-hydrogen atoms and the hydrogen atoms are given in Tables 6-3 and 6-4, respectively. The bond lengths and bond angles for all atoms appear in Tables 6-5 and 6-6. The anisotropic thermal for the non-hydrogen atoms are listed in Table 6-7.

Initially, aluminum was assigned as the central atom, although no seven coordinate aluminum complex has been reported. However, during refinement, fifteen hydrogen atoms were found, indicating the loss of only one hydrogen atom from the dipic and water molecules. If aluminum were the metal ion, two less hydrogen atoms should be present to give a neutrally charged compound.

Table 6-2. Crystallographic Data for Compound **VIII**.

Compound	$Na^+(C_7H_4NO_4^-)(C_7H_5NO_4)\cdot 3H_2O$
Empirical formula	$C_{14}H_9N_2O_8Na\cdot 3H_2O$
Formula wt, g	410.27
Crystal system	Triclinic
Space group	$P\bar{1}$
a, Å	6.905(1)
b, Å	11.141(1)
c, Å	11.209(1)
α, °	85.64(1)
β, °	82.28(1)
γ, °	87.33(1)
V_c, Å^3	851.4(2)
Z	2
D_{calc}, g/cm^3 (298K)	1.600
Radiation, λ (Å)	Mo-Kα, 0.71073
μ, mm^{-1}	0.16
F(000), electrons	424
Crystal dimensions (mm^3)	0.34 × 0.26 × 0.13
2θ range	20.0, 22.0
Observed reflections	3305
Number of parameters	313
Final *R*	4.26
R_w	4.99

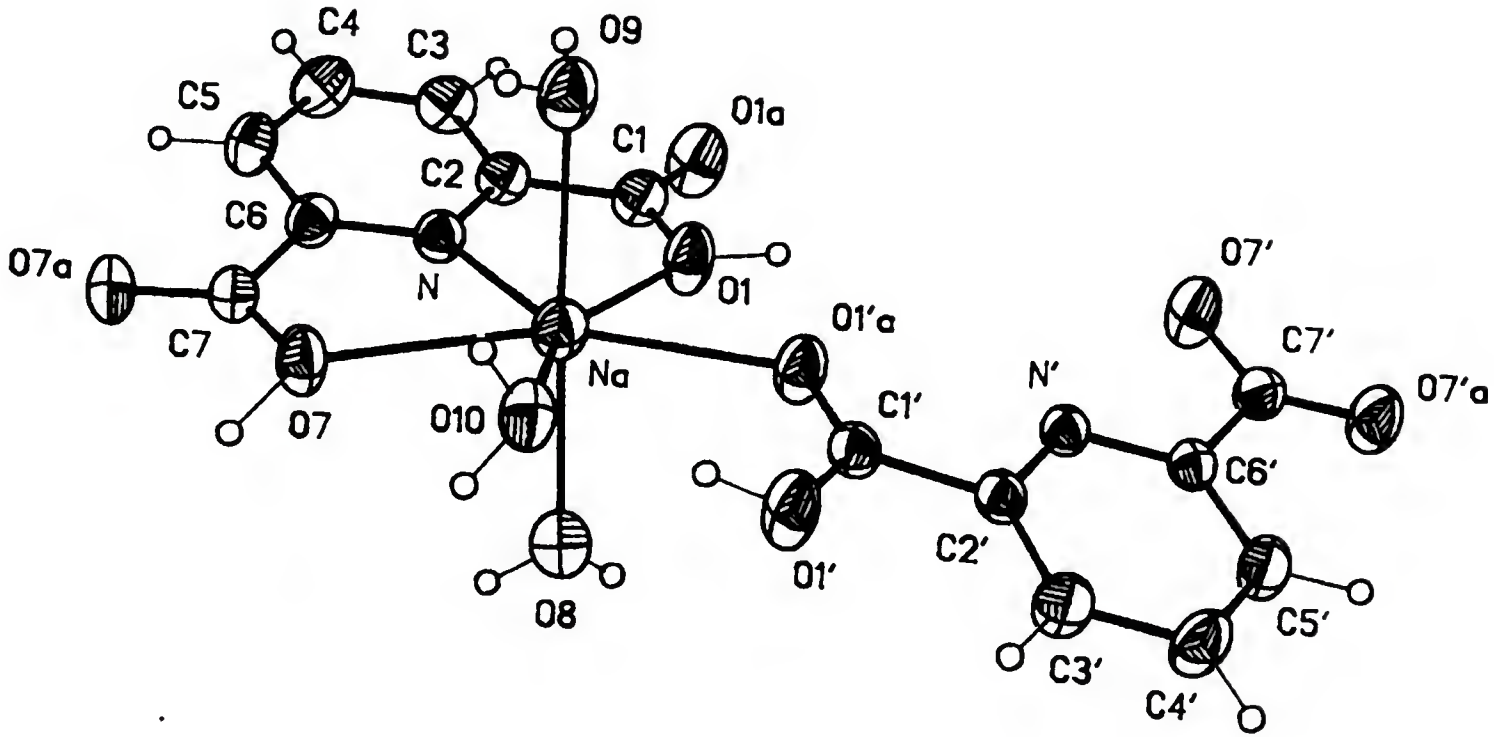

Figure 6-2. ORTEP Representation of **VIII**.

Table 6-3. Final Atomic Coordinates ($\times 10^4$) and Isotropic Thermal Parameters ($Å^2$) for the Non-Hydrogen Atoms of Compound **VIII**. Estimated Standard Deviations are given in Parentheses.

Atom	x	y	z	U
Na	0.3065 (1)	0.7025 (1)	0.0573 (1)	0.0398 (3)
N	0.2625 (3)	0.7675 (2)	-0.1538 (2)	0.0301 (6)
O1	0.2407 (3)	0.5401 (1)	-0.0701 (1)	0.0470 (6)
O1a	0.2179 (3)	0.4779 (1)	-0.2523 (1)	0.0541 (7)
O7	0.2605 (3)	0.9315 (1)	0.0082 (1)	0.0435 (6)
O7a	0.2839 (3)	1.0823 (1)	-0.1346 (2)	0.0462 (6)
C1	0.2374 (3)	0.5573 (2)	-0.1862 (2)	0.0370 (8)
C2	0.2629 (3)	0.6855 (2)	-0.2351 (2)	0.0318 (7)
C3	0.2884 (4)	0.7144 (2)	-0.3591 (2)	0.0381 (8)
C4	0.3164 (4)	0.8324 (2)	-0.3999 (2)	0.0426 (8)
C5	0.3139 (4)	0.9184 (2)	-0.3170 (2)	0.0391 (8)
C6	0.2853 (3)	0.8825 (2)	-0.1949 (2)	0.0317 (7)
C7	0.2767 (3)	0.9739 (2)	-0.1014 (2)	0.0343 (7)
N'	0.2375 (3)	0.2856 (1)	0.2845 (1)	0.0278 (5)
O1'	0.3074 (3)	0.5793 (1)	0.3677 (2)	0.0496 (6)
O1'a	0.3176 (3)	0.5116 (1)	0.1845 (1)	0.0431 (6)
O7'	0.2413 (3)	0.0956 (1)	0.1466 (1)	0.0481 (6)
O7'a	0.1727 (3)	-0.0291 (1)	0.3094 (2)	0.0558 (6)
C1'	0.2899 (3)	0.4955 (2)	0.2935 (2)	0.0315 (7)
C2'	0.2356 (3)	0.3767 (2)	0.3574 (2)	0.0296 (7)
C3'	0.1899 (4)	0.3631 (2)	0.4816 (2)	0.0390 (8)
C4'	0.1419 (4)	0.2502 (2)	0.5346 (2)	0.0432 (8)
C5'	0.1461 (4)	0.1558 (2)	0.4623 (2)	0.0370 (8)
C6'	0.1949 (3)	0.1767 (2)	0.3383 (2)	0.0285 (6)
C7'	0.2021 (3)	0.0715 (2)	0.2597 (2)	0.0347 (7)
O8	-0.0025 (3)	0.7263 (2)	0.1602 (2)	0.0613 (8)
O9	0.6637 (3)	0.6795 (2)	-0.0162 (2)	0.0438 (6)
O10	0.4017 (3)	0.7797 (2)	0.2435 (2)	0.0488 (7)

For anisotropic atoms, the U value is $U_{eq} = \frac{1}{3}\Sigma_i\Sigma_j\ U_{ij}\ a_i^*\ a_j^*\ A_{ij}$ where A_{ij} is the dot product of the ith and j^{th} direct space unit cell vectors.

Table 6-4. Final Atomic Coordinates ($\times 10^4$) and Isotropic Thermal Parameters ($Å^2$) for the Hydrogen Atoms of Compound **VIII**. Estimated Standard Deviations are given in Parentheses.

Atom	x	y	z	U
H1	0.258 (5)	0.459 (3)	-0.041 (3)	0.076 (10)
H7	0.240 (5)	1.011 (3)	0.081 (3)	0.114 (13)
H3	0.292 (4)	0.649 (2)	-0.409 (2)	0.051 (7)
H4	0.334 (4)	0.856 (2)	-0.479 (2)	0.045 (7)
H5	0.326 (3)	1.004 (2)	-0.341 (2)	0.042 (6)
H1'	0.345 (5)	0.644 (3)	0.325 (3)	0.076 (10)
H3'	0.190 (4)	0.431 (2)	0.528 (2)	0.049 (7)
H4'	0.112 (4)	0.236 (2)	0.617 (3)	0.055 (7)
H5'	0.108 (4)	0.072 (2)	0.495 (2)	0.046 (7)
H8a	-0.076 (6)	0.793 (4)	0.147 (3)	0.10 (13)
H8b	-0.085 (7)	0.676 (4)	0.164 (4)	0.12 (2)
H9a	0.689 (6)	0.666 (3)	-0.082 (4)	0.11 (2)
H9b	0.704 (6)	0.736 (4)	-0.012 (4)	0.11 (2)
H10a	0.325 (4)	0.842 (3)	0.271 (3)	0.062 (9)
H10b	0.511 (5)	0.814 (3)	0.223 (3)	0.069 (10)

Table 6-5. Bond Lengths (Å) of all Atoms of Compound **VIII**. Estimated Standard Deviations are given in Parentheses.

Na-N	2.476(2)	Na-O1	2.482(2)
Na-O7	2.584(2)	Na-O1'a	2.474(2)
Na-O8	2.300(2)	Na-O9	2.501(2)
Na-O10	2.495(2)	N-C2	1.338(3)
N-C6	1.337(3)	O1-C1	1.304(3)
O1a-C1	1.219(3)	O7-C7	1.274(3)
O7a-C7	1.238(2)	C1-C2	1.500(3)
C2-C3	1.392(3)	C3-C4	1.372(3)
C4-C5	1.382(3)	C5-C6	1.387(3)
C6-C7	1.510(3)	N'-C2'	1.346(3)
N'-C6'	1.339(2)	O1'-C1'	1.317(3)
O1'a-C1'	1.209(2)	O7'-C7'	1.271(3)
O7'a-C7'	1.226(2)	C1'-C2'	1.495(3)
C2'-C3'	1.383(3)	C3'-C4'	1.385(3)
C4'-C5'	1.373(3)	C5'-C6'	1.390(3)
C6'-C7'	1.514(3)	O1-H1	0.94(3)
O7-H7	1.24(4)	C3-H3	0.95(3)
C4-H4	0.90(3)	C5-H5	0.98(2)
O1'-H1'	0.86(3)	C3'-H3'	0.95(3)
C4'-H4'	0.93(3)	C5'-H5'	1.01(2)
O8-H8a	0.90(4)	O8-H8b	0.81(5)
O9-H9a	0.76(4)	O9-H9a	0.71(4)
O10-H10a	0.90(3)	O10-H10b	0.86(3)

Table 6-6. Bond Angles (°) for all Atoms of Compound **VIII**. Estimated Standard Deviations given in Parentheses.

N-Na-O1	64.28(6)	N-Na-O7	63.67(6)
N-Na-O1'a	137.75(7)	N-Na-O8	103.38(8)
N-Na-O9	86.75(7)	N-Na-O10	141.59(7)
O1-Na-O7	126.54(6)	O1-Na-O1'a	73.53(6)
O1-Na-O8	98.39(8)	O1-Na-O9	89.69(7)
O1-Na-O10	153.54(6)	O7-Na-O1'a	157.32(6)
O7-Na-O8	82.41(7)	O7-Na-O9	98.73(7)
O7-Na-O10	79.87(6)	O1'a-Na-O8	84.17(7)
O1'a-Na-O9	91.12(7)	O1'a-Na-O10	80.26(6)
O8-Na-O9	169.05(9)	O8-Na-O10	82.20(8)
O9-Na-O10	87.27(8)	C2-N-C6	117.8(2)
Na-N-C2	119.99(13)	Na-N-C6	120.31(14)
Na-O1-C1	123.02(14)	Na-O7-C7	119.87(13)
O1-C1-C2	114.3(2)	O1a-C1-C2	121.2(2)
O1-C1-O1a	124.5(2)	N-C2-C3	123.1(2)
C1-C2-C3	120.4(2)	N-C2-C1	116.5(2)
C2-C3-C4	118.4(2)	C3-C4-C5	119.1(2)
C4-C5-C6	1.387(3)	N-C6-C7	116.8(2)
C5-C6-C7	120.6(2)	N-C6-C5	122.6(2)
O7-C7-O7a	124.8(2)	O7-C7-C6	115.9(2)
O7a-C7-C6	119.3(2)	C2'-N'-C6'	116.9(2)
Na-O1'a-C1'	129.10(14)	O1'-C1'-C2'	113.1(2)
O1'a-C1'-C2'	123.0(2)	O1'-C1'-O1'a	123.8(2)
N'-C2'-C3'	123.5(2)	C1'-C2'-C3'	121.7(2)
N'-C2'-C1'	114.7(2)	C2'-C3'-C4'	118.5(2)
C3'-C4'-C5'	118.8(2)	C4'-C5'-C6'	119.1(2)
N'-C6'-C7'	118.3(2)	C5'-C6'-C7'	118.7(2)
N'-C6'-C5'	123.1(2)	O7'-C7'-O7'a	125.5(2)
O7'-C7'-C6'	116.4(2)	O7'a-C7'-C6'	118.1(2)
Na-O1-H1	119.(2)	C1-O1-H1	115.(2)
Na-O7-H7	127.(2)	C7-O7-H7	113.(2)
C2-C3-H3	116.5(15)	C4-C3-H3	125.0(15)
C3-C4-H4	122.(2)	C5-C4-H4	119.(2)
C4-C5-H5	122.4(14)	C6-C5-H5	118.6(14)
C1'-O1'-H1'	108.(2)	C2'-C3'-H3'	119.9(15)
C4'-C3'-H3'	121.6(15)	C3'-C4'-H4'	122.(2)
C5'-C4'-H4'	119.(2)	C4'-C5'-H5'	122.5(14)
C6'-C5'-H5'	118.3(14)	Na-O8-H8a	121.(2)
Na-O8-H8b	123.(3)	H8a-O8-H8b	99.(4)
Na-O9-H9a	115.(3)	Na-O9-H9b	106.(3)
H9a-O9-H9b	106.(5)	Na-O10-H10a	113.(2)
Na-O10-H10b	107.(2)	H10a-O10-H10b	101.(3)
H10a-O10-H1'	113.(2)	H10b-O10-H1'	132.(2)

Table 6-7. Anisotropic Thermal Parameters ($Å^2 \times 10^3$) for the Non-Hydrogen Atoms of Compound **VIII**. Estimated Standard Deviations given in Parentheses.

Atom	U_{11}	U_{22}	U_{33}	U_{12}	U_{13}	U_{23}
Na	58.7(6)	33.0(5)	26.5(5)	-1.7(4)	-2.1(4)	-0.4(3)
N	36.2(10)	27.8(9)	26.4(9)	-2.4(8)	3.5(8)	-1.4(7)
O1	84.8(14)	29.1(9)	26.8(8)	-7.6(8)	-4.9(8)	-0.6(6)
O1a	90.4(15)	39.2(9)	34.9(9)	-18.9(9)	-5.0(9)	-12.6(7)
O7	76.9(12)	23.6(8)	29.9(8)	-5.1(8)	-4.4(8)	-3.1(6)
O7a	57.7(11)	24.6(8)	53.9(10)	-2.6(7)	-3.0(9)	4.7(7)
C1	46.1(14)	35.5(12)	29.6(11)	-6.5(10)	-1.9(10)	-5.7(10)
C2	35.3(12)	33.4(11)	27.2(11)	-3.1(9)	-4.2(9)	-3.3(9)
C3	44.3(12)	44.0(14)	27.4(11)	-2.2(11)	-7.8(10)	-5.6(10)
C4	51.(2)	52.(2)	24.0(12)	-5.8(12)	-6.2(11)	5.0(10)
C5	47.4(15)	35.0(13)	34.6(12)	-5.2(11)	-8.7(10)	8.1(10)
C6	33.0(12)	32.0(11)	29.7(11)	-1.9(9)	-5.3(9)	3.6(9)
C7	37.5(13)	25.2(11)	39.2(12)	-1.7(9)	-3.3(10)	1.7(9)
N'	35.5(10)	22.6(8)	24.7(9)	0.2(7)	-2.1(7)	-2.2(7)
O1'	93.2(15)	24.7(8)	30.7(8)	-14.3(9)	-0.7(9)	-6.6(7)
O1'a	76.2(12)	26.9(8)	25.0(8)	-6.2(8)	-1.0(8)	-1.3(6)
O7'	86.4(14)	27.5(8)	30.3(9)	-11.3(8)	-1.1(8)	-7.4(7)
O7'a	94.0(15)	23.4(9)	44.7(10)	-7.0(9)	12.6(10)	-2.7(7)
C1'	44.1(13)	25.1(10)	24.4(11)	2.0(9)	-1.5(9)	-3.6(8)
C2'	39.9(13)	22.9(10)	25.4(10)	0.6(9)	-1.8(9)	-4.3(8)
C3'	61.(2)	31.1(12)	24.4(11)	-4.4(11)	0.0(10)	-6.2(9)
C4'	66.(2)	40.1(13)	22.2(11)	-6.9(12)	0.3(11)	1.2(10)
C5'	51.2(15)	28.2(12)	30.6(11)	-4.1(10)	-3.4(10)	2.2(9)
C6'	32.9(12)	23.8(10)	28.0(11)	0.0(9)	-1.9(9)	-1.3(8)
C7'	40.8(13)	26.2(11)	35.4(12)	-3.3(9)	2.5(10)	-3.5(9)
O8	64.3(14)	41.0(11)	70.2(14)	4.8(11)	12.7(11)	6.8(10)
O9	65.9(13)	35.2(10)	29.2(10)	-5.1(9)	-3.3(8)	0.6(7)
O10	61.4(13)	27.1(9)	54.8(11)	-6.6(9)	3.6(9)	0.8(8)

The form of the thermal ellipsoid is $\exp[-2\pi^2(h^2a^{*2}U_{11} + k^2b^{*2}U_{22} + l^2c^{*2}U_{33} + 2hka^*b^*U_{12} + 2hla^*c^*U_{13} + 2klb^*c^*U_{23})]$

Sodium coordination

The sodium atom is in a pentagonal bipyramidal environment created by two dipic ligands and three water molecules. The dipic acting as a tridentate ligand has both acid groups formally protonated. The hydroxyl oxygen atoms, O1 and O7, as well as ring nitrogen are coordinated to the central atom at bond lengths of 2.482(2), 2.584(2) and 2.476(2) Å,

respectively. The hydroxyl groups coordinated in reported structures are in deprotonated carboxylate groups instead of acids.[45-51] In the complexes where the acid group is intact, the carbonyl, instead of the hydroxyl, oxygen is coordinated to the metal ion.[46,49] The other dipic has been formally deprotonated, but it did not coordinate the metal ion through the deprotonated hydroxy group. Instead, the carbonyl oxygen, O1'a, of the intact acid group is bonded to sodium at a distance of 2.474(2) Å. The coordination through a carbonyl oxygen of an acid group has been reported for dipic.[46,49] The two axial and the remaining equatorial positions are occupied by water molecules at bond lengths of 2.300(2), 2.501(2) and 2.795(2) Å, respectively.

Hydrogen bonding

Although H7 is formally assigned to O7, it is actually almost equidistant to O7' in the dipic coordinated to an adjacent sodium ion. The symmetry operator for the O7' hydrogen bonded to O7 is X, 1+Y, Z. O7 and the translated O7' are 2.472 Å apart, forming a bond angle of 172° around H7. A symmetrical hydrogen bond of significantly less than (>0.50 Å) two van der Waal's radii constitutes a very strong hydrogen bond.[66] The O7-H7-O7' bond length is just slightly longer than the average value, 2.44 Å, reported for dicarboxylates (RCO_2-H-O_2CR).[66] This interaction creates a network of very strong hydrogen bonded chains throughout the crystal.

Two hydrogen atoms are located on O8, O9 and O10 at bond lengths between 0.71(4) and 0.90(4) Å. The H-O-H bond angles created are 99(4), 106(5) and 101(3)°, respectively. Because these bond angles and lengths are within normal values, it seems reasonable that O8, O9 and O10 are water molecules and not hydroxide ions. In addition, it should be noted that the geometry around O10 is distorted tetrahedral if H1′ and Na are included. The bond angles around O10 range from 101(3) to 132(2)°.

In addition, there are hydrogen bonds that involve the water molecules. H1′ is hydrogen bonded to O10 by a distance of 1.743 Å to create an overall O1′-H1′···O10 bond length of 2.601 Å, at an angle of 175°. O7′a in an adjacent molecule (symmetry operator x, 1+y, z) is hydrogen bonded to H10a at a distance of 1.788 Å to form an angle of 174° with O10. The symmetry related molecule at x, 2+y, z has a hydrogen bond from O7a to H8a in the original molecule. The O7a···H8a interaction has a 1.961 Å bond length and creates an overall 2.842 Å hydrogen bond with an angle of 167° for O8···O7a.

Although a crystal of the desired aluminum compound was not synthesized, an intriguing seven coordinate complex sodium salt has been characterized. An unusual mode of coordination is documented by the bonding of the protonated hydroxyl oxygen atom the central metal ion. Also, no crystal structures, for either simple or complex salts, have been reported for dipic with alkali metal ions.

CHAPTER 7

SYNTHESIS AND STRUCTURE OF A COMPLEX SALT CONTAINING AMMONIUM NITRATE, PICOLINIC ACID AND 2-PYRIDINIUM CARBOXYLATE

Introduction

Picolinic acid, 2-pyridine carboxylic acid, can act as a bidentate ligand by coordinating through the ring nitrogen and a carboxylate oxygen. Also, because of the presence of the accessible oxygen and nitrogen atoms, there is a potential for a network of hydrogen bonding in the absence of a metal ion to coordinate. The structure presented in this chapter, which was synthesized prior to the work discussed in Chapter 1, is another example of a compound, without aluminum, characterized during this investigation.

Experimental

Synthesis

Materials. All materials and solvents were reagent grade and used as supplied from the manufacturer.

Preparation of $(C_5H_4N(CO_2H))(C_5H_4NH(CO_2))(NH_4+)(NO_3^-)$ (**IX**). A 3-neck 300 mL round bottom flask was equipped with a thermometer and condenser. Water (300 mL), $Al(NO_3)_3 \cdot 9H_2O$ (3.029 g, 8.07 mmole), urea (0.7830 g, 13.0 mmole) and pic

(4.009 g, 32.6 mmole) were added to the flask in order listed. A stir bar was added and the mixture stirred until all solids were dissolved. The reaction mixture was immersed in an oil bath and maintained at a temperature of 99 to 102°C for 24 hours. The clear colorless solution, which measured pH 6.5, was removed by filtration from the white solid that had formed during the reaction. After four months, small crystals (**IX**) of x-ray quality had formed.

X-ray Crystallographic Analysis

A clear colorless crystal was mounted on a glass fiber for diffraction studies. All subsequent data were collected on a Nicolet P3 Diffractometer, using filter-monochromated Cu Kα radiation. The unit cell dimensions were determined for 15 automatically centered reflections; space group $P2_1/c$ by intensity statistics and satisfactory structure solution and refinement; 2206 unique reflections, 1573 with $I>3\sigma(I)$; $0\leq h\leq 14$, $0\leq k\leq 9$, $-17\leq l\leq 17$. Two intensity standards measured every 98 reflections showed no change during data collection. The program used for F_{obs} refinement was SHELXTL Revision 5.1 (Sheldrick, 1985) Calculations and figures were performed on a Model 30 Desktop Eclipse computer. Final refinement values for 264 parameters were R = 5.80, R_w = 5.93 and w = 6.75. Atomic scattering factors used were those of the *International Tables of X-ray Crystallography* (1974). All non-hydrogen atoms were located from an E-map. Hydrogen atoms were located by a Difference Fourier map.

Discussion

X-ray Diffraction Analysis

Crystallographic data for compound **IX** is summarized in Table 7-1. The structure of the two organic molecules and the hydrogen bonded network created between them is displayed in Figures 7-1 and 7-2, respectively. The final atomic coordinates are given in Table 7-2. Bond lengths and bond angles are listed in Tables 7-3 and 7-4, respectively. The anisotropic thermal parameters for the non-hydrogen atoms are given in Table 7-5.

Hydrogen Bonding

The most notable feature of **IX**, despite the absence of an aluminum ion, is the placement and bonding of the hydrogen atoms. The carboxylic acid group from one pic is formally deprotonated. The hydrogen atom, H(N), instead appears 0.975 Å from the ring nitrogen N(1) and thereby forms a zwitterion. The other acid is protonated in the normal manner on the carboxylate oxygen O(11).

Each of these hydrogen atoms is bonded to an atom of another pic. H(N) is located 1.798 Å from N(11) of the second ring. H(O) is hydrogen bonded to O(2) in an adjacent pic molecule (symmetry operator is 0.5+x, 0.5-y, 0.5+z). The hydrogen bond created by N(1)-H(N)···N(11) and O(11)-H(O)···O(2) are 0.327 and 0.417 Å shorter than the sum of two van der Waal's radii (3.100 Å for N···N, 3.000 Å for O···O).

Table 7-1. Crystallographic Data for **IX**.

Compound	$(C_5H_4N(CO_2H))(C_5H_4NH(CO_2))(NH_4)(NO_3)$
Formula	$C_{12}H_{14}N_4O_7$
MW	326.27
Crystal system	Monoclinic
Space group	$P\ 2_1/c$
a, Å	12.1985
b, Å	7.9230
c, Å	15.6065
β, °	101.525
V_c, Å^3	1477.94
Z	4
D_{calc}, g/cm^3	1.47
Radiation	Cu $K\alpha$
λ, Å	1.54178
μ, cm^{-1}	10.11
$F(000)$	679.86
Observed reflections	1573
Number of parameters	264
Final R	0.0580
Rw	0.0593

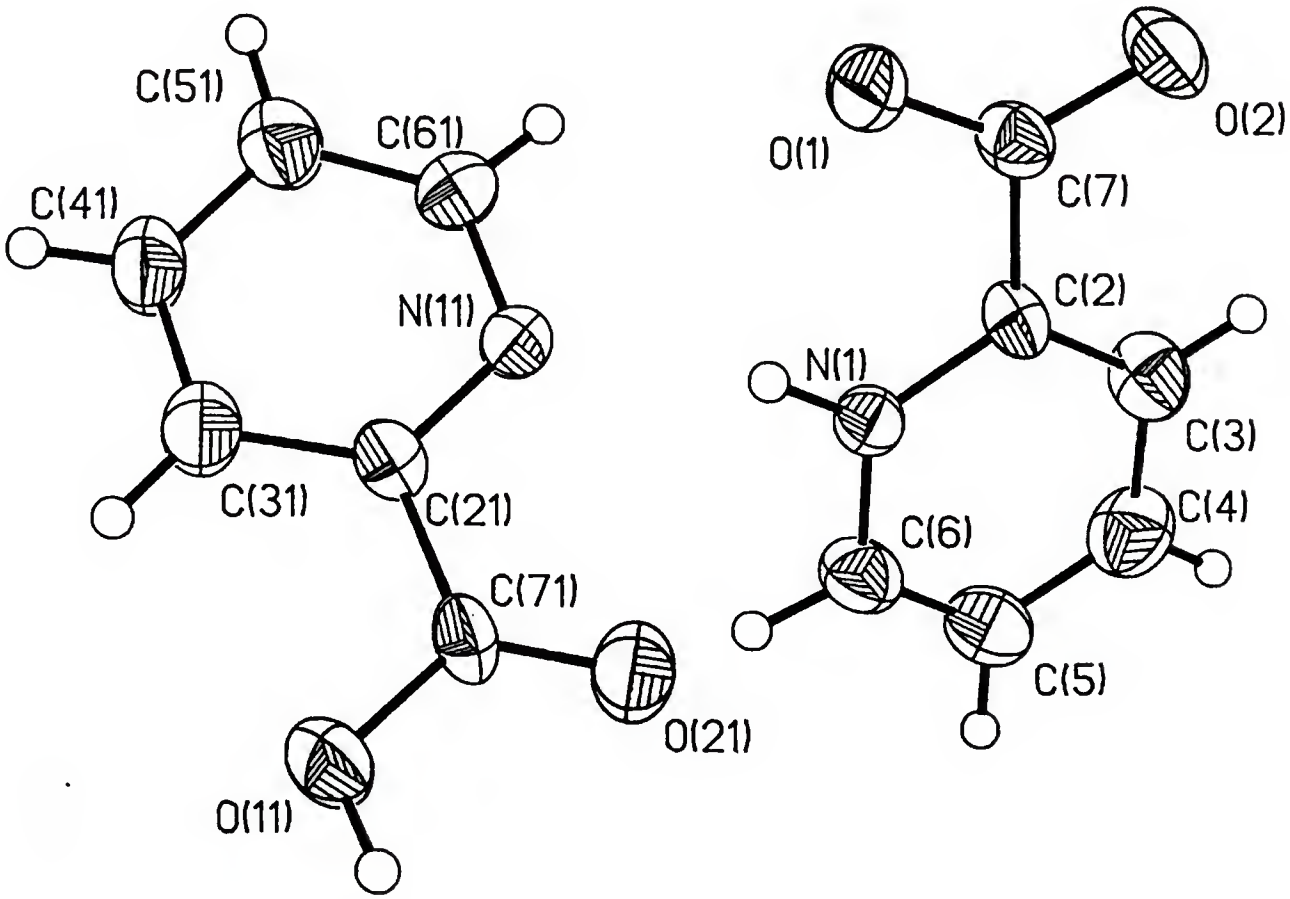

Figure 7-1. ORTEP of Compound **IX**.

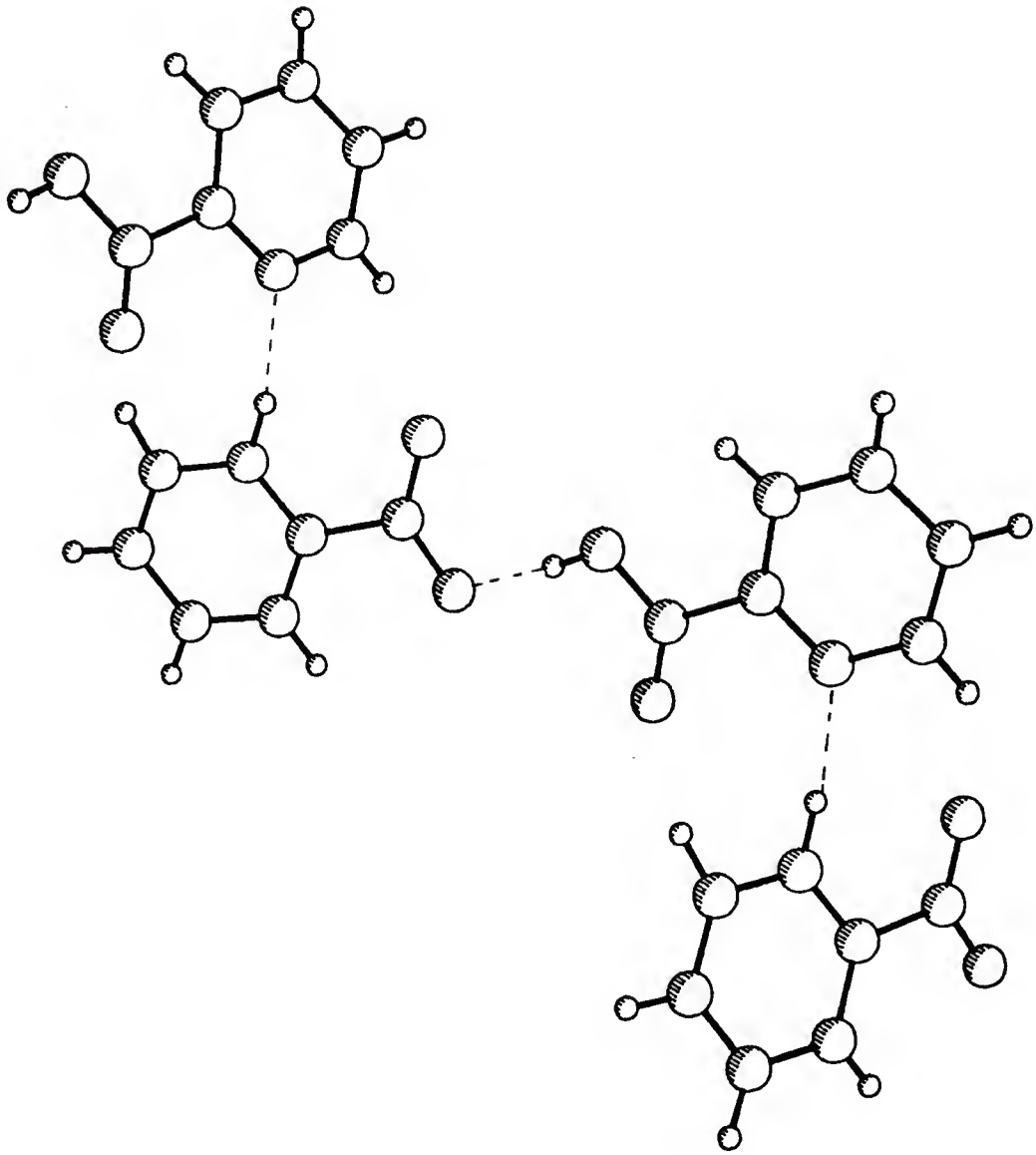

Figure 7-2. Detail Showing Hydrogen Bonding in **IX**.

Table 7-2. Final Atomic Coordinates ($x10^4$) and Isotropic Thermal Parameters ($Å^2x10^3$) for **IX**. Estimated Standard Deviations are given in Parentheses.

	x	y	z	U
N(1)	0.3376 (2)	-0.0187 (4)	0.7255 (2)	33 (1)
C(2)	0.2875 (3)	-0.0038 (4)	0.6405 (2)	33 (1)
C(3)	0.3433 (4)	-0.0584 (5)	0.5778 (3)	45 (2)
C(4)	0.4500 (4)	-0.1256 (7)	0.6024 (3)	55 (2)
C(5)	0.4987 (4)	-0.1375 (6)	0.6891 (3)	51 (2)
C(6)	0.4415 (4)	-0.0815 (6)	0.7503 (3)	42 (2)
C(7)	0.1709 (3)	0.0692 (5)	0.6225 (2)	36 (1)
O(1)	0.1249 (2)	0.0892 (3)	0.6848 (1)	47 (1)
O(2)	0.1316 (2)	0.1052 (3)	0.5431 (1)	50 (1)
N(11)	0.2504 (2)	0.0101 (4)	0.8798 (2)	37 (1)
C(21)	0.3060 (3)	0.0590 (4)	0.9592 (2)	35 (1)
C(31)	0.2699 (4)	0.0224 (6)	1.0353 (2)	46 (2)
C(41)	0.1719 (4)	-0.0674 (7)	1.0301 (3)	60 (2)
C(51)	0.1113 (4)	-0.1153 (6)	0.9488 (3)	51 (2)
C(61)	0.1553 (4)	-0.0758 (6)	0.8770 (3)	44 (2)
C(71)	0.4084 (4)	0.1621 (5)	0.9586 (2)	37 (2)
O(11)	0.4591 (2)	0.2102 (4)	1.0375 (2)	53 (1)
O(21)	0.4405 (2)	0.1991 (3)	0.8928 (1)	54 (1)
N(2)	0.8303 (3)	0.6893 (5)	0.8064 (2)	49 (1)
O(1N)	0.8272 (3)	0.6306 (5)	0.8788 (2)	86 (1)
O(2N)	0.9163 (3)	0.7521 (6)	0.7925 (2)	86 (2)
O(3N)	0.7478 (3)	0.6798 (5)	0.7473 (2)	101 (2)
N(3)	0.1030 (3)	0.0370 (3)	0.3553 (2)	50 (1)

Equivalent isotropic U defined as one third of the trace of the orthogonalized U_{ij} tensor

Table 7-3. Hydrogen Atom Coordinates ($x10^4$) and Isotropic Thermal Parameters ($Å^2x10^3$) for **IX**. Estimated Standard Deviations are given in Parentheses.

	x	y	z	U
H(O)	0.5151 (34)	0.2867 (49)	1.0354 (23)	83 (13)
H(N)	0.2989 (31)	0.0187 (48)	0.7711 (23)	71 (12)
H(3)	0.3120 (26)	-0.0401 (41)	0.5199 (19)	48 (9)
H(4)	0.4919 (30)	-0.1649 (49)	0.5604 (21)	73 (11)
H(5)	0.5729 (27)	-0.1696 (42)	0.7086 (19)	44 (10)
H(6)	0.4657 (24)	-0.0765 (37)	0.8132 (17)	45 (9)
H(31)	0.3108 (23)	0.0578 (35)	1.0886 (16)	35 (8)
H(41)	0.1485 (28)	-0.0839 (44)	1.0807 (21)	66 (10)
H(51)	0.0395 (29)	-0.1688 (45)	0.9438 (20)	59 (10)
H(61)	0.1222 (27)	-0.1070 (41)	0.8227 (19)	47 (9)
H(1N)	0.0310 (28)	-0.0221 (44)	0.3510 (19)	65 (10)
H(2N)	0.1571 (35)	-0.0356 (53)	0.3391 (24)	85 (13)
H(3N)	0.1060 (28)	0.0656 (42)	0.4027 (21)	59 (10)
H(4N)	0.1065 (27)	0.1081 (44)	0.3224 (20)	57 (9)

Equivalent isotropic U defined as one third of the trace of the orthogonalized U_{ij} tensor

Table 7-4. Bond Lengths (Å) for Non-Hydrogen Atoms in **IX**. Estimated Standard Deviations are given in Parentheses.

N(1)-C(2)	1.350(4)	C(2)-C(3)	1.370(5)
C(3)-C(4)	1.387(6)	C(4)-C(5)	1.369(6)
N(1)-C(6)	1.345(5)	C(5)-C(6)	1.363(7)
C(2)-C(7)	1.508(5)	C(7)-O(1)	1.227(5)
C(7)-O(2)	1.268(4)	N(11)-C(21)	1.345(4)
C(21)-C(31)	1.378(5)	C(31)-C(41)	1.380(7)
C(41)-C(51)	1.388(6)	C(51)-C(61)	1.372(6)
N(11)-C(61)	1.338(5)	C(21)-C(71)	1.494(5)
C(71)-O(11)	1.319(4)	C(71)-O(21)	1.207(5)
N(2)-O(1N)	1.231(5)	N(2)-O(2N)	1.219(6)
N(2)-O(3N)	1.223(5)		

Table 7-5. Bond Lengths (Å) involving Hydrogen Atoms in **IX**. Estimated Standard Deviations are given in Parentheses.

N(1)-H(N)	0.975(40)	C(3)-H(3)	0.920(28)
C(4)-H(4)	0.960(38)	C(5)-H(5)	0.931(32)
C(6)-H(6)	0.967(26)	C(31)-H(31)	0.924(24)
C(41)-H(41)	0.901(35)	C(51)-H(51)	0.962(36)
C(61)-H(61)	0.897(29)	O(11)-H(O)	0.919(41)
N(3)-H(1N)	0.986(35)	N(3)-H(2N)	0.947(44)
N(3)-H(3N)	0.766(33)	N(3)-H(4N)	0.769(33)
N(11)···H(N)	1.798(70)	O(2)'···H(O)	1.664(71)

Table 7-6. Bond Angles (°) in **IX**. Estimated Standard Deviations are given in Parentheses.

C(2)-N(1)-C(6)	122.0(0.3)	C(2)-N(1)-H(N)	120.0(2.0)
C(6)-N(1)-H(N)	117.9(2.0)	N(1)-C(2)-C(3)	118.9(0.3)
N(1)-C(2)-C(7)	116.2(0.3)	C(3)-C(2)-C(7)	124.9(0.3)
C(2)-C(3)-C(4)	119.7(0.3)	C(2)-C(3)-H(3)	119.0(2.1)
C(4)-C(3)-H(3)	121.0(2.1)	C(3)-C(4)-C(5)	119.9(0.5)
C(3)-C(4)-H(4)	122.2(1.9)	C(5)-C(4)-H(4)	117.9(2.0)
C(4)-C(5)-C(6)	119.3(0.4)	C(4)-C(5)-H(5)	122.8(2.0)
C(6)-C(5)-H(5)	117.4(2.0)	N(1)-C(6)-C(5)	120.2(0.3)
N(1)-C(6)-H(6)	110.8(1.8)	C(5)-C(6)-H(6)	129.0(1.9)
C(2)-C(7)-O(1)	117.7(0.3)	C(2)-C(7)-O(2)	115.2(0.3)
O(1)-C(7)-O(2)	127.0(0.3)	C(21)-N(11)-C(61)	116.9(0.3)
N(11)-C(21)-C(31)	123.0(0.3)	N(11)-C(21)-C(71)	114.9(0.3)
C(31)-C(21)-C(71)	122.1(0.3)	C(21)-C(31)-C(41)	118.7(0.3)
C(21)-C(31)-H(31)	120.3(1.9)	C(41)-C(31)-H(31)	121.0(1.9)
C(31)-C(41)-C(51)	119.5(0.4)	C(31)-C(41)-H(41)	116.4(2.0)
C(51)-C(41)-H(41)	123.9(2.1)	C(41)-C(51)-C(61)	117.4(0.4)
C(41)-C(51)-H(51)	120.2(1.9)	C(61)-C(51)-H(51)	122.3(1.9)
N(11)-C(61)-C(51)	124.6(0.3)	N(11)-C(61)-H(61)	113.3(2.2)
C(51)-C(61)-H(61)	122.1(2.2)	C(21)-C(71)-O(11)	112.9(0.3)
C(21)-C(71)-O(21)	123.4(0.3)	O(11)-C(71)-O(21)	123.7(0.4)
C(71)-O(11)-H(O)	111.7(2.2)	O(1N)-N(2)-O(2N)	120.1(0.4)
O(1N)-N(2)-O(3N)	119.9(0.4)	O(2N)-N(2)-O(3N)	119.9(0.4)
H(1N)-N(3)-H(2N)	110.6(3.2)	H(1N)-N(3)-H(3N)	94.4(3.2)
H(1N)-N(3)-H(4N)	117.9(2.9)	H(2N)-N(3)-H(3N)	122.4(3.3)
H(2N)-N(3)-H(4N)	97.6(3.6)	H(3N)-N(3)-H(4N)	115.5(3.6)

Table 7-7. Anisotropic Thermal Parameters ($Å^2 x10^3$) for Non-Hydrogen Atoms in **IX**. Estimated Standard Deviations are given in Parentheses.

Atom	U_{11}	U_{22}	U_{33}	U_{23}	U_{13}	U_{12}
N(1)	37(2)	35(2)	29(1)	1(1)	9(1)	3(1)
C(2)	36(2)	32(2)	28(2)	-2(1)	1(1)	2(2)
C(3)	50(3)	53(3)	31(2)	-2(2)	7(2)	11(2)
C(4)	57(3)	66(3)	47(3)	-2(3)	22(2)	16(3)
C(5)	36(3)	64(3)	52(3)	7(2)	9(2)	12(2)
C(6)	41(3)	44(3)	35(2)	8(2)	-2(2)	7(2)
C(7)	40(2)	37(2)	29(2)	-5(2)	3(2)	2(2)
O(1)	41(1)	66(2)	35(1)	-2(1)	9(1)	10(1)
O(2)	48(2)	67(2)	32(1)	6(1)	2(1)	17(1)
N(11)	36(2)	46(2)	29(1)	0(1)	5(1)	-4(1)
C(21)	37(2)	34(2)	32(2)	1(1)	4(2)	-1(2)
C(31)	50(3)	60(3)	28(2)	-5(2)	8(2)	-12(2)
C(41)	63(3)	84(4)	38(3)	2(2)	24(2)	-16(3)
C(51)	39(3)	67(3)	47(3)	8(3)	10(2)	-12(3)
C(61)	40(3)	53(3)	36(2)	-1(2)	2(2)	-10(2)
C(71)	42(3)	39(3)	30(2)	-2(2)	4(2)	-1(2)
O(11)	54(2)	67(2)	35(1)	-2(1)	0(1)	-23(2)
O(21)	60(2)	66(2)	38(1)	-5(1)	15(1)	-24(1)
N(2)	48(3)	57(3)	42(2)	3(2)	10(2)	-5(2)
O(1N)	112(3)	104(3)	51(2)	8(2)	39(2)	-13(2)
O(2N)	53(2)	117(4)	86(3)	39(3)	9(2)	-27(2)
O(3N)	63(2)	129(3)	95(2)	20(2)	-27(2)	-7(2)
N(3)	50(2)	68(3)	38(2)	4(2)	19(2)	5(2)

The form of the thermal ellipsoid is $\exp[-2\pi^2(h^2a^{*2}U_{11} + k^2b^{*2}U_{22} + l^2c^{*2}U_{33} + 2klb^*c^*U_{23} + 2hla^*c^*U_{13} + 2hka^*b^*U_{12})]$

Even though the bond lengths are significantly less than the sum of the two radii, neither H(N) nor H(O) are centered but instead are covalently bonded to a parent atom. Because of the dissimilar bond lengths, these two interactions should be classified as weak hydrogen bonds.[66]

The two other hydrogen bonds are also classified as weak. The overall bond lengths for N(3)-H(1N)···O(1)'' and N(3)-H(4N)···O(2N)''', 3.038 and 2.895 respectively, are barely less than the sum of the radii for an oxygen atom and a

nitrogen atom, 3.050 Å. The remaining hydrogen interactions have bond lengths greater than the sum of the two van der Waal's radii and, therefore, do not qualify as even weak hydrogen bonds.[66]

Although neither ammonia nor the ammonium ion were added to the reaction mixture, NH_4^+ was present in the crystal analyzed. When urea is heated, especially in the presence of acid, it decomposes by according to the following chemical reaction. Under the slightly acidic conditions in the

$$H_2NCONH_2 \quad + \quad H_2O \quad \rightarrow \quad 2\ NH_3 \quad + \quad CO_2$$

filtrate, the ammonia was converted the its conjugate acid.

The four hydrogen atoms of the ammonium ion refined to reasonable parameters. The four N-H bond lengths are 0.766, 0.769, 0.947 and 0.986 Å, within normal limits. Also, the six angles created by the hydrogen atoms around the nitrogen range from 94.9° to 122.4°.

Nature of the Products

The reaction mixture involved approximately a 4 : 3 : 1 ratio of ligand to base to aluminum ions. An excess of pic was employed to ensure that the maximum amount of aluminum could react. In consideration of the nature of the insoluble white solid produced in later experiments, it seems reasonable that the white solid formed in this synthesis contains aluminum and pic. Since there was an excess of ligand used, the unreacted pic was free to crystalize in a manner that

produced spaces suitable for the spatial requirements of ammonium and nitrate ions.

CHAPTER 8

ABSOLUTE CONFIGURATION OF SODIUM HYDROGEN (+)-TARTRATE MONOHYDRATE

Introduction

In a study not covered in this work, the coordination and crystal growth of aluminum with ligands, such as tartaric acid, without a donor nitrogen was investigated.[67] A solution of the aluminum complex formed a glass upon evaporation. The subject of this chapter, which does not contain aluminum, was one of a few crystals grown from a mixed solvent system.

Structures of several bitartrate salts with alkali metals and ammonium have been previously reported. However, the only two to give absolute configurations are the isomorphous potassium hydrogen (+)-tartrate and ammonium hydrogen (+)-tartrate.[68,69] As yet, there has been no structural data published for the absolute configuration of a monohydrate of a bitartrate salt.

Experimental

Synthesis

Materials. All materials and solvents were reagent grade and used as supplied from manufacturer.

Preparation of $Na^+C_4H_5O_6^- \cdot H_2O$ (**X**). In 15 mL H_2O, (+)-tartaric acid (1.475 g, 9.83 mmole) and $Al(NO_3)_3 \cdot 9H_2O$ (1.223 g, 3.26 mmole) was dissolved. $NaHCO_3$ (1.658 g, 19.7 mmole) was added and bubbling ensued. When the solution was treated with ethanol, a tacky white solid formed. The solution was separated from the solid by filtration. From the filtrate, large colorless hexagonal cylinders (**X**) (and characteristic cubic $NaNO_3$ crystals) were obtained after evaporating overnight. Elemental analysis: **X**: 24.64(10) % C, 3.55(3) % H, 0.21(9) % N, measured. $C_4H_7O_6Na$: 27.60 % C, 4.05 % H, 0 % N, calculated.

X-ray Crystallographic Analysis

A single crystal measuring approximately 0.8 x 0.8 x 0.6 mm was mounted on a glass fiber. All data were collected on a Nicolet P3 Diffractometer, using graphite-monochromated Mo Kα radiation. The unit cell dimensions were determined from 18 automatically centered reflections, $3.7<\theta<13.7°$; space group $P2_12_12_1$ by intensity statistics and satisfactory structure solution and refinement; 1465 unique reflections, 1152 with $I>3\sigma(I)$, $0 \le h \le 9$, $-11 \le k \le 11$, $-13 \le l \le 13$. Two intensity standards measured every 98 reflections showed no change during data collection. All non-hydrogen atoms were located from an E-map. Four of the seven hydrogen atoms were located from Fourier maps but no others from a difference Fourier map. The program used for F_{obs} refinement was SHELXTL Revision 5.1 (Sheldrick, 1985). Final refinement values were

R = 4.38, wR = 5.62 and w = 4.38 for 109 parameters. Atomic scattering factors used were those of *International Tables for X-ray Crystallography*, vol. IV.

Discussion

X-ray Diffraction Study

Crystallographic data for **X** is summarized in Table 8-1. Atomic positions for **X** are given in Table 8-2. The molecule and atomic numbering scheme are given in Figure 8-1. All bond lengths and angles including the sodium ion coordination are listed in Table 8-3. The anisotropic thermal parameters for the non-hydrogen atoms are given in Table 8-4.

One of the carboxylic acid groups in the tartaric acid was deprotonated. O(5) is bonded to H(3) at a bond length of 1.000 Å to form the intact carboxylic acid group. Of the oxygen atoms in the molecule, O(5) is the only donor atom that is not within 3.0 Å of a sodium atom. H(3) is hydrogen bonded at a distance of 1.568 Å to O(1) in an adjacent hydrogen tartrate ion. The O(5)-H(3)···O(1)′ hydrogen bond is 0.43 Å shorter than the sum of two oxygen van der Waal's radii, but is classified as a weak hydrogen bond because the H(3) is not centered.[66]

The sodium ion is surrounded by eight oxygen atoms with bond lengths between 2.426 and 2.827 Å. Figure 8-2 shows a detail of the coordination around the sodium atom. The deviations from the least squares planes analysis for the

Table 8-1. Crystallographic Data for **X**.

Complex	$Na^+(C_4H_5O_6)^- \cdot H_2O$
Formula	$C_4H_7O_7Na$
MW	190.08
Crystal system	Orthorhombic
Space group	$P2_12_12_1$
a, Å	7.2393
b, Å	8.6735
c, Å	10.5928
V_c, Å^3	665.12
Z	4
D_{calc}, g/cm^3	1.899
Radiation	Mo $K\alpha$
λ, Å	0·71069
μ(Mo$K\alpha$), cm^{-1}	2.24
F(000)	388
Crystal dimensions	0.8 × 0.8 × 0.6 mm
Observed reflections	1152
Number of parameters	109
Final R	4.38
Rw	5.62

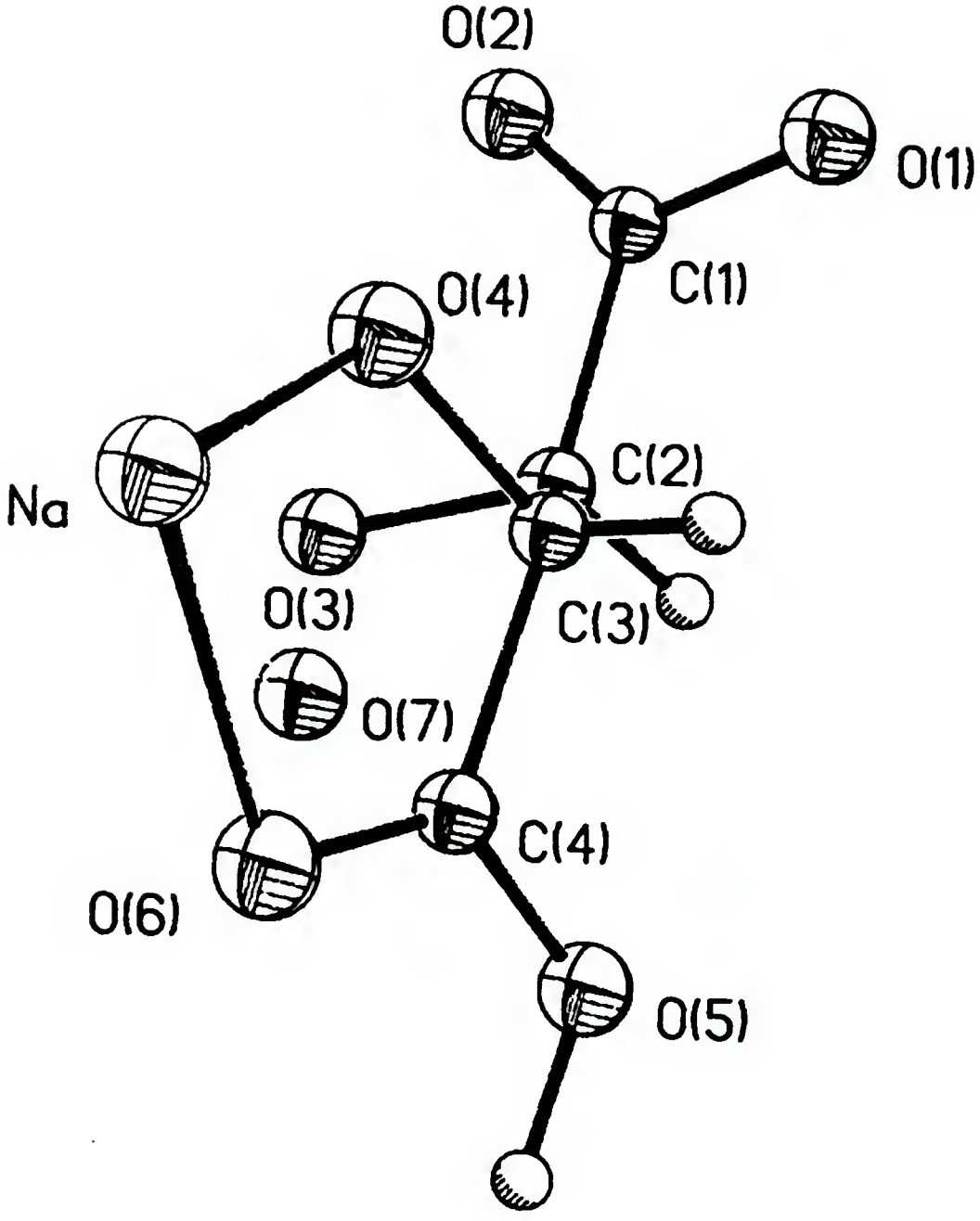

Figure 8-1. ORTEP Drawing of **X** Showing the Atomic Numbering Scheme.

Table 8-2. Final Atomic Coordinates ($x10^4$) and Isotropic Thermal Parameters ($Å^2x10^3$) for **X**. Estimated Standard Deviations are given in Parentheses.

Atom	x	y	z	U_{eq}*
Na	0.0891(2)	-0.2074(2)	-0.5731(2)	0.0264(5)
O(1)	0.5928(3)	-0.2861(3)	-0.1605(3)	0.0255(8)
O(2)	0.5694(4)	-0.0356(3)	-0.1102(3)	0.0263(9)
O(3)	0.2106(4)	-0.0054(3)	-0.1288(3)	0.0239(8)
O(4)	0.2807(4)	-0.1668(4)	-0.3660(3)	0.0266(9)
O(5)	-0.0846(4)	-0.2826(3)	-0.1586(2)	0.0239(8)
O(6)	-0.0888(4)	-0.1869(3)	-0.3552(3)	0.0280(8)
C(1)	0.4874(5)	-0.1563(4)	-0.1356(4)	0.017(1)
C(2)	0.2762(5)	-0.1578(4)	-0.1363(4)	0.016(1)
C(3)	0.2026(5)	-0.2365(4)	-0.2561(3)	0.017(1)
C(4)	-0.0054(5)	-0.2319(4)	-0.2625(4)	0.019(1)
H(1)	0.246(7)	-0.209(7)	-0.054(5)	0.03(1)
H(2)	0.236(8)	-0.370(7)	-0.260(5)	0.05(2)
H(3)	-0.221(7)	-0.297(6)	-0.166(5)	0.05(2)
O(7)	0.0417(4)	-0.5245(3)	-0.0093(3)	0.0257(9)

$*U_{eq}=\frac{1}{3}\Sigma_{ij}U_{ij}a_i*a_j*\mathbf{a}_i.\mathbf{a}_j$.

Table 8-3. Bond Lengths (Å) and Angles (°) for **X**. Estimated Standard Deviations are given in Parentheses.

(a) Bond distances (Å) for the bitartrate ion.

O(1)-C(1)	1.283(5)	C(1)-C(2)	1.527(5)
O(2)-C(1)	1.230(5)	C(2)-C(3)	1.540(6)
O(3)-C(2)	1.404(5)	C(3)-C(4)	1.508(6)
O(4)-C(3)	1.428(5)	C(2)-H(1)	1.00(5)
O(5)-C(4)	1.314(5)	C(3)-H(2)	1.18(6)
O(6)-C(4)	1.218(5)	O(5)-H(3)	1.00(5)

(b) Bond angles (°) for the bitartrate ion.

O(1)-C(1)-C(2)	114.6(3)	C(2)-C(3)-C(4)	111.8(3)
O(2)-C(1)-C(2)	119.4(3)	O(4)-C(3)-C(4)	110.3(3)
O(1)-C(1)-O(2)	125.9(3)	O(6)-C(4)-C(3)	122.7(3)
C(1)-C(2)-C(3)	110.9(3)	O(5)-C(4)-O(6)	124.5(3)
O(3)-C(2)-C(1)	109.2(3)	O(5)-C(4)-C(3)	112.8(3)
O(3)-C(2)-C(3)	110.4(3)	C(4)-O(5)-H(3)	111(3)
O(4)-C(3)-C(2)	110.3(3)		

Table 8-3 -- Continued.

(c) Torsion angles (°) for the bitartrate ion.

O(1)-C(1)-C(2)-O(3)	-170.3(3)	
O(1)-C(1)-C(2)-C(3)	-48.4(4)	
O(2)-C(1)-C(2)-O(3)	10.7(5)	**
O(2)-C(1)-C(2)-C(3)	132.6(4)	
O(3)-C(2)-C(3)-O(4)	67.4(4)	**
O(3)-C(2)-C(3)-C(4)	-55.7(4)	
C(1)-C(2)-C(3)-O(4)	-53.7(4)	
C(1)-C(2)-C(3)-C(4)	-176.8(3)	**
O(4)-C(3)-C(4)-O(5)	-174.4(3)	
O(4)-C(3)-C(4)-O(6)	6.2(5)	**
C(2)-C(3)-C(4)-O(5)	-51.3(4)	
C(2)-C(3)-C(4)-O(6)	129.3(4)	

(d) Distances (Å) and Symmetry Operators for Sodium Ion Coordination.

Na-O(4)	2.616(3)
Na-O(6)	2.648(3)
Na-O(7)	2.416(4)
Na-O(2^2)	2.429(3)
Na-O(3^2)	2.422(3)
Na-O(1^3)	2.827(3)
Na-O(4^3)	2.566(3)
Na-O(6^4)	2.622(3)

Symmetry operators: (2) 0.5-x, -y, -0.5+z; (3) 0.5-x, -1-y, 0.5+z; (4) 0.5+x, -0.5-y, -1-z

(e) Bonds (Å) and Angles (°) around the Sodium Ion.

O...Na...O	O-O	O-Na-O
O(4)...O(6)	2.681(4)	61.2(1)
O(6)...O(2^2)	3.322(4)	81.6(1)
O(2^2)...O(3^2)	2.616(4)	65.2(1)
O(4)...O(3^2)	3.160(4)	77.6(1)
O(4)...O(2^2)	4.022(4)	105.6(1)
O(6)...O(3^2)	4.322(4)	116.9(1)
O(7)...O(4^3)	2.912(5)	71.5(1)
O(4^3)...O(1^3)	3.160(4)	71.5(1)
O(1^3)...O(6^4)	3.370(4)	76.3(1)
O(7)...O(6^4)	3.033(5)	73.9(1)
O(7)...O(1^3)	4.168(5)	105.0(1)
O(4^3)...O(6^4)	4.571(4)	123.6(1)

Table 8-4. Anisotropic Thermal Parameters ($Å^2 \times 10^3$) for Non-Hydrogen Atoms in **X**. Estimated Standard Deviations are given in Parentheses.

Atom	U_{11}	U_{22}	U_{33}	U_{23}	U_{13}	U_{12}
Na	25(1)	23(1)	31(1)	5(1)	-2(1)	-2(1)
O(1)	13(1)	25(1)	38(2)	-6(1)	2(1)	1(1)
O(2)	18(1)	23(1)	38(2)	-2(1)	-5(1)	-3(1)
O(3)	19(1)	17(1)	35(2)	-6(1)	1(1)	2(1)
O(4)	24(1)	40(2)	16(1)	3(1)	6(1)	-8(1)
O(5)	15(1)	36(1)	20(1)	2(1)	1(1)	-2(1)
O(6)	25(1)	31(1)	27(1)	8(1)	-6(1)	-2(1)
O(7)	15(2)	28(2)	40(2)	-7(1)	3(2)	5(2)
C(1)	13(2)	21(2)	17(2)	2(2)	0(2)	-1(2)
C(2)	13(2)	18(2)	17(2)	-2(2)	-1(2)	1(1)
C(3)	15(2)	21(2)	13(2)	0(2)	2(1)	-2(2)
C(4)	18(2)	18(2)	19(2)	-5(2)	-1(1)	-1(2)

The anisotropic temperature factor exponent takes the form: $\exp[-2\pi 9h^2a^{*2}U_{11} + k^2b^{*2}U_{22} + l^2c^{*2}U_{33} + 2hka^*b^*U_{12} + 2hla^*c^*U_{13} + 2klb^*c^*U_{23})]$

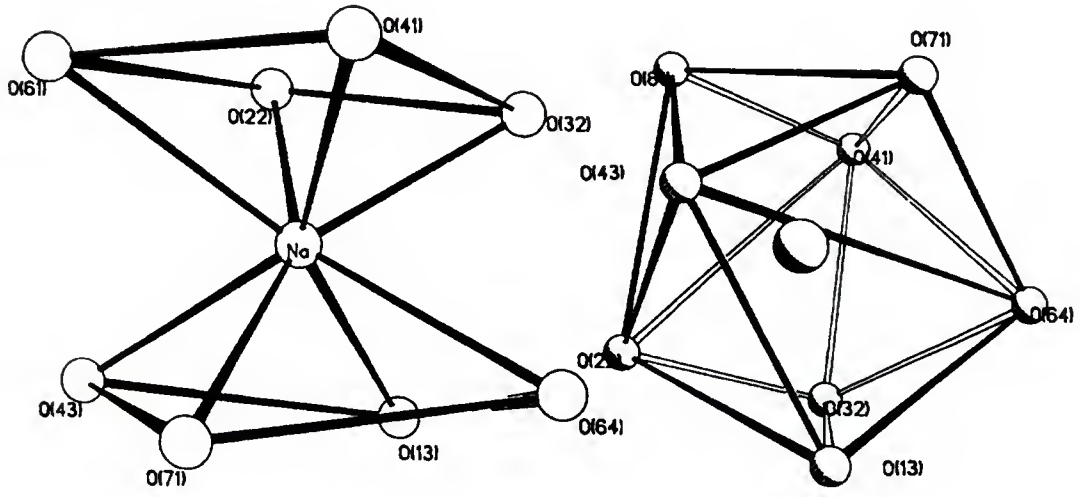

Figure 8-2. Sodium Ion Coordination in **X**, Showing the Square Antiprismatic, left, and Dodecahedral, right, Orientations.

Table 8-5. Least Squares Planes Analysis of Square Antiprismatic and Dodecahedral Geometries for **X**.

Least Squares Planes Atoms

Square Antiprism
(1) O13, O43, O64, O71
(2) O22, O32, O41, O61

Triangular Dodecahedron
(3) O22, O32, O43, O71
(4) O13, O41, O61, O64

	Square Antiprism		Dodecahedron	
	Deviations, Δ, from Least Squares Planes			
	(1)	(2)	(3)	(4)
Na	-	-	0.1213	0.0240
O13	-0.1585	-	-	0.2073
O22	-	0.1014	0.3952	-
O32	-	-0.1065	-0.2929	-
O41	-	0.1043	-	0.4179
O43	0.1860	-	-0.3538	-
O61	-	-0.0993	-	-0.2759
O64	0.1686	-	-	-0.3493
O71	-0.1961	-	0.2515	-
Rmsd	0.1779	0.1029	0.3281	0.3224

Rmsd takes the form $[(\Sigma\Delta^2)/2]^{1/2}$

	Least Squares Planes Equation Coefficients			
A	-0.16(54)	0.33(39)	-1.2(1.2)	1.39(91)
B	7.31(38)	7.33(64)	1.88(81)	8.5(1.0)
C	5.69(20)	5.64(16)	10.18(39)	-1.04(39)
D	-6.19(13)	-3.301(81)	-6.46(23)	-1.06(23)

Equations for Least Squares Planes take the form:

$$Ax + By + Cz = D$$

square antiprismatic and triangular dodecahedral geometries are given in Table 8-5. The fit to the two sets of planes is closer for square antiprismatic, but not significantly close. The angles between the two least squares planes are 3.8° and 85.1°, respectively. The angles in the idealized geometry are 0° and 90°. The geometry around the sodium ion is intermediate between the two idealized geometries for octacoordinate centers.[70,71]

To check the absolute configuration of the compound, least squares refinements for all non-hydrogen atom coordinates were compared with those of the enantiomer. No measurable difference was noted between the R or R_w values of X, Y, Z and -X, -Y, -Z. A probable reason for the inconclusive test results is low anomalous scattering factors for Mo Kα for atoms as small as sodium.[61,72,73] These values are used to correct for x-rays that are dispersed upon striking a specific atom.[61] The more x-rays disperse, the greater the difference between the fit of the data for X, Y, Z and -X, -Y, -Z. If radiation that has larger scattering factors had been used, one enantiomer should refine slightly better and, thereby, prove the absolute configuration of a compound.[61]

CHAPTER 9

CONCLUSION

Characterization of Aluminum Coordination Compounds

The coordination chemistry of aluminum with N,O donor ligands was investigated. Although a complex was formed with each of the ligands in this study, only two were completely characterized. Complexes **I** and **II** were sufficiently soluble in ethanol or methanol to be recrystallized, while all others were insoluble in every common solvent. It was determined that the other compounds must not be the sodium salts of the ligands, because the sodium salts were found to be very soluble in water. The only methods that could be used to characterize compounds **III** through **VII** were elemental analysis, FABMS and Infra-red and Al-27 NMR spectroscopies.

Elemental Analysis

Since each ligand has a specific number of carbon and nitrogen atoms, the presence of an organic solvent molecule or an ammonium ion in a synthesized compound can easily be confirmed. However, the amount of oxygen associated with water can not be accurately determined because of the uncertainty in the amount of hydrogen present. In addition, since there is only a 2 g/mole difference between the mass of

an aluminum and a sodium with two hydrogen atoms, it is difficult to prove of disprove the presence of aluminum, as opposed to sodium, based on CHN data.

The data confirms the presence of the ligand in each of the compounds because the molar ratios of carbon to nitrogen are, for the most part, very close to those of the ligands. However, because the amount of hydrogen is high, most likely due to the presence of water molecules, the molar ratios involving hydrogen do not correspond to those of the deprotonated ligands. No further conclusions can be drawn from this technique.

Infra-red Spectroscopy

The information provided by Infra-red spectroscopy includes the stretching frequency of the carbonyl group, and therefore, also on its environmnet, length, strength and double bond character. The C=O group in a carboxylic acid has stretch in the region 1760 to 1700 cm^{-1}, while that for a salt of the carboxylic acid shifts to between 1650 and 1550 cm^{-1}, because the sodium ion causes a perturbation. Theoretically, in a complex involving the carboxylate group, the stretching frequency for the carbonyl group would probably be different from that of the acid and the sodium salt.

Each aluminum compound has a carbonyl stretching frequency between 1660 and 1690 cm^{-1}, distinctly different than the characteristic carboxylic acid and carboxylate ion regions.[52] For **III** and **V**, the single peak occurs between the

peaks for the sodium salt and the ligand. For mpic, the stretching frequency is low, but the value for **IV** is comparable to **III** and **V**. This would indicate that in the aluminum compound, the ligand is coordinated to the metal ion producing an environment different from that in either the carboxylic acid and carboxylate ion. For **VII**, there are two peaks present. The peak at 1666 cm^{-1} is in the region of the other aluminum compounds and is, therefore, probably due to a coordinated carboxylate group. The other peak could be due to a differently reacting carboxylate group in one compound or another compound with differently bonded carboxylate groups. Despite the presence of more than one aluminum environment in **III**, **IV** and **V** indicated by Al-27 NMR, there is only one visible carbonyl stretching band. Either, the coordination is so similar that the peaks are indistinguishable or the aluminum is coordinated by a bond of the same strength in every compound in the mixture.

Fast Atom Bombardment Mass Spectrometry

FABMS generally works well for large molecules by providing structural evidence from fragmentation. It is due to the occurrence of fragmentation that the ratios for the mixtures in the samples could not be determined. For the spectra of **IV**, **V** and **VI**, the m/z for the ligand is the largest peak present. If the primary component of the solids were the ligands, they would have been soluble. For **III**, the largest peak was probably due to $Al(pic)(H_2O)_3^+$. There were also two

reasonable sized peaks that would correspond to combinations of aluminum, the ligand and hydroxide. However, there was a small peak (0.11%) that would indicate the presence of the tris complex. For **IV**, in addition to the ligand and its decarboxylated fragment, there were three peaks probably due to aluminum combined with one, two and three ligands. For **V**, there were few large peaks; however, there is a small peak (1.06%) that would indicate the tris complex. For **VI**, there is no peak hear the mass for $Al(hyp)_3$, but there is a small peak (0.41%) that could be the tris complex after the loss of part of one of its rings.

In each spectra, fragmentation has occurred to a significant extent. The data for **III**, **IV**, and **V** indicate that the tris complex was present; however, in all four spectra, no conclusive results were found concerning the ratios of the compounds in the sample mixtures.

Aluminum-27 NMR Spectroscopy

Aluminum-27 NMR would have proved a valuable technique if the scale were more fully calibrated. The shift of the peak is indicative of the geometry, symmetry and the type of atoms surrounding the metal center. Since most of the research reported for Al-27 NMR refers to exclusively oxygen atoms bonded to the aluminum, it is not as useful as it could have been. Most of the octahedral AlO_6 groups have shifts very near 0 ppm, whereas the tetrahedral AlO_4 groups are shifted to near 80 ppm. However, the shifts reported for tris complexes

of O,O bidentate ligands in distorted octahedral environments range from 36 to 41 ppm. The data reported for hexacoordinate aluminum complexes of N,O donor atoms, which includes a study using aminopolycarboxylic acids and AlN_3O_3 compounds, list the chemical shift range from 8.1 to 41.2 ppm. The spectra of solids **Ia** and **IIa** revealed a mixture of aluminum environments. For **Ia**, a large peak at 54 ppm and a smaller at 221 ppm. For **IIa**, there are two peaks of equal height at 5 and 73 ppm. The spectrum collected for **IIb** provided a single peak at 54 ppm. Because the structure was confirmed by a second x-ray analysis, the environment of the aluminum complex in solution is known to be $Al(ox)_3$ -- a distorted octahedral environment with three nitrogen and three oxygen atoms. A shift range of 54 to 73 ppm is probably due to the distorted meridional AlO_3N_3 center and should be added to the range of chemical shifts reported for an octahedral environment around an aluminum ion. Also, the difference could be due to the solvent molecule present.

All of the solids except for **V** produced more than one peak using Al-27 NMR. It is clear that each of these contains a mixture of aluminum environments. However, in each solution, there is a peak near 68 ppm which is rather close to 73 ppm. This could confirm the presence of a tris aluminum complex or a common DMSO solvated aluminum species in solution. Also, there are no peaks near 70 for any of the solid samples except for **VI** with hypoxanthine. Since no

chemical shifts for aluminum coordination compounds have been reported for the variety of chemical shifts present in the spectra, little information can be gained about the environment of the aluminum ions in the compounds that have been analyzed.

The spectra for compound **V**, with pyrazinoic acid, each has only one peak for the solid and solution phases. The solution peak is at 70 ppm similar to the other solutions. However, the solid has a peak at 0 ppm, characteristic of $Al(H_2O)_6^{3+}$.

X-ray Crystallography

X-ray crystallography is used to determine the location and type of each atom present in the complex. The greatest disadvantage to x-ray diffraction techniques is the need for a single crystal approximately 0.2 mm in each dimension. Since compounds **III** through **VII** could not be recrystallized, a variety of crystal growth techniques, including urea decomposition, vapor and aqueous gel diffusion, variation of the solvent system and the base strength, were investigated.

Crystal Growth Techniques

Urea Decomposition

For urea decomposition, the crystals that formed with each ligand were neither large nor of high quality. There was a rather large incidence of twinned crystals and inseparable

clusters of crystalline product, possibly as a result of the higher temperature.

Vapor Diffusion

For the diffusion of ammonia vapor, a crystalline product began to form in each experiment after a few days. However, either the crystals were too small or in inseparable clusters. The ammonia reacted immediately upon contact with the surface of the solution. The only single crystals discovered were on the bottom of the beaker. Once a crystal became too heavy to be supported by surface tension, it sank to the bottom and did not grow any larger. The clusters which continued to grow on the surface probably did not sink because of the increased surface tension created by the irregular surface.

Gel Diffusion

For gel diffusion experiments, a crystalline product was produced in most of the trials. The exceptions were when a white band was produced in every case using hyp and twice with mpic. The white band indicates that either very fine crystals formed or only $Al(OH)_3$ was produced. For the most part, he crystals produced were too small, twinned or clusters. However, one experiment, which yielded suitable single crystals, led to the x-ray analysis of compound **VIII**.

Base Strength

For experiments varying the strength of the base, no suitable crystals were formed except for the $KAl(SO_4)_2 \cdot 12H_2O$ reactant. Although the reactions did proceed slower than with

the concentrated bicarbonate ion as the base, single large crystals were not produced.

Solvent System

When methyl or ethyl alcohol was employed as the solvent, experiments did not produce a compound other than the sodium salt of the ligand unless a substantial amount of water was present. However, in the presence of water, pic and pza produce characteristic unsuitable crystal forms. In DMSO, pic and pza both produced a white solid that when heated to 100°C to remove water, a clear but brightly colored solution was formed. The same result was produced when a similar solution of the sodium salt was heated. In addition, no solid remained after the evaporation of the heated DMSO reaction mixture.

Aluminum Isopropoxide

When aluminum isopropoxide was employed, the solids formed using aluminum isopropoxide were non-crystalline and insoluble in any common solvent.

Crystal Growth Results

All of the trials with pic and pza gave consistent results. For pic, large crystals were produced; however, all of these were either twinned or double-twinned. Twinned crystals, which are formed when two crystals grow together along a common face, are not usually suitable for x-ray diffraction studies. Pza consistently produced fairly large crystalline structures that were flower-like in appearance. Examination with a microscope revealed that each had the four

striated branches arranged in a tetrahedral orientation around a central point.

X-ray Diffraction Studies

Despite many attempts with a variety of crystal growth techniques, several compounds, **I**, **II**, and **VIII** through **X**, were studied using x-ray crystallography.

Aluminum Complexes

Compound **I**, $Al(meox)_3 \cdot CH_3OH \cdot H_2O$, and compound **II**, $Al(ox)_3 \cdot CH_3OH$, were the only aluminum-containing compounds characterized by x-ray crystallography. In each complex, the aluminum ion is in a distorted octahedral environment created by three ligands. The three nitrogen and three oxygen atoms are arranged in the meridional as opposed to the facial conformation. Although **II** is quite similar to **I**, there are notable differences in bond lengths and angles between the aluminum, nitrogen and oxygen atoms. In $Al(meox)_3$, the average Al-O bond lengths are shorter than for $Al(ox)_3$. In addition, the Al-N bond lengths for Al-N bonds are an average of 0.100 Å longer for $Al(meox)_3$. It seems reasonable that as the Al-O bond gets shorter, the ligand molecule pivots to also provide a longer Al-N bond distance. The average intraligand O-Al-N bond angle for **I** is 82.5° which is slightly more acute than the average of 82.9° for **II**. The interligand bond angles around aluminum average to 92.8° for $Al(meox)_3$. For $Al(ox)_3$, these bond angles, have an average value of 92.5°. The trans

bond angles for **I** and **II** have an average deviation of 9.4° and 8.8°, respectively, from the ideal 180° angle. All of these measurements prove that the $Al(ox)_3$ is closer to the ideal octahedral environment than $Al(meox)_3$. The steric interaction of the methyl groups with the aromatic rings is probably responsible for the increased distortion from the octahedral environment in the tris(2-methyloxinato)aluminum(III) complex.

<u>$Na(C_7H_4NO_4)(C_7H_5NO_4)\cdot 3H_2O$</u>

For compound **VIII**, aluminum was initially assigned as the central atom, although no seven coordinate aluminum complex has been reported. However, during refinement, the number of hydrogen atoms found indicated the loss of only one hydrogen atom from the dipic and water molecules. A sodium ion was then assigned as the metal ion to give a neutrally charged compound.

The sodium ion is in a pentagonal bipyramidal environment created by two dipic ligands and three water molecules. One dipic, which has both acid groups deprotonated, acts as a tridentate ligand. The bond lengths for the hydroxyl oxygen atoms and the ring nitrogen 2.482(2), 2.584(2) and 2.476(2) Å, respectively. The other dipic, which has been formally deprotonated, is coordinated to the metal ion only through the carbonyl oxygen of the acid group, at a distance of 2.474(2) Å, rather than the deprotonated hydroxy group. The remaining equatorial and the two axial positions are occupied by water

molecules at bond lengths of 2.795(2), 2.300(2) and 2.501(2) Å, respectively. Because there are two hydrogen atoms each on O8, O9 and O10 at bond lengths between 0.71(4) and 0.90(4) Å, which create H-O-H bond angles between 99(4) and 106(5)°, it seems reasonable that O8, O9 and O10 are water molecules and not hydroxide ions.

There is extensive hydrogen bonding in **VIII**. H7 is formally assigned to O7, but it is actually almost equidistant between O7 and O7′ in an adjacent dipic. The two oxygen atoms are 2.472 Å apart and form a bond angle of 172° around H7. The O7-H7-O7′ bond length is just slightly longer than the average value, 2.44 Å, reported for very strong hydrogen bonds in similar compounds. Also, there is a hydrogen bond between H1′ and the equatorial water oxygen O10 and subsequently between H10a and O7′a in an adjacent molecule. In addition, H8a is hydrogen bonded to O7a.

<u>$(C_5H_4N(CO_2H))(C_5H_4NH(CO_2))(NH_4^+)(NO_3^-)$</u>

Compound **IX** is a complex salt of two pic molecules, ammonium and nitrate. Although it is lacking an aluminum ion, the compound does provide extensive discussion of the placement and bonding of the hydrogen atoms. One pic is protonated, by H(O), in the normal acid conformation. However, the carboxylic acid group on the other pic is formally deprotonated and, instead the hydrogen atom, H(N) is located 0.975 Å from the ring nitrogen.

A hydrogen-bonding network exists linking the pic molecules to pic in other unit cells. H(N) is located 1.798 Å from the nitrogen atom in the second ring. H(O) is hydrogen bonded to O(2) in an adjacent pic molecule. Although, the bond lengths for each of these hydrogen bonds are significantly shorter that the sum of the two van der Waal's radii, neither is considered strong hydrogen bond because of the hydrogens are not centered. The two other hydrogen bonds, N(3)-H(1N)···O(1)'' and N(3)-H(4N)···O(2N)''', are also classified as weak because the bond lengths are barely less than the sum of the radii for oxygen and nitrogen. The remaining hydrogen interactions do not qualify as even weak hydrogen bonds.

<u>$Na^{+}C_4H_5O_6^{-}\cdot H_2O$</u>

Compound **X** is sodium hydrogen (+)-tartrate monohydrate. Although aluminum is not present in this compound, its structure provides a discussion of octacoordinate geometries, hydrogen bonding and absolute configuration. All of the oxygens in the compound are coordinated to the sodium with the notable exception of O(5), the hydroxyl oxygen from the protonated carboxylic acid group. The sodium ion is surrounded by eight oxygen atoms, from four different tartrate ions, with bond lengths between 2.426 and 2.827 Å. Calculations of the deviations from the least squares planes for square-antiprismatic and triangular dodecahedral geometries indicate that, although the geometry is

intermediate of the two, the fit is closer for square antiprismatic.

The only non-coordinated oxygen, O(5), is located 1.000 Å from H(3), which is, in turn, hydrogen bonded at a distance of 1.568 Å to O(1) in an adjacent hydrogen tartrate ion. Although it is significantly shorter than the sum of two van der Waal's radii, this hydrogen bond is classified as weak because the H(3) is not centered.

To check the absolute configuration of the compound, least squares refinements for all non-hydrogen atom coordinates were compared with those of the enantiomer. No measurable difference was noted, probably because of the low anomalous scattering factors for Mo Kα for atoms as small as sodium. If radiation that has larger scattering factors had been used, one enantiomer should have refined slightly better.

Summary

With the current focus on the health and environmental issues related to aluminum, research in this field will most certainly continue. However, because of the lack of definitive characterization techniques, the progress in the study of aluminum complexes with N,O donor ligands will proceed slowly.

LIST OF REFERENCES

(1) Liss, L., ed. "Aluminum Neurotoxicity"; Tathopox Publishing, Inc., New York, 1980.

(2) Graves, A. B.; White, E.; Koepsell, T. D.; Reifler, B. V.; van Belle, G; Larson, E. B. *J. Clin. Epidemiol.* **1990**, *43*, 35-44.

(3) Flaten, T. P. *Proc. Sec. Intn. Symp. Geochem. Health* **1987**, London, Apr. 22-24, 1987.

(4) Goldgraber, D.; Lerman, M. I.; McBride, O. W.; Saffiotti, U.; Gajdusek, D. C. *Science* **1987**, *235*, 877-880.

(5) Gitelman, H. J., ed. "Aluminum and Health: A Critical Review"; Marcell Dekker, Inc., New York, 1989.

(6) Kaehny, W. D.; Hegg, A. P.; Alfrey, A. C. *N. Engl. J. Med.* **1977**, *296*, 1389-1390.

(7) Sherrard, D. J. *Sem. Nephrol.* **1986**, *6*, No. 4, 5-11.

(8) Mayor, G. H.; Burnatowska-Hledin, M. *Sem. Nephrol.* **1986**, *6*, No. 4, 1-4.

(9) Edwardson, J. A.; Candy, J. M. *Ann. Med.* **1989**, *21*, 95-97.

(10) Greenwood, N. N.; Earnshaw, A. "Chemistry of the Elements"; Pergamon Press, Ltd., Oxford, 1986.

(11) Lewis, T. E., ed. "Environmental Chemistry and Toxicology of Aluminum"; Lewis Publishers, Inc., Chelsea, Michigan, 1989.

(12) Tam, S. C.; Williams, R. J. P. *J. Inorg. Biochem.* **1986**, *26*, 35-44.

(13) Driscoll, C. T. *J. Royal Neth. Chem. Soc.* **1987**, *106*, 402.

(14) Williams, R. J. P. *J. Royal Neth. Chem. Soc.* **1987**, *106*, 401.

(15) Motekaitis, R. J.; Martell, A. E. *Inorg. Chem.* **1984**, *23*, 18-23.

(16) Marklund, E.; Öhman, L.-O. *Acta Chem. Scand.* **1990**, *44*, 353-357.

(17) Nelson, W. O.; Karpishin, T. B.; Rettig, S. J.; Orvig, C. *Inorg. Chem.* **1988**, *27*, 1045-1051.

(18) Finnegan, M. M.; Lutz, T. G.; Nelson, W. O.; Smith, A.; Orvig, C. *Inorg. Chem.* **1987**, *26*, 2171-2176.

(19) Lutz, T. G.; Clevette, D. J.; Rettig, S. J.; Orvig, C. *Inorg. Chem.* **1989**, *28*, 715-719.

(20) Taylor, D. *Aust. J. Chem.* **1978**, *31*, 1455-1462.

(21) Muetterties, E. L.; Guggenberger, L. J. *J. Am. Chem. Soc.* **1972**, *94*, 8046-8054.

(22) McClelland, B. W. *Acta Cryst.* **1975**, *B31*, 2496-2498.

(23) Feng, T. L.; Gurian, P. L.; Healy, M. D.; Barron, A. R. *Inorg. Chem.* **1990**, *29*, 408-411.

(24) Sattin, A; Muhoberac, B. B.; Aprison, M. H.; Schauf, C. L. *Medical Hypotheses* **1989**, *29*, 155-159.

(25) Schmidbaur, H; Lettenbauer, J.; Wilkinson, D. L.; Müller, G.; Kumberger, O. *Z. Naturforsch*, **1991**, *46b*, 901-911.

(26) Liu, S.; Rettig, S. J.; Orvig, C. *Inorg. Chem.*, **1992**, *31*, 5400-5407.

(27) Hoveyda, H. R.; Karunaratne, V.; Rettig, S. J.; Orvig, C. *Inorg. Chem.*, **1992**, *31*, 5408-5416.

(28) Bossek, U.; Hanke, D.; Wieghardt, K.; Nuber, B. *Polyhedron*, **1993**, *12*, 1-5.

(29) Liu, S.; Wong, E.; Karunaratne, V.; Rettig, S. J.; Orvig, C. *Inorg. Chem.*, **1993**, *32*, 1756-1765.

(30) Simonsen, S. H.; Bechtel, D. W. *American Crystallographic Association, Ser. 2*, **1980**, *7*, 23.

(31) Ul-Haque, M.; Horne, W.; Lyle, S. J. *J. Cryst. Spect. Res.* **1991**, *21*, 411-417.

(32) Kushi, Y.; Fernando, Q. *J. Am. Chem. Soc.* **1970**, *92*, 91-95.

(33) DeSimone, J. M.; Stangle, M.; Riffle, J. S.; McGrath, J. E. *Makromol.Chem., Macromol. Symp.*, **1991**, *42/43*, 373-385.

(34) Feng, T. L.; Tsangaris, J. M.; Barron, A. R. *Monatshefte für Chemie*, **1990**, *121*, 113-118.

(35) Karweer, S. B.; Pillai, B. P.; Iyer, R. K. *Magn. Res. Chem.* **1990**, *28*, 922-924.

(36) Jøns, O.; Johansen, E. S. *Inorg. Chim. Acta*, **1988**, *151*, 129-132.

(37) Dzugan, S. T.; Goedken, V. L. *Inorg. Chim. Acta*, **1988**, *154*, 169-175.

(38) Addy, P.; Evans, D. F.; Sheppard, R. N. *Inorg. Chim. Acta*, **1987**, *127*, L19-20.

(39) Gurian, P. L.; Cheatham, L. K.; Ziller, J. W.; Barron, A. R. *J. Chem. Soc. Dalton Trans.*, **1991**, 1449-1456.

(40) Komatsu, N.; Uokoi, M.; Kubota, E. *Bull. Chem. Soc. Jpn.*, **1988**, *61*, 3746-3748.

(41) Heřmánek, S.; Fusek, J.; Kříž, O.; Čásenský, B.; Černý, Z. *Z. Naturforsch*, **1987**, *42b*, 539-545.

(42) Barron, A. R.; Lyons, D.; Wilkinson, G.; Motevalli, M.; Howes, A.J.; Hursthouse, M. B. *J. Chem. Soc. Dalton Trans.*, **1986**, 279-285.

(43) Shirk, A. E.; Shirk, J. S. *Inorg. Chem.*, **1983**, *22*, 72-77.

(44) Findlow, J. A.; Duffield, J. R.; Evans, D. A.; Williams, D. R. *J. Royal Neth. Chem. Soc.* **1987**, *106*, 403.

(45) Thich, J. C.; Ou, C. C.; Powers, D.; Vasiliou, B.; Mastopaolo, D.; Potenza, J. A.; Schugar, H. J. *J. Am. Chem. Soc.*, **1976**, *98*, 1425-1433.

(46) Quaglieri, P. P.; Loiseleur, H.; Thomas, G. *Acta Cryst.*, **1972**, *B28*, 2583-2590.

(47) Strahs, G.; Dickerson, R. E. *Acta Cryst.*, **1968**, *B24*, 571-578.

(48) Palmer, K. J.; Wong, R. Y.; Lewis, J. C. *Acta Cryst.*, **1972**, *B28*, 223-228.

(49) Biagini-Cingi, M.; Chiesi-Villa, A.; Guastini, C.; Nardelli, M. *Gazz. Chim. Ital.*, **1972**, *102*, 1026-1033.

(50) Beveridge, K. A.; Bushnell, G. W. *Can. J. Chem.*, **1979**, *57*, 2498-2503.

(51) Ou, C.-C.: Borowski, W. J.; Potenza, J. A.; Schugar, H. J. *Acta Cryst.*, **1977**, *B33*, 3246-3248.

(52) Silverstein, R. M.; Bassler, G. C.; Morrill, T. C. "Spectrometric Identification of Organic Compounds" 4th ed., John Wiley and Sons, New York, 1981.

(53) Cotton, F. A.; Wilkinson, G. "Advanced Inorganic Chemistry: A Comprehensive Text"; Oxford University Press, New York, 1985.

(54) Akitt, J. W. *Prog. in NMR Spec.*, **1989**, *21*, 1-149.

(55) Wu, Y.; Chmelka, B. F.; Pines, A.; Davis, M. E.; Grobet, P. J.; Jacobs, P. A. *Nature*, **1990**, *346*, 550-553.

(56) Dirken, P. J.; Jansen, J. B. H.; Schuiling, R. D. *Amer. Miner.*, **1992**, *77*, 718-724.

(57) Iyer, R. K.; Karweer, S. B.; Jain, V. K. *Magn. Reson. in Chem.*, **1989**, *27*, 328-334.

(58) Polynova, T. N.; Bel'Skaya, N. P.; Banus, D. T. G.; Porai-Koishits, M. A.; Martynanko, L. I. *J. Struct. Chem.*, **1970**, *11*, 158.

(59) Rinehart, K. L., Jr *Science*, **1982**, *218*, 254-260.

(60) Reynolds, D. R.; Burn, J. L. E.; Boggess, B.; Cook, K. D.; Woods, C. *Inorg. Chem.*, **1993**, *32*, 5517-5521.

(61) Glusker, J. P.; Trueblood, K. N. "Crystal Structure Analysis: A Primer" 2nd ed., Oxford University Press, New York, 1985.

(62) Desiraju, G. R.; Curtin, D. Y.; Paul, I. C. *J. Am. Chem. Soc.*, **1977**, *99*, 6148.

(63) March. J. "Advanced Organic Chemistry: Reactions, Mechanisms and Structure" 3rd ed., John Wiley and Sons, New York, 1985.

(64) Hollinshead, R. G. W. "Oxine and its Derivatives" part I; Butterworths, London, 1954.

(65) Heitsch, C. W.; Nordman, C. E.; Parry, R. W. *Inorg. Chem.*, **1963**, *2*, 508-512.

(66) Emsley, J. *Chem. Soc. Rev.*, **1980**, *9*, 91-124.

(67) Browning, K. R. Unpublished results.

(68) Buschman, J.; Luger, P. *Acta Cryst. C*, **1985**, *41*, 201-203.

(69) Spek, A. L. *Acta Cryst. C*, **1987**, *43*, 1633-1634.

(70) Hoard, J. L.; Silverton, J. V. *Inorg. Chem.*, **1963**, *2*, 235-243.

(71) Lippard, S. J.; Russ, B. J. *Inorg. Chem.*, **1968**, *7*, 1686-1688.

(71) Cromer, D. T.; Liberman, D. *J. Chem. Phys.*, **1970**, *53*, 1891-1898.

(72) Dauben, C. H.; Templeton, D. H. *Acta Cryst.*, **1955**, *8*, 841-842.

BIOGRAPHICAL SKETCH

Kim Browning was born in Orlando, Florida, on February 4, 1965. She graduated with honors from Maynard Evans High School in 1983. In 1987, Kim graduated summa cum laude from the University of Central Florida with a B.S. in chemistry and began graduate studies at the University of Florida. Starting in August 1992, she was an Instructor of Chemistry at the Louisiana School for Math, Science and the Arts. Following nomination by one of her students, Kim Browning was named to Who's Who Among America's Teachers for 1994.

I certify that I have read this study and that in my opinion it conforms to acceptable standards of scholarly presentation and is fully adequate, in scope and quality, as a dissertation for the degree of Doctor of Philosophy.

Gus J. Palenik, Chairman
Professor of Chemistry

I certify that I have read this study and that in my opinion it conforms to acceptable standards of scholarly presentation and is fully adequate, in scope and quality, as a dissertation for the degree of Doctor of Philosophy.

James M. Boncella
Associate Professor of Chemistry

I certify that I have read this study and that in my opinion it conforms to acceptable standards of scholarly presentation and is fully adequate, in scope and quality, as a dissertation for the degree of Doctor of Philosophy.

David E. Richardson
Professor of Chemistry

I certify that I have read this study and that in my opinion it conforms to acceptable standards of scholarly presentation and is fully adequate, in scope and quality, as a dissertation for the degree of Doctor of Philosophy.

Wallace S. Brey
Professor of Chemistry

I certify that I have read this study and that in my opinion it conforms to acceptable standards of scholarly presentation and is fully adequate, in scope and quality, as a dissertation for the degree of Doctor of Philosophy.

Koppaka V. Rao
Professor of Medicinal Chemistry

This dissertation was submitted to the Graduate Faculty of the Department of Chemistry in the College of Liberal Arts and Sciences and to the Graduate School and was accepted as partial fulfillment of the requirements for the degree of Doctor of Philosophy.

May 1995

Dean, Graduate School

LD
1780
1995
.B885

UNIVERSITY OF FLORIDA
3 1262 08554 5548